UC Merced

UC Merced Electronic Theses and Dissertations

Title

Genetic regulation of antifungal drug resistance in Candida albicans and Candida auris

Permalink

https://escholarship.org/uc/item/96f5x7jv

Author

Ennis, Craig Lewis

Publication Date

2021

Copyright Information

This work is made available under the terms of a Creative Commons Attribution License, availalbe at https://creativecommons.org/licenses/by/4.0/

Peer reviewed|Thesis/dissertation

eScholarship.org Powered by the California Digital Library
University of California

UNIVERSITY OF CALIFORNIA, MERCED

Genetic regulation of antifungal drug resistance in *Candida albicans* and *Candida auris*

A dissertation submitted in partial satisfaction of the

requirements for the degree of

Doctor of Philosophy

in

Quantitative and Systems Biology

by

Craig Lewis Ennis

Committee in charge:

Professor Aaron Hernday, Chair of Advisory Committee

Professor Miriam Barlow

Professor Kirk Jensen

Professor Clarissa Nobile, Supervisor

2021

Copyright
Craig Lewis Ennis, 2021
All Rights Reserved

The dissertation of Craig Lewis Ennis, titled, “Genetic regulation of antifungal drug resistance in *Candida albicans* and *Candida auris*”, is approved, and is acceptable ion quality and form for publication on microfilm and electronically:

_____ Date _____

Professor

_____ Date _____

Professor

Supervisor _____ Date _____

Professor

Chair _____ Date _____

Professor

University of California, Merced

2021

This is dedicated to my mom, sisters, and nephew.

Table of Contents

I. List of Abbreviations

UV	Ultraviolet
TSA	Tryptic soy agar
TSB	Tryptic soy broth
YPD	Yeast peptone dextrose
DSB	Double strand break
HDR	Homology directed repair
NHEJ	Non-homologous end joining
tracrRNA	Trans-activating CRISPR RNA
dDNA	Donor DNA
gRNA	Guide RNA
NAT	Nourseothricin
HYG	Hygromycin
DAPI	4′,6-diamidino-2-phenylindole
ConA	Concanavalin A
SC	Synthetic complete
SpiderG	Spider media supplemented with 1% glucose
TF	Transcription factor

II. List of Figures

Figure **Page**

IV. Acknowledgments

The work presented in this dissertation was made possible through the help and support of many people. I would like to express my gratitude to my advisor and mentor Dr. Clarissa Nobile. I have grown tremendously as a scientist with the technical and professional expertise. Clarissa provided my first foray into lab work and the space to explore and grow in the process. Thank you for always believing in me, I would not be where I am today without your guidance and support.

Next, I would like to thank my thesis committee members, whose assistance and approval have helped me develop as an independent scientist. Dr.'s Miriam Barlow, Aaron Hernday, and Kirk Jensen, whose expertise in each of their specialties contributed to my growth. A special thank you to Miriam for the mentorship she has provided since I was an undergraduate – I have learned a lot and will miss our hallway chats.

I am grateful for support from the National Institutes of Health's NICDR (National Institute for Dental and Craniofacial Research) for supporting my ideas and providing the independence to expand my research in areas I could not have imagined. This fellowship would not have been possible without the support of UC Merced's Health Sciences Research Institute (HSRI) and the wonderful staff (Prosper Godonoo, Leann Nascimento, and Carmen Middleton) who aided with submission and management of the award. I appreciate the support you provided through the entire process.

I would like to thank my colleagues past and present their support and feedback throughout my journey at UC Merced. In particular Drs. Megha Gulati, Melanie Ikeh, James Goodwine, Priyanka Bapat, Ashley Valle Arevalo, Diana Rodriguez, Akshay Paropkari, Thaddeus Seher, and Clement Laksana, Deepika Gunasekaran, Mohammad Qasim, Namkha Nguyen, Austin Perry, Morgan Quail, and Pegah Mosharaf. I have learned a great deal from each of you and I have enjoyed our fun talks in the lab over the years.

I'd like to also thank my friends who made the time here enjoyable. Thank you to Drs. Kinsey Brock, Jackie Shay, Mo Kaze, and Cristie Donham along with Candace Cole, Lillie Pennington, Sonia Vargas, Rhondene Wint, and Jade Fee.

Finally I'd like to acknowledge the many students whom I mentored during my graduate work. Thank you to Ihoema Chieke, Lonnie Saetern, Tamy Do, Christian Montiel, Gabriel Viramontes, and Viviana Muñoz, for your many contributions to this and other works.

V. Vita for Craig Lewis Ennis

Education:

PhD	University of California, Merced, Quantitative and Systems Biology	2021
MS	University of California, Merced, Quantitative and Systems Biology	2019
BS/BA	University of California, Merced, Biology & Psychology	2016

List of Publications:

Ennis, C.L., Hernday, A.D., Nobile, C.J. (2021) A markerless CRISPR-mediated system for genome editing in *Candida auris* reveals a conserved role for Cas5 in the caspofungin response. *Microbiology Spectrum*.

Fan, S., Yue, H., Zheng, Q., Bing, J., Tian, S., Chen, J., **Ennis, C.L.**, Nobile, C.J., Huang, G., Du, H. (2021) Morphological diversity is a general characteristic of *Candida auris* clinical isolates. *Medical Mycology.*

Lohse, M.B., **Ennis, C.L.**, Hartooni, N., Johnson, A.D., Nobile, C.J. (2020) A screen for small molecules to target *Candida albicans* biofilms. *Journal of Fungi*.

Du, H., Bing, J., Hu, T., **Ennis, C.L.**, Nobile, C.J., Huang, G. (2020) *Candida auris*: epidemiology, biology, antifungal resistance, and virulence. *PLoS Pathogens.*

Du, H., **Ennis C.L.**, Hernday, A.D., Nobile, C.J., Huang, G. (2020) N-acetylglucosamine (GlcNAc) sensing, utilization, and functions in *Candida albicans*. *Journal of Fungi*.

Nobile, C.J., **Ennis, C.L.**, Hartooni, N., Johnson, A.D., Lohse, M.B. (2020) A selective serotonin-reuptake inhibitor, a proton pump inhibitor, and two calcium channel blockers target *Candida albicans* biofilms. *Microorganisms*.

Gulati, M., Lohse, M.B., **Ennis, C.L.**, Gonzalez, R.E., Perry, A.M., Bapat, P., Valle Arevalo, A., Rodriguez, D.L., Nobile, C.J. (2018) *In vitro* culturing and screening of *Candida albicans* biofilms. *Current Protocols in Microbiology*.

Gulati, M., **Ennis, C.L.**, Rodriguez, D.L., Nobile, C.J. (2017) Visualization of biofilm formation in Candida albicans using an automated microfluidic device. *Journal of Visualized Experiments*.

Awards and Fellowships:

2020 President's Award for Outstanding Student Leadership 2020
University of California, Office of the President
(Awarded to RadioBio, Selected by UC President Janet Napolitano)

QSB Summer Research Fellowship 2020
UC Merced School of Natural Sciences

University Friends Circle (UFC) Community Service Award 2020
UC Merced's University Friends Circle (Awarded to RadioBio)

GradSLAM! Finalist 2020
UC Merced Graduate Division

Graduate Student Travel Award 2019
American Society for Microbiology

University Friends Circle (UFC) Community Service Award 2019
UC Merced's University Friends Circle (Awarded to RadioBio)

NIH Ruth L. Kirschstein Predoctoral Individual NSRA 2019 - 2023
National Institute of Dental and Craniofacial Research (F31DE028488)

Aristotle House Fellow (Declined) 2019 - 2020
UC Merced School of Natural Sciences

GradSLAM! Third Place Award 2019
UC Merced Graduate Division

GradSLAM! Finalist 2019
UC Merced Graduate Division

Aristotle House Fellow 2018 - 2019
UC Merced School of Natural Sciences

QSB Summer Research Fellowship 2018
UC Merced School of Natural Sciences

University Friends Circle (UFC) Community Service Award 2018
UC Merced's University Friends Circle (Awarded to RadioBio)

GradSLAM! Third Place Award 2018
UC Merced Graduate Division

GradSLAM! Finalist 2018
UC Merced Graduate Division

Outstanding Graduate Poster Presentation Second Place Award 2018
Northern California American Society for Microbiology

Sonoma County Mycological Society Graduate Award 2017
Sonoma County Mycological Society

Three Minute Thesis First Place Award 2017
Northern California American Society for Microbiology

Competitive Edge Summer Bridge Fellowship 2016
UC Merced Graduate Division

Select Presentations:

Ennis, C.L., Nobile C.J. Identifying the Transcriptional Network Controlling Biofilm Development in *Candida auris*. Poster presentation at: Cold Springs Harbor Laboratory Meeting on Microbial Pathogenesis & Host Response 2021, September 21-24, 2021.

Ennis, C.L., Nobile C.J. Identifying the Transcriptional Network Controlling Biofilm Development in *Candida auris*. Poster presentation at: FASEB's The Microbial Pathogenesis Conference: Mechanisms of Infectious Diseases 2021, July 13-15, 2021.

Ennis, C.L. Identifying the Transcriptional Network Controlling Biofilm Development in *Candida auris*. Oral presentation at: World Microbe Forum (ASM General Meeting), June 23, 2021.

Ennis, C.L., Hernday, A.D., Nobile C.J. Marker-less CRISPR/Cas9 Mediated Genome Editing in *Candida auris*. Poster presentation at: *Candida* and Candidiasis 2021, March 23, 2021.

Ennis, C.L. Genetic Regulation of Antifungal Resistance in *Candida albicans*. Webinar presentation at: Fluxion Biosciences, February 28, 2020.

Ennis, C.L., Nobile C.J. Identifying New Regulators of Antifungal Resistance in *Candida albicans* Biofilms. Poster presentation at: ASMicrobe 2019, June 22, 2019.

Ennis, C.L. Identifying New Regulators of Antifungal Resistance in *Candida albicans* biofilms. Oral presentation at: 20th Annual Cal Microbiology Symposium, April 27, 2019.

Ennis, C.L., Nobile C.J. Identifying New Regulators of Antifungal Resistance in *Candida albicans* Biofilms. Poster presentation at: 14th ASM Conference on *Candida* and Candidiasis 2018, April 17, 2018.

Ennis, C.L., Nobile C.J. Identifying New Regulators of Antifungal Resistance in *Candida albicans* Biofilms. Poster presentation at: Northern California American Society for Microbiology Spring 2018 Meeting, March 3, 2018.

Ennis, C.L. Genetic Control of Antifungal Resistance in *Candida albicans*. Oral presentation at: UC Merced Molecular and Cell Biology Seminar, November 13, 2018.

Ennis, C.L. There is a Fungus Among Us: *Candida albicans* and Human Health. Invited oral presentation at: Mycological Society of San Francisco's 48th Annual Fungus Fair, December 3, 2017.

VI. Abstract

Genetic regulation of antifungal drug resistance in *Candida albicans* and *Candida auris*

Craig Lewis Ennis

Doctor of Philosophy

University of California, Merced

2021

Supervisor: Professor Clarissa J. Nobile

Fungal pathogens are responsible for millions of infections worldwide every year. These infections are caused by several fungal species, yet the *Candida* species of fungal pathogens are the most frequently isolated from humans. They cause superficial to life-threatening disseminated infections, where individuals with compromised immune systems, individuals with changes in their resident microbiota, and those undergoing antibiotic treatments are at highest risk for developing severe *Candida* infections. A longstanding limitation in the field is the ability to make precise genome edits in the *Candida* species to identify genes and pathways involved in virulence and antifungal resistance. Chapter 1 of this dissertation describes the identification of *Candida albicans* transcriptional regulators controlling cell aggregation in response to the antifungal drug caspofungin. This led to the identification of a novel adhesin mediating aggregation and a cell wall protein critical for the caspofungin response. Chapter 2 describes the development and optimization of the first markerless CRISPR/Cas9 system for genome editing in the emerging fungal pathogen *Candida auris*. I show the versatility of this tool to perform genome edits in clinical isolates and identify a conserved role for a transcription factor involved in the caspofungin response. Chapter 3 describes my work on the efficacy of a novel oxidizing disinfectant agent capable of disrupting biofilms, surface attached microbial communities, of pathogenic fungal and bacterial species. Finally, Chapter 4 summarizes my conclusions from the first three chapters and discusses future directions for the work. Overall, this body of work provides new tools for the genetic manipulation of an emerging fungal pathogen and expands our understanding of how *Candida* species respond to antifungal drug treatment.

Chapter 1

Cfl11 is a new mediator of caspofungin-induced flocculation in *Candida albicans*

In preparation for submission; Authors: Craig L. Ennis, Gabriel Viramontes, Austin M. Perry, & Clarissa J. Nobile

1.1 Abstract

Candida albicans is a commensal of the human microbiota, but is also the most common fungal pathogen of humans. Perturbations in the host microbiota, immune system, and changes in pH can lead to the over proliferation of *C. albicans*, causing life threatening, disseminated infections. Three antifungal drug classes (the azoles, echinocandins, and polyenes) are approved for treating *Candida* infections. Caspofungin, an antifungal drug of the echinocandin class, is commonly prescribed to treat disseminated candidiasis. Caspofungin works by inhibiting the synthesis of β-(1,3)-D-glucans, reducing stability of the fungal cell wall, and ultimately leading to fungal cell death. Interestingly, *C. albicans* yeast cells flocculate, tightly adhere to one another, in response to treatment with caspofungin. These adhered cells (or "flocs") are microbial communities with some similarities to biofilms, surface attached microbial communities encased in a secreted extracellular matrix. Screening an existing homozygous transcription factor (TF) deletion mutant library, we identified three regulators required for flocculation, all of which overlap with the regulators of the biofilm transcriptional network. Using RNA-sequencing, we identified putative target genes of these regulators, and with a CRISPR/Cas9 system, we deleted genes of interest, and assessed their flocculation phenotypes. Based on this work, we identified Cfl11 as a new mediator of caspofungin-induced flocculation and propose a mechanism for its contribution to adhesion. We also identified Pga23 as an essential mediator of the caspofungin response. Together, these findings improve our understanding of how microbial communities develop in response to stress and the molecular mechanisms that underpin adhesion and antifungal drug resistance in human fungal pathogens.

1.2 Introduction

Candida albicans is a commensal fungus of the human microbiota, but is also the most common fungal pathogen of humans (1). *C. albicans* can exist as a commensal on the skin, in the mouth, gut, and genitourinary tract of healthy humans (2). Individuals with immune defects, those undergoing long-term antibiotic treatment, or those having undergone surgical procedures are at highest risk of developing a *Candida* infection (3-6). One virulence trait of *C. albicans* is its ability to form recalcitrant surface-attached microbial communities called biofilms (7). These three-dimensional structures can form on biotic and abiotic substrates and can seed infections at other locations within the human host (8). Biofilm development begins with the attachment of yeast-form cells to a surface, a process supported by cell surface adhesins (9). Once attached, the yeast-form cells elongate forming hyphae and pseudohyphae and the cells secrete a protective extracellular matrix material (10-12). Once the biofilm has matured, yeast-form cells are dispersed and can seed niches elsewhere in the body (13, 14).

Three antifungal drug classes are used to treat *C. albicans* infections (the azoles, polyenes, and echinocandins) (15). Caspofungin, an antifungal drug of the echinocandin class, is frequently used to treat disseminated infections and has some reported efficacy against biofilm-based infections (16). Caspofungin works by inhibiting the synthesis of β-(1,3)-D-glucans, structural components of the fungal cell wall, resulting in fungal cell wall instability and subsequent fungal cell death (17). During treatment with caspofungin *in vitro*, free-floating (planktonic) *C. albicans* cells flocculate, forming tightly adhered "biofilm-like" three dimensional structures called "flocs" (18). This phenotypic response is not unique to caspofungin treatment and similar aggregation in *C. albicans* has been observed when *C. albicans* cells are starved for certain amino acids or when they are co-cultured with specific anaerobic bacteria (19, 20). Previous groups have studied aggregation in response to caspofungin treatment, identifying the transcription factor Efg1 as an essential regulator of *ALS1*, a gene that encodes a cell surface adhesin protein; both *EFG1* and *ALS1* are essential for caspofungin-induced flocculation (18).

Several proteins are encoded in the *C. albicans* genome that facilitate adhesion to other microorganisms, host tissues, or implanted medical devices. This is mediated by the *ALS*, *HYR*, and *HWP* gene families in the *C. albicans* genome and many transcriptional factors contribute to the expression of *C. albicans* adhesins (9, 21-24). Furthermore, the majority of these adhesins have functionally redundant roles, where, when lost, can complement the function of others (22). Adhesion is a general property of *Candida* species and distantly related non-pathogenic fungal species. Aggregation has been extensively studied in the brewer's yeast, *Saccharomyces cerevisiae*, and has also observed in bacteria. Across kingdoms, aggregation can be influenced by carbon source availability, changes in pH, growth phase, or sublethal antimicrobial concentrations (18, 20, 25-27). In the related non-pathogenic yeast *S. cerevisiae*, aggregation is mediated by the Flo1, Flo5, Flo9, and Flo10 cell wall proteins, as well as the Flo8 transcriptional regulator (25). *C. albicans* and *S. cerevisiae* diverged approximately 200 million years ago (28); however, *C. albicans* retained a homolog of Flo8 (29, 30). In *C. albicans*, Flo8 regulates biofilm development and adhesion (31), yet its role in antifungal drug-induced aggregation was not previously known. Complex phenotypes are typically regulated by multiple transcriptional regulators

(32), thus unidentified regulators are likely also contributing to antifungal drug-induced aggregation.

Concomitant with the upregulation of genes encoding adhesins during caspofungin treatment, *C. albicans* also upregulates cell wall damage response genes (33). Several putative response genes have been identified by RNA-sequencing (RNA-seq), many of which are regulated by the transcription factors Cas5, Rlm1, and Sko1, and result in remodeling of the fungal cell wall composition to withstand drug exposure (34-37). For instance, elevated cell wall chitin levels can increase resistance and tolerance of *C. albicans* to echinocandins (38, 39). Cell wall remodelers, adhesins, and upstream transcriptional regulators together contribute to the caspofungin response and the ability of *C. albicans* to tolerate antifungal drug treatment.

In this work, we performed a genetic screen to identify a complete set of transcriptional regulators required for flocculation in response to caspofungin. Using RNA-seq we identified putative target genes of these regulators and with a CRISPR/Cas9 system, we deleted several genes of interest. From this we identified Cfl11 as a new mediator of caspofungin-induced flocculation and Pga23 as an essential mediator of the caspofungin response. These findings further our understanding of how *C. albicans* colonizes surfaces and responds to cell wall stresses, pathways that can be exploited in the development of new antifungal drugs.

1.3 Results

Bcr1, Flo8, and Efg1 regulate caspofungin-induced flocculation

Treatment of free-floating *C. albicans* cells with caspofungin is known to induce flocculation, and this response is regulated by Efg1 which regulates *ALS1*, a gene encoding a cell surface adhesin protein (19). Adhesion in *C. albicans* is regulated by several transcription factors (19, 24, 25), and we reasoned that caspofungin-induced flocculation is likely controlled by additional unidentified transcription factors. To identify transcription factors involved in caspofungin-induced flocculation, we screened an existing library of 211 homozygous transcription factor deletion mutant strains for their abilities to flocculate in the presence of caspofungin (32, 41). Mutants TF137 (*bcr1*Δ/Δ), TF156 (*efg1*Δ/Δ), and TF175 (*flo8*Δ/Δ) were significantly defective in caspofungin-induced

flocculation; and TF33 (*cas5*Δ/Δ), TF59 (*ace2*Δ/Δ), and TF117 (*tup1*Δ/Δ) had significantly increased levels of caspofungin-induced flocculation (Figure 1.1A).

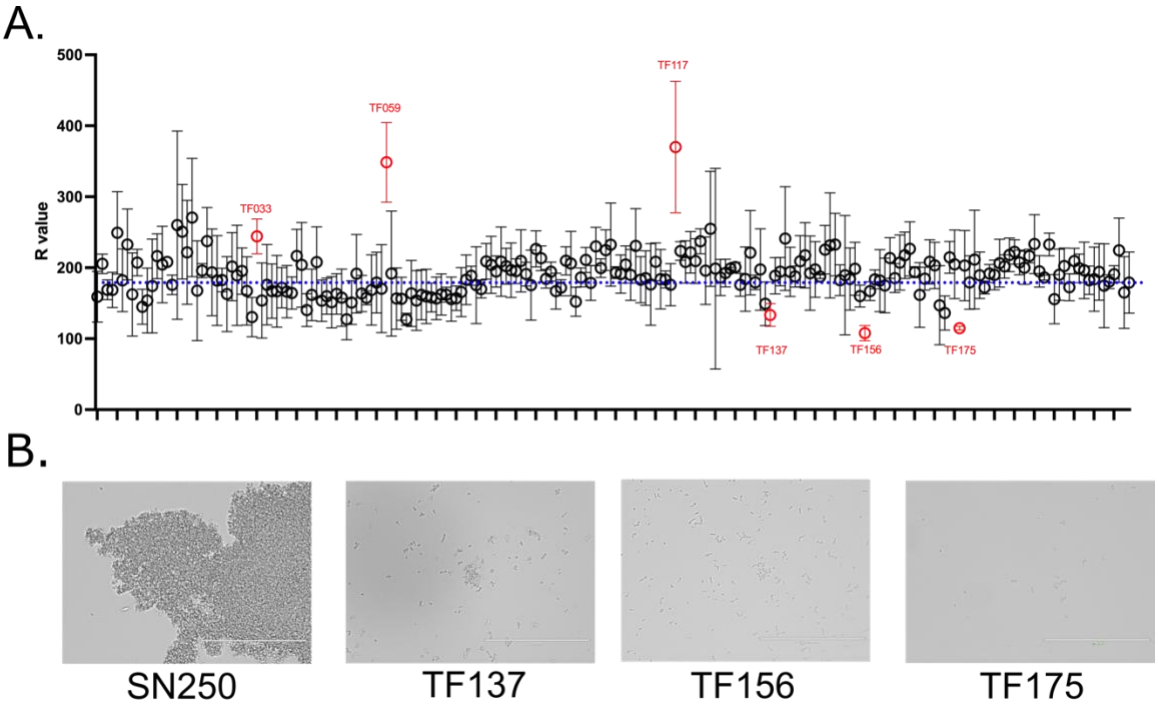

Figure 4.1 Bcr1, Efg1, and Flo8 are regulators of caspofungin-induced flocculation. (A) A complete library of 211 C. albicans transcription factor deletion mutant strains were screened for their abilities to flocculate in response to caspofungin. Cells were grown in caspofungin at a concentration of 62.5 ng/mL, shaking, for 3 h, and flocculation was measured in an optical density sedimentation assay. Optical density (OD_{600}) was measured at two time points (OD_1 and OD_2) to compute the R value [(OD_1*100)/OD_2], i.e., the relative level of sedimentation. Each transcription factor deletion mutant strain was tested on three separate occasions and the average of the tests is shown. The blue dotted line represents the average wildtype strain R value across all experiments performed. Transcription factor deletion mutants with a statistically significant change in R values are denoted in red. Statistical significance was determined using a two-tailed students t-test with a p value < 0.05. (B) Brightfield microscopy at 20X magnification of the wildtype, *bcr1*Δ/Δ, *efg1*Δ/Δ, and *flo8*Δ/Δ strains grown in RPMI-1640 supplemented with 62.5 ng/mL caspofungin. Scale bars represent 200 μm.

This flocculation assay measures the ability of cells to settle over time such that flocculating strains will settle faster due to increased size and density than strains that do not flocculate. Additionally, strains that are hypersensitive to caspofungin will settle faster due to increased cell lysis. Cas5 is a well characterized regulator of the caspofungin response in *Candida* species, and it is likely that cells of the *cas5*Δ/Δ strain are settling faster relative to the wildtype because of their hypersensitivity to the drug (34, 38, 42), and thus we chose not to further study the roles of Cas5 in the context of flocculation. To control for strains that flocculate in the absence of caspofungin, we performed the same assay in

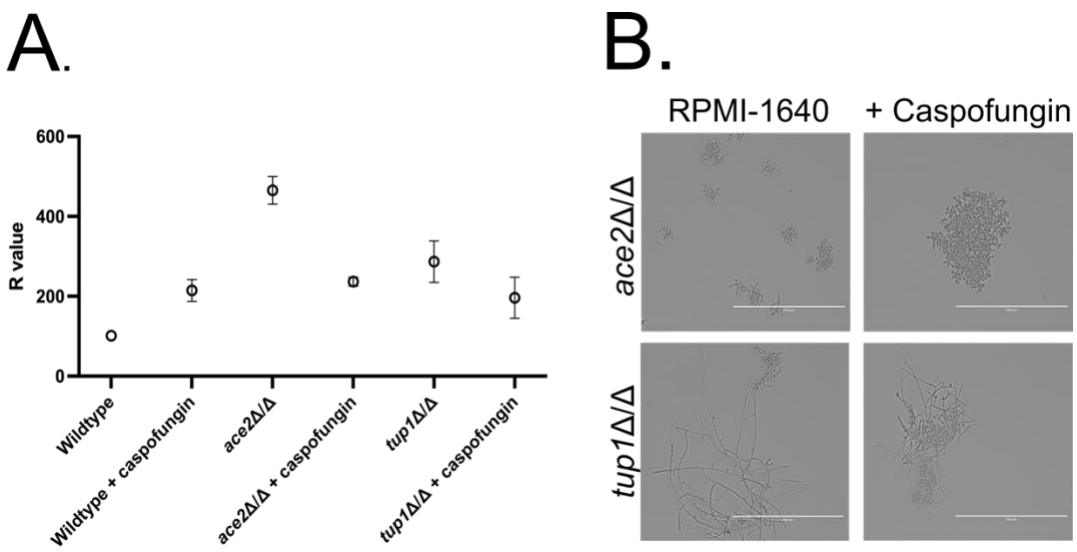

S Figure 1.1 ace2Δ/Δ and tup1Δ/Δ sedimentation and microscopy experiments indicate a pleiotropic phenotype. (A) Sedimentation of the *ace2*Δ/Δ and *tup1*Δ/Δ deletion mutant strains in the presence and absence of 62.5 ng/mL caspofungin. (B) Brightfield microscopy of the wildtype, *ace2*Δ/Δ and *tup1*Δ/Δ deletion mutant strains in the presence and absence of 62.5 ng/mL caspofungin. Images were acquired with a 20X objective. Scalebars represent 200 μm.

RPMI-1640 alone, finding that *ace2*Δ/Δ and *tup1*Δ/Δ deletion mutant strains have increased sedimentation (and thus increased flocculation) even in the absence of caspofungin (S Figure 1.1A and B). Deletion of *ACE2* in *C. albicans* and other yeast species is known to result in reduced cell separation, potentially explaining the high degree of aggregation observed in both conditions (43-45). Tup1 negatively regulates filamentation (46), and a *tup1*Δ/Δ strain is locked in the hyphal state, forming dense, interconnected cell masses due to expression of high levels of hyphal specific genes and cell-surface adhesins (47, 48). Interestingly the *tup1*Δ/Δ mutant strain treated with caspofungin formed large cell masses containing both hyphae and yeast, indicating that caspofungin inhibits hyphal morphogenesis in an otherwise hyphal locked strain (Figure S1B). Nonetheless, loss of either of these regulators resulted in a pleiotropic effect, and as a result they were not studied further. The phenotypes of the flocculation defective mutant strains (*bcr1*Δ/Δ, *efg1*Δ/Δ, and *flo8*Δ/Δ) were also confirmed with brightfield microscopy. Under caspofungin treatment, the wildtype strain forms large, dense clusters of primarily yeast-form cells greater than 200 μm in size (Figure 1.1B). The *bcr1*Δ/Δ, *efg1*Δ/Δ, and *flo8*Δ/Δ mutant strains, however, did not form large cell masses like the wildtype, rather the cells were largely non-adherent (Figure 1B). Lastly, we confirmed that the flocculation defective mutant strains are not sensitive to caspofungin. We next performed growth rate measurements in the presence and absence of caspofungin, and discovered that the growth of *bcr1*Δ/Δ, *efg1*Δ/Δ, and *flo8*Δ/Δ strains is not impacted by the concentration of caspofungin used (S Fig 1.2). Complementation of these transcription factor mutant strains

with the wildtype allele restores flocculation in these strains, confirming the roles of Bcr1, Efg1, and Flo8 as regulators of caspofungin-induced flocculation (Figure 1.1C).

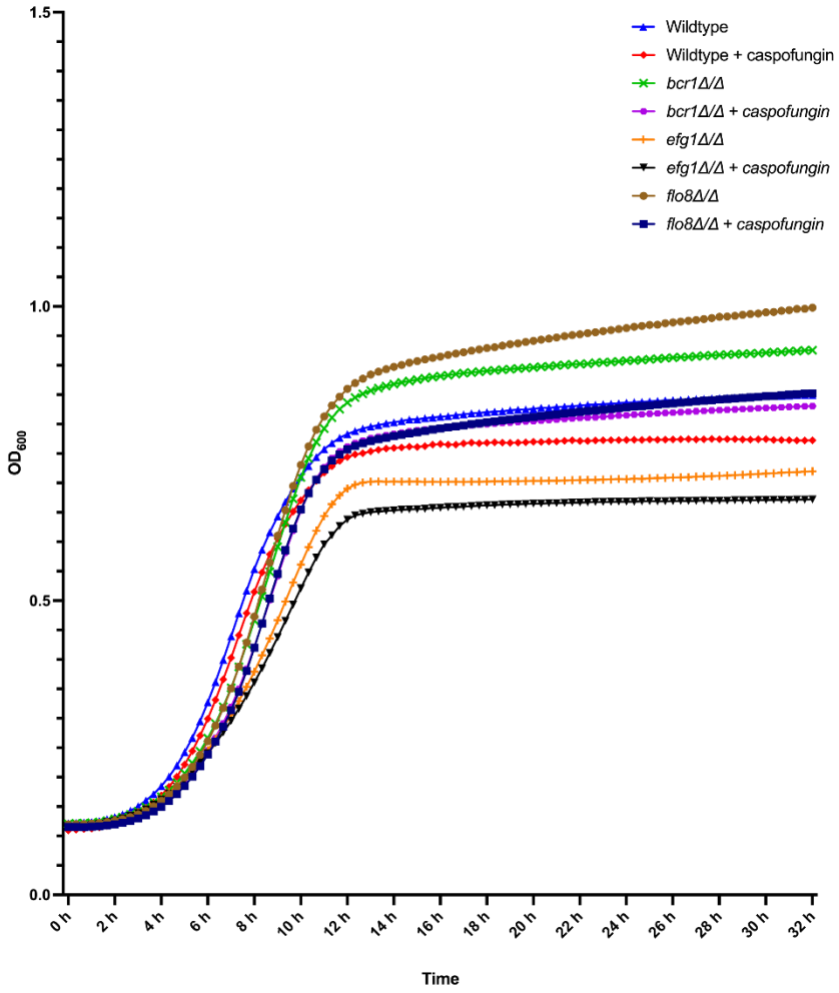

S Figure 1.2 Growth rate experiments of the wildtype and flocculation defective transcription factor mutant strains. Growth of the wildtype and flocculation defective transcription factor mutant strains was measured in RPMI-1640 alone and in the presence of 62.5 ng/mL caspofungin over 32 h. Twelve technical replicates were tested per experiment and the average of two biological replicates is presented.

RNA-sequencing of the wildtype and caspofungin treated transcription factor mutant strains identifies genes and pathways involved in flocculation

Next, we sought to explore the molecular mechanisms contributing to cell aggregation in response to caspofungin. The *C. albicans* genome contains approximately 6,000 protein coding genes and nearly 20% of these genes are unique to this pathogen (49, 50). To identify additional genes and pathways involved in adhesion, we performed single-

end 3' Tag-Seq on the wildtype and *bcr1*Δ/Δ, *efg1*Δ/Δ, and *flo8*Δ/Δ strains in the presence and absence of caspofungin.

Differential gene expression analysis of wildtype strain in the presence versus absence of caspofungin identified 149 genes significantly upregulated and 46 genes significantly downregulated in the presence of caspofungin (Figure 1.2, S Data 1). Many of the genes with significant fold changes were identified in previous studies (e.g., *PGA23*, *DDR48*, and *ALS1*) (34, 38), validating our sequencing approach. The cell wall encoding adhesin gene *ALS1* was significantly upregulated in the wildtype strain in response to caspofungin, yet we did not detect increases in expression for other *ALS* genes encoding other adhesins within the *ALS* gene family (S Data 1). Comparing the changes in gene expression of the *bcr1*Δ/Δ, *efg1*Δ/Δ, and *flo8*Δ/Δ mutant strains to the wildtype strain in the presence of caspofungin, *ALS1* was significantly downregulated in all deletion mutant strains (Figure 1.2, S Data 1). Furthermore, we identified three additional genes (*CFL11*, *RBT1*, and *ALS3*) that were significantly downregulated in the *bcr1*Δ/Δ, *efg1*Δ/Δ, and *flo8*Δ/Δ mutant strains relative to the wildtype strain, in the presence of caspofungin.

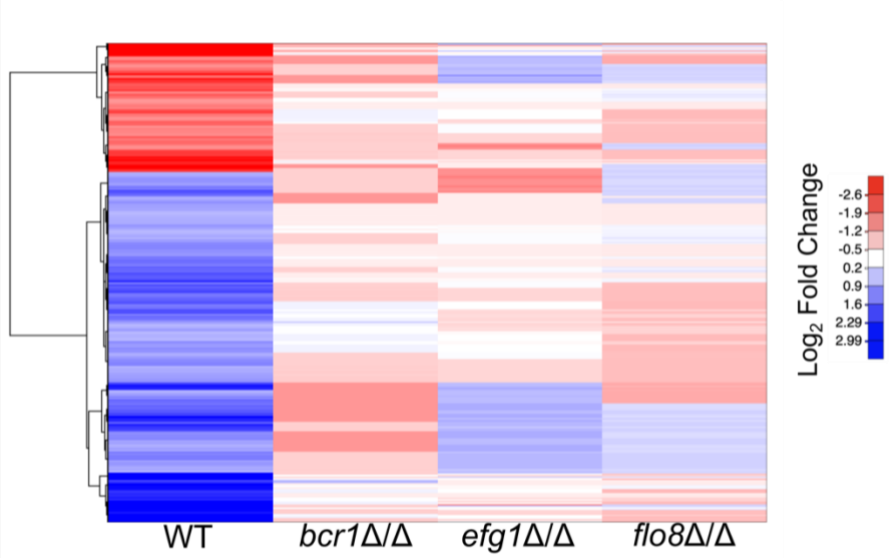

Figure 1.2 Differentially expressed genes of the wildtype and flocculation defective mutant strains. Heatmap of RNA-seq experiments to identify adhesins contributing to cell-cell aggregation. The left most column of the heatmap compares the wildtype in the presence of caspofungin to the untreated control. Each sequential column represents a different transcription factor deletion mutant strain under flocculation inducing conditions (i.e., in the presence of caspofungin) compared to the wildtype strain in the same condition.

To better understand the cellular processes associated with the upregulated genes, we performed Gene Ontology (GO) analysis for biological processes. We first compared the caspofungin treated wildtype to the untreated wildtype control, where we observed

enrichment for oxidation-reduction processes, cell wall-related metabolism, cell wall organization, and adhesion. This is consistent with the findings that *C. albicans* undergoes cell wall remodeling in response to caspofungin (34, 35, 38, 39). Furthermore, genes associated with metal ion transport and homeostasis related genes were significantly downregulated under these conditions. In comparison, *bcr1*Δ/Δ, *efg1*Δ/Δ, and *flo8*Δ/Δ deletion mutant strains did not have the same enrichment for adhesion or oxidation-reduction processes, suggesting that these regulators contribute to the regulation of these mechanisms during caspofungin exposure. This observation is consistent with previous findings that Efg1 contributes to cell wall remodeling upon caspofungin treatment (51, 52). Taken together, Bcr1, Efg1, and Flo8 contribute to the regulation of several processes (adhesion, oxidation reduction, and cell wall remodeling) in response to caspofungin treatment.

CFL11 is required for caspofungin-induced flocculation and initial adherence of biofilm cells

We next sought to identify other mediators of cell aggregation in response to caspofungin treatment. RNA-seq experiments identified *ALS1*, *ALS3*, *CFL11*, and *RBT1* as significantly downregulated genes in the flocculation defective transcription factor deletion mutant strains compared to the wildtype under flocculation inducing conditions. The *cfl11*Δ/Δ, *als1*Δ/Δ, and *als3*Δ/Δ strains were previously constructed in the isogenic (SN250) genetic background (53, 54), and we created an isogenic *rbt1*Δ/Δ strain in this study using CRISPR/Cas9. Als1 was previously identified as a mediator of caspofungin-induced flocculation, and its deletion mutant strain was consistently defective in cell-cell adhesion under these conditions (Figure 1.3A) (19). One additional mutant strain, *cfl11*Δ/Δ (*orf19.701*Δ/Δ), was defective in flocculation induced by caspofungin in this screen. This gene encodes an NADPH oxidase (NOX) enzyme with previously published roles in reactive oxygen species (ROS) production during hyphal development (55). Mutant strains lacking *CFL11* were unable to efficiently propagate and maintain hyphae *in vivo* and *in vitro*, linking H_2O_2 production to hyphal development.

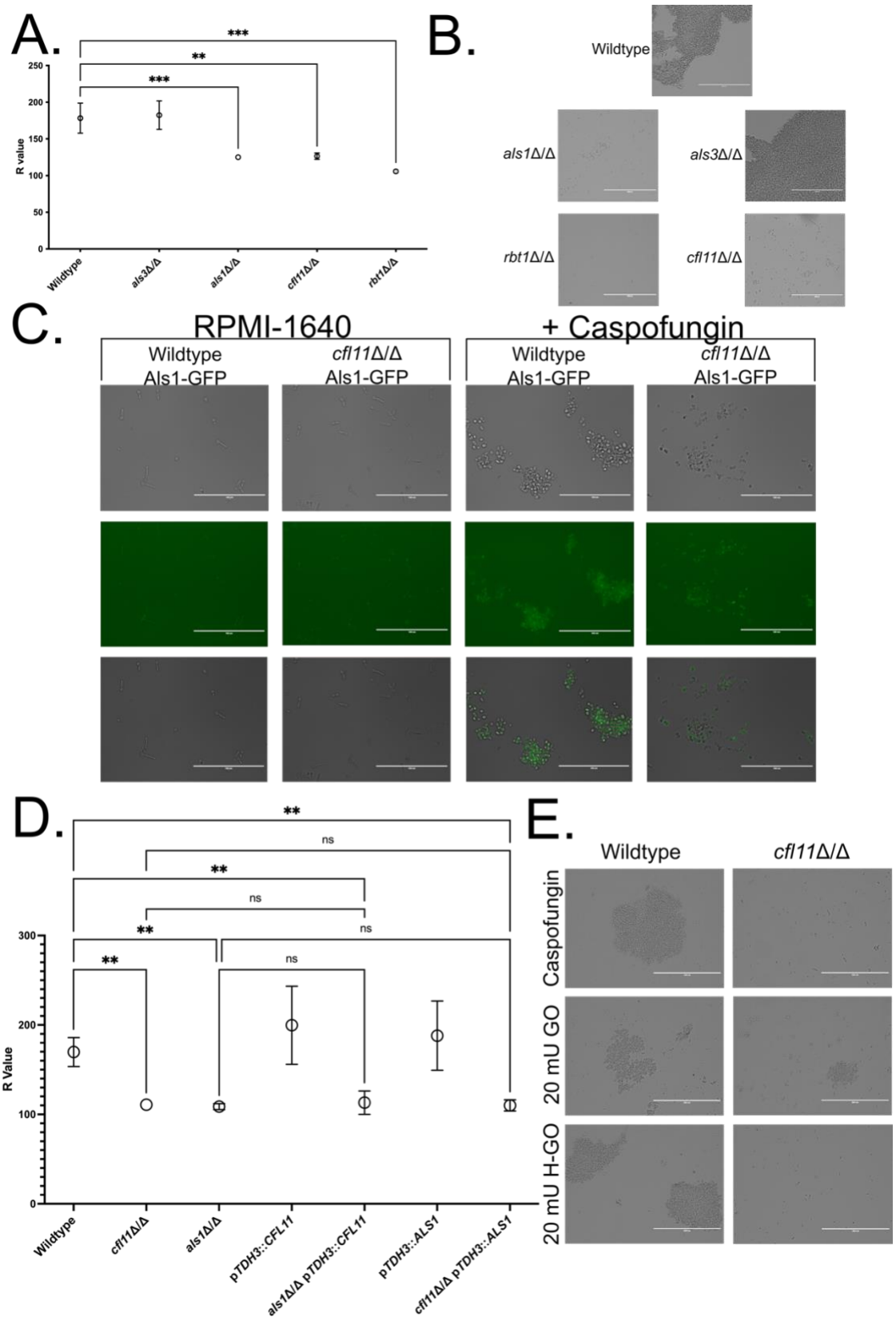
A.
R value
Wildtype
als3Δ/Δ
als1Δ/Δ
cfl11Δ/Δ
rbt1Δ/Δ
B.
Wildtype
als1Δ/Δ
als3Δ/Δ
rbt1Δ/Δ
cfl11Δ/Δ
C.
RPMI-1640
+ Caspofungin
Wildtype Als1-GFP
cfl11Δ/Δ Als1-GFP
D.
R Value
Wildtype
cfl11Δ/Δ
als1Δ/Δ
pTDH3::CFL11
als1Δ/Δ pTDH3::CFL11
pTDH3::ALS1
cfl11Δ/Δ pTDH3::ALS1
E.
Wildtype
cfl11Δ/Δ
Caspofungin
20 mU GO
20 mU H-GO

Figure 1.3 Cfl11 mediates adhesion through the production of reactive oxygen species. (A) Sedimentation experiment of target genes identified from RNA-seq experiments. The wildtype, *als1*Δ/Δ, *als3*Δ/Δ, and *cfl11*Δ/Δ strains were grown in 62.5 ng/mL caspofungin and the ability to flocculate was measured. Three biological replicates were tested and the average of the three is displayed. Statistical significance was determined with a two-tailed students t-test; p-value < 0.05 (*), < 0.01 (**), < 0.001 (***). (B) The wildtype, *als1*Δ/Δ, als3Δ/Δ, and cfl11Δ/Δ strains were incubated under flocculation inducing conditions and imaged with a bright field microscope at 20X magnification. Scale bar represents 200 μm. (C) Fluorescence and bright field microscopy of the wildtype and *cfl11*Δ/Δ Als1-GFP internally tagged strains grown in RPMI-1640 with and without 62.5 ng/mL caspofungin. GFP fluorescence was imaged with the GFP fluorescence channel, and all images were acquired with 20X magnification. Scale bar represents 200 μm. (D) The wildtype, *als1*Δ/Δ, *cfl11*Δ/Δ, *CFL11*^{OE}, *ALS1*^{OE}, *als1*Δ/Δ *CFL11*^{OE}, and *cfl11*Δ/Δ *ALS1*^{OE} strains were grown in RPMI-1640 for 3 h to induce flocculation and the degree of flocculation was measured. Three biological replicates were tested for each strain and the average of all experiments is presented. Statistical significance was determined with a two-tailed students t-test; p-value < 0.05 (*), < 0.01 (**), < 0.001 (***). (E) Bright field microscopy of the wildtype and *cfl11*Δ/Δ grown in RPMI-1640 supplemented with 1% glucose and 62.5 ng/mL caspofungin. 20 mU *Aspergillus niger* glucose oxidase (GO) was tested for the ability to complement the *cfl11*Δ/Δ deletion strain phenotype and 20 mU heat inactivated GO (H-GO) was included as a control.

We further sought to characterize the role of Cfl11 in adhesion. Als1 is a well characterized adhesin with roles in promoting adhesion to biotic and abiotic surfaces, and we reasoned that Cfl11 either interacts with Als1 or functions on its own. In eukaryotes, some NOX enzymes have regulatory roles that propagate signals affecting gene expression (56). We constructed an Als1-GFP tagged strain to further explore the impact of *cfl11*Δ/Δ on Als1 expression and function. Initially the GFP tag was inserted at the C-terminus using a RIPLING amino acid sequence linking Als1 to GFP as previously described (57), however C-terminal tagging of Als1 interfered with flocculation in the wildtype strain background (results not shown). As a result, we developed an Als1-GFP internal tag construct were GFP is flanked by a GSGG amino acid linker, and this construct was incorporated after amino acid position V1002. The V1002 position was selected because it occurs after the agglutinin-like sequence repeats annotated on the *Candida* Genome Database and was distant from the GPI-anchor motif. This Als1-GFP internal tag was incorporated in both the wildtype and *cfl11*Δ/Δ deletion mutant strains. Upon caspofungin treatment, the wildtype Als1-GFP internally tagged strain flocculated as expected (Figure 1.2C). Both the wildtype and *cfl11*Δ/Δ Als1-GFP strains exhibited bright GFP fluorescence in the caspofungin treatment condition and Als1-GFP properly localizes to the cell periphery. This suggests that *ALS1* is expressed at similar levels in the wildtype and *cfl11*Δ/Δ mutant and that Als1 localization is not dependent on Cfl11.

In previous work characterizing Cfl11, it was reported that the *cfl11*Δ/Δ strain is defective in an *in vivo* central venous rat catheter biofilm model yet it did not have the same defect under laboratory conditions (55). Having identified a role in cell-to-cell adhesion, we sought to further characterize the contribution of Cfl11 during biofilm development. We assessed initial biofilm adherence and biofilm development at 24 h of the wildtype, *cfl11*Δ/Δ, and *als1*Δ/Δ mutant strains. In both optical density and plating methods to measure adherence during the early stages of biofilm development, both the *cfl11*Δ/Δ and *als1*Δ/Δ strains were severely defective in initial adherence (S Figure 1.3). Taken together our results suggest that Cfl11 is important for early stages of biofilm development under laboratory conditions, yet dispensable at later time points.

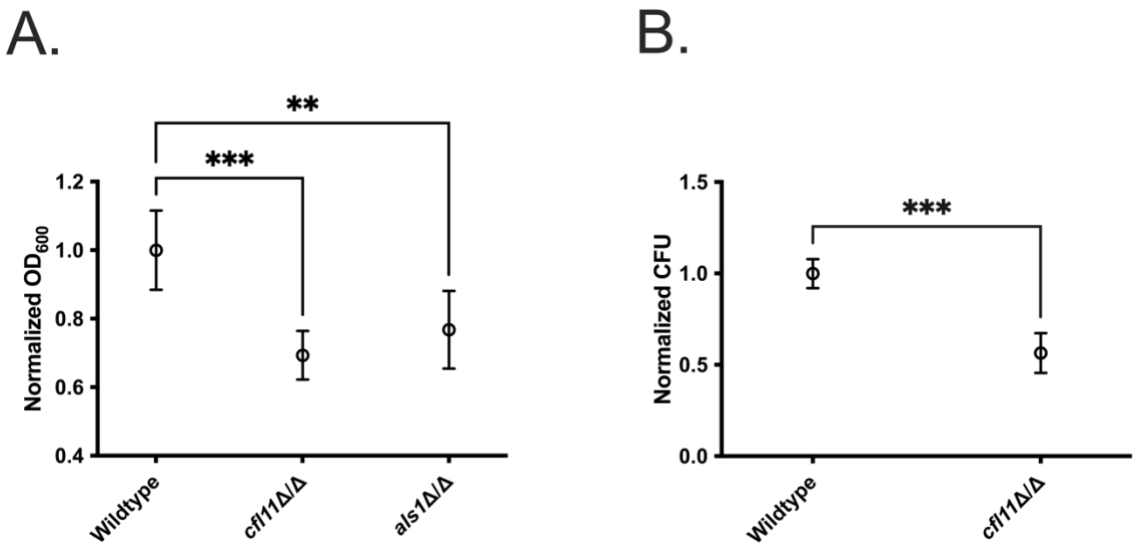

S Figure 1.3 CFL11 is required for initial biofilm adherence but is dispensable for other stages of biofilm formation in vitro (A) Measurement of overall cell attachment after 90 min incubation by scanning optical density readings. Each experiment included six technical replicates per strain and was repeated on two occasions. Optical density readings were normalized to the wildtype values and significance was determined with a two-tailed students t-test; p-value < 0.05 (*), < 0.01 (**), < 0.001 (***). (B) Measurement of the overall cell attachment after 90 min incubation by diluting, plating, and enumerating resulting colonies. Attached cells were vigorously scraped and diluted $2 * 10^5$ across four technical replicates; two biological replicates were performed, and the average results are presented. Statistical significance was determined with a two-tailed students t-test; p-value < 0.05 (*), < 0.01 (**), < 0.001 (***).

To better characterize a possible relationship between Cfl11 and Als1, we overexpressed *CFL11* and *ALS1* in the wildtype and in their deletion mutant strain backgrounds. Overexpression strains were constructed with CRISPR/Cas9 using a gRNA targeting NEUT5L and an overexpression cassette with the *TDH3* promoter and *ACT1* terminator driving expression of the gene of interest flanked between 300 bp up and

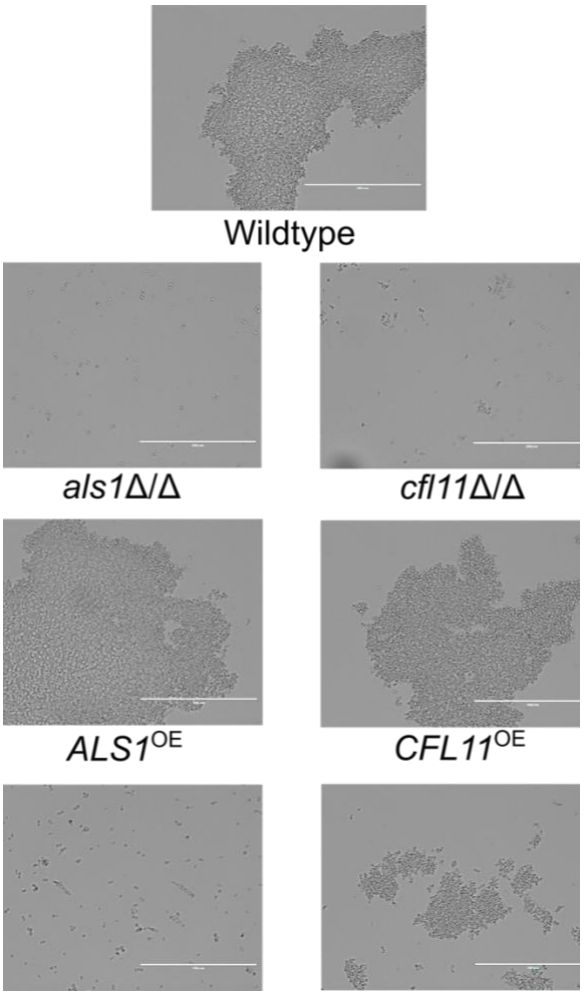

S Figure 1.4 Brightfield microscopy of ALS1 and CFL11 overexpression strains reveals an Als1-Cfl11 co-dependency. Evaluation of the overexpression mutant strains in Figure 1.3D by bright field microscopy. Scale bar represents 200 μm.

downstream homology to NEUT5L. Both *CFL11* and *ALS1* were overexpressed in the wildtype and opposing deletion mutant strain, creating wildtype *ALS1*^{OE} and *cfl11*Δ/Δ *ALS1*^{OE} strains in addition to wildtype *CFL11*^{OE} and *als1*Δ/Δ *CFL11*^{OE} strains. Under flocculation inducing conditions, the wildtype strains overexpressing either *ALS1* or *CFL11* had increased flocculation relative to the isogenic wildtype strain (Figure 1.3D, S Figure 1.4). The *cfl11*Δ/Δ *ALS1*^{OE} and *als1*Δ/Δ *CFL11*^{OE} strains, however, did not flocculate in the presence of caspofungin. This was confirmed with brightfield microscopy. We note that the *cfl11*Δ/Δ *ALS1*^{OE} strain does have a partial improvement in adhesion relative to the *cfl11*Δ/Δ strain, but the cell masses are limited in size relative to the wildtype strain (S Figure 1.4). These results suggest a co-dependence between Cfl11 and Als1 contributing to adhesion.

Cfl11 functions by creating reactive oxygen bursts at the cell surface enabling hyphal and biofilm development *in vivo* and the hyphal defect of the *cfl11*Δ/Δ mutant can be complemented with the addition of ROS forming enzymes (55). We used *Aspergillus niger* glucose oxidase (GO), an enzyme that metabolizes glucose to create H_2O_2 bursts. The wildtype, *cfl11*Δ/Δ, and *als1*Δ/Δ deletion mutants were grown in flocculation inducing media with either 20 mU/mL GO or 20 mU/mL heat inactivated GO. Growth of the *cfl11*Δ/Δ deletion strain in media with caspofungin and GO partially restored cell-to-cell adhesion and the heat inactivated GO condition resulted in predominantly diffuse cells that were not attached (Figure 1.3E). These results together suggest that Cfl11 contributes to cell aggregation through the development of ROS which appear to be important for Als1 function.

PGA23 provides protection to cell stress and is essential for the caspofungin response

We next sought to identify additional cell surface adhesins involved in the caspofungin response. Towards the identification of adhesion related genes, we filtered the differential expression results for genes encoding proteins that cell surface localize or have secretion signals. The top ten differentially expressed genes were selected for further study, (*PGA31*, *LDG2*, *LDG3*, *LDG4*, *PGA23*, *CRH11*, *MNN1*, and *ORF19.675*). Deletion mutants for these genes, however, did not result in flocculation defects, yet we did note that some settled faster than the wildtype strain, suggesting that cell death may be occurring in these strains (Data not shown). We further screened the gene deletion mutants in growth rate experiments in the presence and absence of caspofungin over the course of 32 hours and measured the rate of exponential growth to quantitatively assess differences in growth rates. The *pga23*Δ/Δ (*orf19.3470*Δ/Δ) and *crh11*Δ/Δ mutant strains had significantly

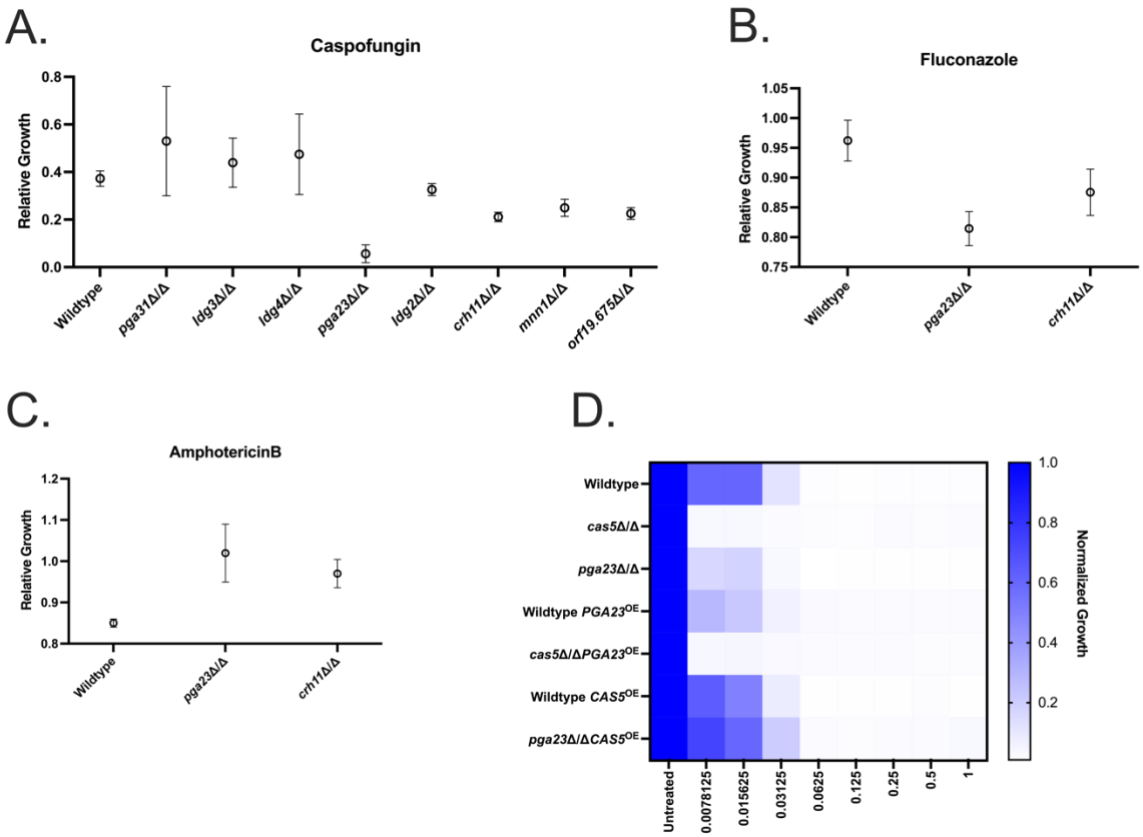

Figure 1.4 Pga23 is a cell surface protein critical for the response to caspofungin. Target gene deletion mutants were diluted in RPMI-1640 in a 384 well plate and grown in the presence and absence of (A) 62.5 ng/mL caspofungin, 32 h. The rate of exponential growth was calculated with the Growth Rates Made Easy software package *(1)*. Six replicates were included per experiment and the relative growth was determined by averaging the unpaired ratios of the treated strain over the untreated control. The average of these results across two experiments is presented. The wildtype, *pga23*Δ/Δ, and *crh11*Δ/Δ mutant strains growth were assessed in the presence of (B) 0.2 μg/mL fluconazole, and (C) 2 μg/mL amphotericinB for 32 h shaking and were analyzed similarly in Fig 4A. (D) Caspofungin susceptibility assay of the wildtype, *pga23*Δ/Δ, *cas5*Δ/Δ, and overexpression strains. Caspofungin was made at a stock concentration of 2 μg/mL and serially diluted 1:1 eight times and diluted C. albicans strains were added in a 1:1 ratio. Two technical replicates were tested for each biological replicate and the average of two biological replicates is presented.

impaired growth in the presence of caspofungin (Figure 1.4A). Intrigued by the response to caspofungin, we tested the *pga23*Δ/Δ and *crh11*Δ/Δ mutant strains in the presence of fluconazole (Figure 1.4B) and amphotericin B (Figure 1.4C), representative antifungal drugs from the azole and polyene drug classes, respectively. Under these growth conditions, the *pga23*Δ/Δ deletion mutant had reduced growth in the presence of

fluconazole. Deletion of *PGA23* results in diminished growth in the presence of the two antifungal drugs, and thus this it is likely a general cell stress responsive gene.

The *pga23*Δ/Δ phenotype in the presence of caspofungin (Figure 1.4A) resembles the published results of the *cas5*Δ/Δ mutant phenotype under similar conditions (38, 58). Experiments measuring RNA PolII occupancy found significantly decreased occupancy in a *cas5*Δ/Δ mutant in the presence of caspofungin compared to the wildtype at the *PGA23* locus, indicating a direct regulatory relationship between Cas5 and Pga23 during caspofungin treatment (38). We asked whether increased expression of *PGA23* can overcome caspofungin hypersensitivity in a *cas5*Δ/Δ mutant by constructing wildtype and *cas5*Δ/Δ strains overexpressing *PGA23*. Overexpressing *PGA23* in the wildtype strain results in increased susceptibility to caspofungin compared to the isogenic wildtype strain, and overexpression of *PGA23* in the *cas5*Δ/Δ strain does not complement the loss of the transcription factor (Figure 1.4D). Interestingly, overexpression of *CAS5* in the *pga23*Δ/Δ strain complements the phenotype, thus there are likely unidentified Cas5-dependent genes that can complement *PGA23* when expressed at high levels.

Flocculation in response to Caspofungin is conserved across the Candida clade

Echinocandin compounds are widely used to treat not just *C. albicans*, but other pathogenic *Candida* species and are frequently used to treat azole resistant *Candida glabrata* infections. We asked if the caspofungin-induced aggregation observed in *C. albicans* is conserved in other *Candida* species. Towards this we used a library of clinical isolates from the Center for Disease Control's Antimicrobial Resistance Isolate bank. This library includes isolates from clinically important *Candida* clade species that encode the CUG codon as serine instead of leucine (e.g. *Candida tropicalis, Candida parapsilosis, Candida lusitaniae, Candida auris*) (59) and related species that are phylogenetically positioned outside of the *Candida* clade (*Candida krusei* and *Candida glabrata*). We

assessed the ability of these clinical isolates to aggregate in response to caspofungin and examined both echinocandin-sensitive and resistant isolates if available.

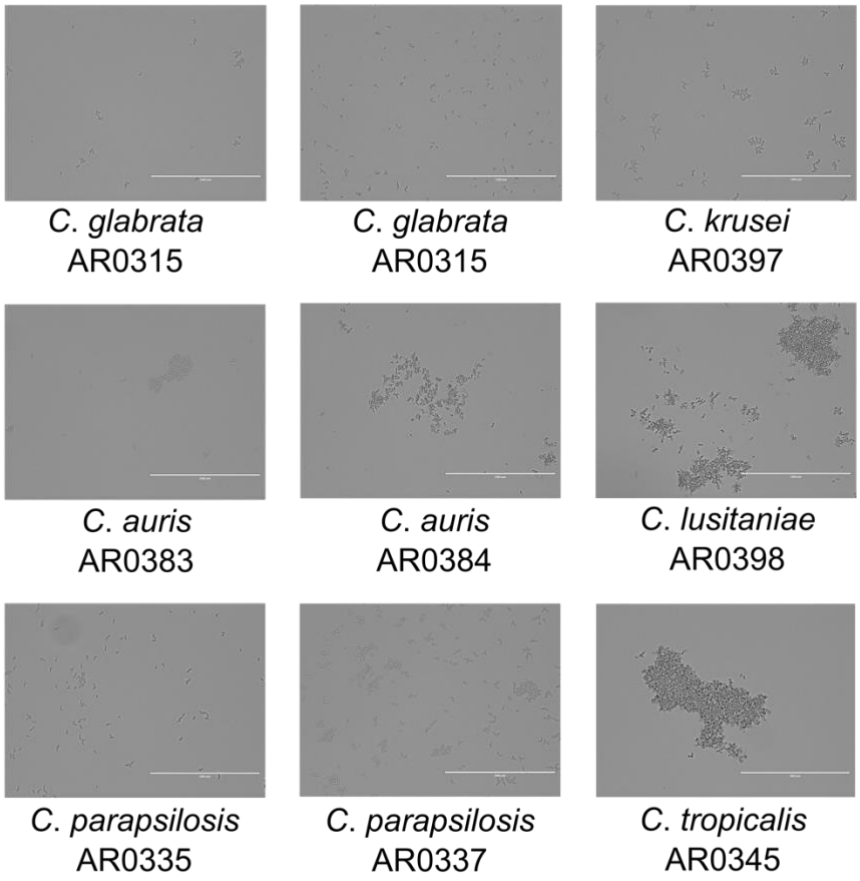

Figure 1.5 Conservation of the flocculation response across *Candida* species. Brightfield microscopy of clinical isolates of *Candida* species from the Center for Disease Control Antimicrobial Resistance Isolate Library. *Candida* species were grown under flocculation inducing conditions with 62.5 ng/mL caspofungin for 3 h. Cells were washed and transferred to slides and imaged with 20 X magnification. Scale bar represents 200 μm.

We did not identify flocculation in either *C. glabrata* or *C. krusei* species (Figure 5). We did however identify that several *Candida* clade species flocculate in response to caspofungin. *C. tropicalis* and *C. lusitaniae* formed large cell masses in response to caspofungin treatment similar to *C. albicans* (Figure 1.1B and 1.5). Both *C. auris* and *C. parapsilosis* formed small aggregates, yet not to the same magnitude as *C. albicans*, *C. tropicalis*, and *C. lusitaniae*. The aggregation in response to caspofungin appears to be pervasive within the *Candida* clade species, yet variation exists between and within species.

1.4 Discussion

Here we present a genetic screen identifying Bcr1 and Flo8 as additional regulators of cell aggregation in response to caspofungin. Using RNA-seq we identified a novel role for Cfl11 in cell-cell adhesion expanding the known roles of this protein and our results suggest it is important for the function of Als1. Lastly, we identified critical cell surface proteins (Pga23 and Crh11) that mediate the response to caspofungin and deletion of either *PGA23* or *CRH11* results in hypersensitivity to the drug.

Genome-wide screens using transcription factor deletion mutants has been an effective method for identifying *C. albicans* regulatory pathways and downstream target genes. Using such methods, we identified two new regulators of caspofungin-induced cell aggregation, Bcr1 and Flo8. These findings are in line with other studies that have identified Bcr1, Efg1, and Flo8 as regulators of initial cell attachment, biofilm maturation, and aggregation in response to anaerobic bacteria (20, 24, 31, 53). It is not particularly surprising that these regulators control adhesion in this context, however their contribution to aggregation in response to cell stress is novel. Growth within the biofilm state provides protection from chemical perturbation and aggregation may be a mechanism to protect cells from chemical stress.

Testing significantly downregulated target genes shared by the *bcr1*Δ/Δ, *efg1*Δ/Δ, and *flo8*Δ/Δ strains, we confirmed a role for Als1 in flocculation and identified a novel contributor, Cfl11. Our findings suggest a unique link between the development of ROS and adhesion. A previous study linked the propagation of hyphae to ROS creation (54), yet a connection to adhesion has not been described. Under laboratory conditions, *CFL11* is dispensable for biofilm maturation yet is required for initial adherence (S Figure 1.3); however *in vivo CFL11* is critical for biofilm development (54). We hypothesize that functionally redundant enzymes complement *CFL11* under laboratory conditions, yet this gene is essential for biofilm development within the host. A number of genes with putative oxidoreductase activity (e.g. *orf19.1473*, *CFL2*, *CFL4*, *CFL5*, and *SOD4*) were upregulated in the wildtype, *bcr1*Δ/Δ, *efg1*Δ/Δ, and *flo8*Δ/Δ mutant strain (S Data 1) all of which are upregulated in mature biofilms with the exception of *ORF19.1473* (53). Our RNA-seq results also suggest a regulatory relationship between Bcr1, Efg1, and Flo8 contributing to the positive regulation of *CFL11*, although *CFL11* was not directly bound by these TFs in previously published genome-wide binding studies (53, 61). Therefore, the TFs directly regulating *CFL11* remain elusive or may be dependent on the host niche or growth condition. Intriguingly, Cfl11 is unique to *C. albicans*, *C. dubliniensis*, and *C. tropicalis*, with more distantly related *Candida* species lacking an ortholog, although Als1 orthologs are found in several *Candida* species. It is possible other conserved enzymes with oxidoreductase activity are catalyzing the creation of ROS species within the context of adhesion. Given its localization on the cell surface and importance for biofilm development, Cfl11 and other ROS producing enzymes may be promising biofilm specific therapeutic targets.

Searching for additional cell surface adhesins, we serendipitously identified genes required for the response to caspofungin. Testing these gene deletion mutants for growth in caspofungin containing media, the *pga23*Δ/Δ strain exhibited severe hypersensitivity. In the presence of caspofungin, *C. albicans* upregulates cell surface genes many of which are

regulated by the transcription factor Cas5, and *PGA23* is no exception (33, 37). A screen for haploinsufficiency in the presence of four antifungal drug classes found loss of one copy of *PGA23* resulted in minor sensitivity to the antifungal, amphotericin B (62). Our findings in conjunction with published works suggests Pga23 is a generalist that contributes broadly to ameliorate *C. albicans* cell stress. Presently the function of Pga23 is unclear, however we suspect it may be involved in cell wall remodeling, maintenance, and/or integrity. Putative orthologs of Pga23 are present in most *Candida* species (i.e. *Candida dubliniensis*, *Candida tropicalis*, and *Candida parapsilosis*), however an ortholog was not identified in more distantly related species, such as the emergent pathogen, *Candida auris* (29).

A final question that remains unanswered is why *C. albicans* and related species flocculate in response to cell wall stress. We present two hypotheses. In the first, adhesion may be a mechanism of protection for stressed cells. This could be an example of altruism, a behavior that is costly to perform at the individual level, but that benefits the population (63). Within the context of flocculation, the upregulation of adhesins may be a mechanism to protect cells within the inner masses from cell stress while the outermost ones succumb to treatment. In theory, this would allow the surviving cells in the center to propagate once antifungal treatment has ended. Other forms of altruism are seen in viruses and bacteria, and it has been proposed that biofilms generally promote altruistic behaviors (64, 65). Interestingly, however, flocculation defective mutant strains do not have significantly impaired growth, suggesting that the protective mechanism is dispensable. An additional hypothesis is that flocculation is a specific feature of caspofungin treatment, rather than a survival mechanism. Under treatment of sublethal antibiotic concentrations within a zebrafish gut, bacterial species *Vibrio cholera* and *Enterococcus cloacae* aggregate resulting in a gel-like mass that is more effectively expelled from the host compared to free-floating cells (27). Caspofungin is a frequently administered to individuals with severe *Candida* infections. Aggregation in *C. albicans* may be a mechanism in which the cells are more effectively expelled from the body. Both scenarios are not mutually exclusive and provide interesting, testable hypotheses that can aid in better understanding of microbial behaviors and their mechanisms of action during treatment with this important antifungal drug.

In sum, we further our understanding of the molecular mechanisms underlying adhesion and cell wall stress response in a clinically important fungal pathogen. Together these findings present potential mechanisms by which to prevent and treat life threatening *C. albicans* infections.

1.5 Methods

Media and Solutions

All *Candida spp.* strains were plated on YPD (2% Bacto Peptone, 2% Dextrose, 1% Yeast Extract) and incubated at 30 °C. A single colony was selected and inoculated in 4 mL YPD and grown overnight shaking at 30 °C. *C. albicans* CRISPR/Cas9 transformants were selected for on YPD+clonNAT200 (YPD + 200 μg/mL nourseothricin). Removal of CRISPR/Cas9 components was performed by streaking edited C. albicans cells on SD lacking leucine (2% Dextrose, 6.7% YNB with ammonium sulfate, and auxotrophic

supplements). Flocculation experiments were performed with RPMI-1640 without sodium bicarbonate and buffered with MOPS. Caspofungin was a kind gift from Merck.

Strains and Mutant Construction

The *Candida albicans* strains utilized in this study are listed in Table S1, except for the transcription factor mutant library, select target genes [SN274 (*cfl11*Δ/Δ), STT82 (*als1*Δ/Δ), and STT200 (*orf19.3499*Δ/Δ)], transcription factor complementation strains [CJN2318 (*EFG1*), CJN2322 (*BCR1*), CJN2813 (*FLO8*)], and the respective wildtypes (SN250 and SN425). These strains were constructed for previous studies (40, 52, 53). Strains created for this study were created in their isogenic background (SN250) utilizing markerless CRISPR/Cas9 mediated genome editing as previously published (57). Briefly, a 20bp guide RNA (gRNA) was selected and utilized to direct Cas9 to the locus of interest. Donor DNA (dDNA) with 50 bp or greater homology to the *C. albicans* genome was provided to repair the double strand break. Cells were plated on YPD + clonNAT200 to select for colonies that integrated the Cas9 and gRNA constructs and individually transformed colonies were verified by PCR for the correct genome modification. Colonies with the correct deletion or integration were plated on SC media lacking leucine to remove CRISPR components and *NAT* resistance markers. Colonies that grew on SC media lacking leucine were tested to confirm that *NAT* resistance was lost and were stored at -80 °C. A complete list of primers used for creation of *C. albicans* strains can be found in File S2.

Gene deletion strains CEC24 (*orf19.675*Δ/Δ), CEC25 (*pga23*Δ/Δ), CEC26 (*crh11*Δ/Δ), CEC27 (*orf19.6484*Δ/Δ), CEC30 (*orf19.6486*Δ/Δ), CEC46 (*orf19.6487*Δ/Δ), CEC91 (*mnn1*Δ/Δ), and DLR80 (*orf19.5302*Δ/Δ) were created with CRISPR/Cas9 and the gene was replaced with a 23 bp AddTag sequence (CGAGACGAGTGCTCGACATGAGG) described in several studies for facile complementation of the wildtype allele to the native locus (57, 66).

The internal Als1-GFP tagged strains (CEC12 and CEC13) were created in the wildtype (SN250) and *cfl11*Δ/Δ mutant (SN274) respectively. Donor DNA to integrate GFP was amplified with primers from pCE1 which contains *Candida* optimized monomeric GFP. This created donor DNA with > 50 bp homology to the *ALS1* open reading frame and a GSGG amino acid linker sequence to integrate GFP. The GFP and flanking GSGG linkers were integrated after V1002 to create an internal Als1-GFP tag. Correct integration of GFP at the *ALS1* locus was confirmed by colony verification with primers amplifying across flanking integration sites.

Overexpression mutant strains CEC107 (p*TDH3*::*CFL11*), CEC109 (*als1*Δ/Δ p*TDH3*::*CFL11*), CEC118 (p*TDH3*::*ALS1*), CEC120 (p*TDH3*::*PGA23*), CEC121 (*cfl11*Δ/Δ p*TDH3*::*ALS1*), CEC122 (*cas5*Δ/Δ p*TDH3*::*PGA23*), CEC184 (p*TDH3*::*CAS5*) and CEC185 (*pga23*Δ/Δ p*TDH3*::*CAS5*) were created as follows. Over expression construct pMQ14 which utilizes the *TDH3* promoter and *ACT1* terminator flanked between 300 bp of homology to *C. albicans* NEUT5L to overexpress the gene of interest at a neutral locus. This expression construct was digested with *Bgl*II and *Eco*52I and amplified. Genes of interest (*PGA23*, *ALS1*, *CFL11*, and *CAS5*) were amplified from genomic DNA with > 20 bp flanking homology to linearized pMQ14 and circularized by gap repair with chemically competent *E. coli* creating pCE37 (*CFL11*), pCE39 (*PGA23*), pCE40 (*ALS1*),

and pCE42 (*CAS5*). Over expression plasmids and NEUT5L gRNA (pADH143-23) plasmids were digested with *Mss*I creating dDNA and gRNA for transformation. Integration of the overexpression construct was confirmed by PCR colony verification of the integration sites.

Complementation of the *cfl11*Δ/Δ and *pga23*Δ/Δ deletion strains utilized the overexpression plasmids pCE37 and pCE39 respectively to overexpress *CFL11* and *PGA23* in their respective deletion background. Both the dDNA and gRNA plasmid (pADH143-23) were *Mss*I digested and transformed as described creating strains CEC### (*cfl11*Δ/Δ $CFL11^{OE}$) and CEC### (*pga23*Δ/Δ $PGA23^{OE}$).

Flocculation Assay

The flocculation assay was performed as described previously with minor modifications (18). Briefly, we measured the OD_{600} of *Candida* species overnight culture and diluted in RPMI 1640 + 62.5 ng/mL caspofungin to an OD_{600} of 0.3. Diluted cultures were placed at 30 °C shaking for 3 h. Subsequently cultures were vigorously mixed, and 1 mL was transferred to a clean cuvette and OD_{600} was measured (OD_1). Cuvettes were left at room temperature for 15 min to allow cells to settle and the OD_{600} was measured again (OD_2). The two OD values obtained (OD_1 and OD_2) were used to calculate the degree of flocculation (R value) where $R = (OD_1 \times 100)/(OD_2)$. Three biological replicates were tested for each individual strain and significance was determined with a two-tailed t-test at a significance cutoff of $p < 0.05$.

Glucose oxidase rescue experiments

Experiments assaying the ability of recombinant glucose oxidase to rescue flocculation were performed as follows. Overnight *C. albicans* optical density was measured and cells diluted in RPMI-1640 supplemented with 1% glucose. Recombinant Type VII *Aspergillus niger* glucose oxidase (GO) (Sigma Aldrich, Catalog G2133-10KU) was added at a concentration of 20 mU/mL. Heat inactivated (H-GO) was included as a control for GO activity. Diluted cells in GO or H-GO containing media were incubated at 30 C shaking for 3 h and flocculation was assessed by bright field microscopy at 20X magnification.

Growth Rates Experiment

Overnight culture was diluted 1:10 into RPMI-1640 and cell density measured by optical density readings at OD_{600}. Cells were further diluted to 10^5 CFU/mL and diluted 3:4 in RPMI or RPMI containing 62.5 ng/mL caspofungin. All growth rates experiments were performed in 384-well plates with six or twelve replicates per strain and condition in each plate. Plates were incubated at 30 °C with linear shaking and optical density readings were measured every twenty minutes over the course of thirty-two hours in a Biotek Cytation5 Cell Imaging Multi-Mode Reader. Growth rates were calculated with the Growth Rates Made Easy package (67).

Microscopy

Samples prepared for bright field and fluorescence microscopy were grown at 30 °C shaking in RPMI-1640 supplemented with 62.5 ng/mL caspofungin for 3 h. Samples were

washed and resuspended in sterile water and transferred to a poly-L-lysine coated slide. Brightfield and fluorescence microscopy images were acquired on an EVOS® FL Cell Imaging System (Thermo Fisher Scientific). Als1-GFP strains were imaged using the GFP channel. All images were acquired using the 20X objective.

Adherence Assay

Optical density and diluting and plating adherence assays were performed as previously published (68, 69). Briefly overnight cell culture was diluted to an OD_{600} of 0.5 in a 96 well polystyrene plate with RPMI-1640 buffered with MOPS. Cells were allowed to adhere to the surface for 90 minutes shaking at 250 rpm at 37 °C in an ELMI Shaker. Wells were washed twice with 1X PBS to remove non-adhered cells. For the optical density adherence assay, OD_{600} 5x5 area scans of the washed wells were measured and averaged for each well, with six replicates included per experiment. For CFU enumeration, attached cells were scraped from the surface of each well and serially diluted $2 * 10^5$ in PBS and plated on YPD.

RNA-seq Cell Harvesting and Analysis

The optical density of overnight culture was measured as previously described. Flasks with RPMI and caspofungin were inoculated with strains to an optical density of 0.1 and incubated at 30 °C for 3 h shaking. Samples were centrifuged and media decanted. The remaining cell pellet was snap frozen with liquid nitrogen and stored at -80 °C. Two biological replicates were collected for each strain and condition. RNA was extracted using the RiboPure RNA Purification Kit for yeast (Invitrogen). 500 ng total RNA was prepared for mature poly(A) RNA selection for 100 bp single-end sequencing using QuantSeq 3' mRNA-seq Library Prep Kit FWD (Lexogen). Samples were sequenced on an Illunima HiSeq 4000 by the UC Davis Genome Center. Poor quality reads and adapters were trimmed with bbduk (version 38.87 [https://jgi.doe.gov/data-and-tools/bbtools/bb-tools-user-guide/bbmap-guide/]) and the trimmed read files were mapped to the assembly 21 SC5314 genome and gene counts quantified using STAR (version 2.7.4.a (70)). Differentially expressed genes were identified with the limma (version 3.33.0 (71)) and edgeR (version 3.14 (72)) software packages in R (version 3.6.3 (73)). Genes with a Log_2 fold change $> | \pm 1.5 |$ and an adjusted p value < 0.05 were considered differentially expressed. Gene ontology analysis was performed with the differential gene expression results using computationally and manually curated gene ontology terms available on the Candida Genome Database (CGD) (74, 75). Using a lower threshold of differential regulation of a Log_2 fold change $> | \pm 0.5 |$ enabling the capture of additional biological processes.

1.6 References

1. Nobile CJ, Johnson AD. 2015. Candida albicans biofilms and human disease. Annual review of microbiology 69:71-92.
2. Romo JA, Kumamoto CA. 2020. On Commensalism of Candida. J Fungi (Basel) 6.

3. Stamm WE. 1991. Catheter-associated urinary tract infections: epidemiology, pathogenesis, and prevention. The American journal of medicine 91:S65-S71.
4. Sangeorzan JA, Bradley SF, He X, Zarins LT, Ridenour GL, Tiballi RN, Kauffman CA. 1994. Epidemiology of oral candidiasis in HIV-infected patients: colonization, infection, treatment, and emergence of fluconazole resistance. The American journal of medicine 97:339-346.
5. Pfaller MA, Diekema DJ. 2007. Epidemiology of invasive candidiasis: a persistent public health problem. Clinical microbiology reviews 20:133-163.
6. Leroy O, Gangneux JP, Montravers P, Mira JP, Gouin F, Sollet JP, Carlet J, Reynes J, Rosenheim M, Regnier B, Lortholary O, AmarCand Study G. 2009. Epidemiology, management, and risk factors for death of invasive Candida infections in critical care: a multicenter, prospective, observational study in France (2005-2006). Crit Care Med 37:1612-8.
7. Lohse MB, Gulati M, Johnson AD, Nobile CJ. 2018. Development and regulation of single-and multi-species Candida albicans biofilms. Nature Reviews Microbiology 16:19-31.
8. Nobile CJ, Mitchell AP. 2007. Microbial biofilms: e pluribus unum. Current Biology 17:R349-R353.
9. McCall AD, Pathirana RU, Prabhakar A, Cullen PJ, Edgerton M. 2019. Candida albicans biofilm development is governed by cooperative attachment and adhesion maintenance proteins. NPJ biofilms and microbiomes 5:1-12.
10. Gulati M, Nobile CJ. 2016. Candida albicans biofilms: development, regulation, and molecular mechanisms. Microbes and infection 18:310-321.
11. Zarnowski R, Westler WM, Lacmbouh GA, Marita JM, Bothe JR, Bernhardt J, Lounes-Hadj Sahraoui A, Fontaine J, Sanchez H, Hatfield RD. 2014. Novel entries in a fungal biofilm matrix encyclopedia. MBio 5:e01333-14.
12. Nobile CJ, Nett JE, Hernday AD, Homann OR, Deneault J-S, Nantel A, Andes DR, Johnson AD, Mitchell AP. 2009. Biofilm matrix regulation by Candida albicans Zap1. PLoS biology 7:e1000133.
13. Nobile CJ, Fox EP, Hartooni N, Mitchell KF, Hnisz D, Andes DR, Kuchler K, Johnson AD. 2014. A histone deacetylase complex mediates biofilm dispersal and drug resistance in Candida albicans. MBio 5:e01201-14.
14. Uppuluri P, Acosta Zaldívar M, Anderson MZ, Dunn MJ, Berman J, Lopez Ribot JL, Köhler JR. 2018. Candida albicans dispersed cells are developmentally distinct from biofilm and planktonic cells. MBio 9:e01338-18.
15. Cowen LE, Sanglard D, Howard SJ, Rogers PD, Perlin DS. 2014. Mechanisms of Antifungal Drug Resistance. Cold Spring Harb Perspect Med 5:a019752.
16. Bachmann SP, VandeWalle K, Ramage G, Patterson TF, Wickes BL, Graybill JR, Lopez-Ribot JL. 2002. In vitro activity of caspofungin against Candida albicans biofilms. Antimicrob Agents Chemother 46:3591-6.
17. Abruzzo GK, Flattery AM, Gill CJ, Kong L, Smith JG, Pikounis VB, Balkovec J, Bouffard A, Dropinski J, Rosen H. 1997. Evaluation of the echinocandin antifungal MK-0991 (L-743,872): efficacies in mouse models of disseminated aspergillosis, candidiasis, and cryptococcosis. Antimicrobial Agents and Chemotherapy 41:2333-2338.

18. Gregori C, Glaser W, Frohner IE, Reinoso-Martín C, Rupp S, Schüller C, Kuchler K. 2011. Efg1 controls caspofungin-induced cell aggregation of Candida albicans through the adhesin Als1. Eukaryotic cell 10:1694-1704.
19. Cleary I, MacGregor N, Saville S, Thomas D. 2012. Investigating the Function of Ddr48p in Candida albicans. Eukaryotic cell 11:718-724.
20. Fox E, Cowley E, Nobile C, Hartooni N, Newman D, Johnson A. 2014. Anaerobic bacteria grow within Candida albicans biofilms and induce biofilm formation in suspension cultures. Current biology 24:2411-2416.
21. Staab JF, Bradway SD, Fidel PL, Sundstrom P. 1999. Adhesive and mammalian transglutaminase substrate properties of Candida albicans Hwp1. Science 283:1535-1538.
22. Nobile CJ, Schneider HA, Nett JE, Sheppard DC, Filler SG, Andes DR, Mitchell AP. 2008. Complementary adhesin function in C. albicans biofilm formation. Current biology 18:1017-1024.
23. Nobile CJ, Andes DR, Nett JE, Smith Jr FJ, Yue F, Phan Q-T, Edwards Jr JE, Filler SG, Mitchell AP. 2006. Critical role of Bcr1-dependent adhesins in C. albicans biofilm formation in vitro and in vivo. PLoS pathogens 2:e63.
24. Finkel JS, Xu W, Huang D, Hill EM, Desai JV, Woolford CA, Nett JE, Taff H, Norice CT, Andes DR. 2012. Portrait of Candida albicans adherence regulators. PLoS pathogens 8:e1002525.
25. Soares EV. 2011. Flocculation in Saccharomyces cerevisiae: a review. J Appl Microbiol 110:1-18.
26. Sampermans S, Mortier J, Soares EV. 2005. Flocculation onset in Saccharomyces cerevisiae: the role of nutrients. J Appl Microbiol 98:525-31.
27. Schlomann BH, Wiles TJ, Wall ES, Guillemin K, Parthasarathy R. 2019. Sublethal antibiotics collapse gut bacterial populations by enhancing aggregation and expulsion. Proc Natl Acad Sci U S A 116:21392-21400.
28. Taylor JW, Berbee ML. 2006. Dating divergences in the Fungal Tree of Life: review and new analyses. Mycologia 98:838-49.
29. Fitzpatrick DA, O'Gaora P, Byrne KP, Butler G. 2010. Analysis of gene evolution and metabolic pathways using the Candida Gene Order Browser. BMC genomics 11:1-14.
30. Byrne KP, Wolfe KH. 2005. The Yeast Gene Order Browser: combining curated homology and syntenic context reveals gene fate in polyploid species. Genome research 15:1456-1461.
31. Fox EP, Bui CK, Nett JE, Hartooni N, Mui MC, Andes DR, Nobile CJ, Johnson AD. 2015. An expanded regulatory network temporally controls C andida albicans biofilm formation. Molecular microbiology 96:1226-1239.
32. Sorrells TR, Johnson AD. 2015. Making sense of transcription networks. Cell 161:714-23.
33. Bruno VM, Kalachikov S, Subaran R, Nobile CJ, Kyratsous C, Mitchell AP. 2006. Control of the C. albicans cell wall damage response by transcriptional regulator Cas5. PLoS Pathog 2:e21.

34. Heredia MY, Gunasekaran D, Ikeh MAC, Nobile CJ, Rauceo JM. 2020. Transcriptional regulation of the caspofungin-induced cell wall damage response in Candida albicans. Curr Genet 66:1059-1068.
35. Heredia MY, Ikeh MAC, Gunasekaran D, Conrad KA, Filimonava S, Marotta DH, Nobile CJ, Rauceo JM. 2020. An expanded cell wall damage signaling network is comprised of the transcription factors Rlm1 and Sko1 in Candida albicans. PLoS Genet 16:e1008908.
36. Rauceo JM, Blankenship JR, Fanning S, Hamaker JJ, Deneault JS, Smith FJ, Nantel A, Mitchell AP. 2008. Regulation of the Candida albicans cell wall damage response by transcription factor Sko1 and PAS kinase Psk1. Mol Biol Cell 19:2741-51.
37. Xie JL, Qin L, Miao Z, Grys BT, Diaz JC, Ting K, Krieger JR, Tong J, Tan K, Leach MD, Ketela T, Moran MF, Krysan DJ, Boone C, Andrews BJ, Selmecki A, Ho Wong K, Robbins N, Cowen LE. 2017. The Candida albicans transcription factor Cas5 couples stress responses, drug resistance and cell cycle regulation. Nat Commun 8:499.
38. Yang F, Zhang L, Wakabayashi H, Myers J, Jiang Y, Cao Y, Jimenez-Ortigosa C, Perlin DS, Rustchenko E. 2017. Tolerance to Caspofungin in Candida albicans Is Associated with at Least Three Distinctive Mechanisms That Govern Expression of FKS Genes and Cell Wall Remodeling. Antimicrobial Agents and Chemotherapy 61:e00071-17.
39. Lee KK, Maccallum DM, Jacobsen MD, Walker LA, Odds FC, Gow NA, Munro CA. 2012. Elevated cell wall chitin in Candida albicans confers echinocandin resistance in vivo. Antimicrob Agents Chemother 56:208-17.
40. Homann OR, Dea J, Noble SM, Johnson AD. 2009. A phenotypic profile of the Candida albicans regulatory network. PLoS genetics 5:e1000783.
41. Holland LM, Schroder MS, Turner SA, Taff H, Andes D, Grozer Z, Gacser A, Ames L, Haynes K, Higgins DG, Butler G. 2014. Comparative phenotypic analysis of the major fungal pathogens Candida parapsilosis and Candida albicans. PLoS Pathog 10:e1004365.
42. Wakade RS, Ristow LC, Stamnes MA, Kumar A, Krysan DJ. 2020. The Ndr/LATS Kinase Cbk1 Regulates a Specific Subset of Ace2 Functions and Suppresses the Hypha-to-Yeast Transition in Candida albicans. mBio 11.
43. Sbia M, Parnell EJ, Yu Y, Olsen AE, Kretschmann KL, Voth WP, Stillman DJ. 2008. Regulation of the yeast Ace2 transcription factor during the cell cycle. J Biol Chem 283:11135-45.
44. Kelly MT, MacCallum DM, Clancy SD, Odds FC, Brown AJ, Butler G. 2004. The Candida albicans CaACE2 gene affects morphogenesis, adherence and virulence. Mol Microbiol 53:969-83.
45. Braun BR, Johnson AD. 1997. Control of filament formation in Candida albicans by the transcriptional repressor TUP1. Science 277:105-9.
46. Braun BR, Head WS, Wang MX, Johnson AD. 2000. Identification and characterization of TUP1-regulated genes in Candida albicans. Genetics 156:31-44.

47. Bastidas RJ, Heitman J, Cardenas ME. 2009. The protein kinase Tor1 regulates adhesin gene expression in Candida albicans. PLoS Pathog 5:e1000294.
48. Butler G, Rasmussen MD, Lin MF, Santos MA, Sakthikumar S, Munro CA, Rheinbay E, Grabherr M, Forche A, Reedy JL, Agrafioti I, Arnaud MB, Bates S, Brown AJ, Brunke S, Costanzo MC, Fitzpatrick DA, de Groot PW, Harris D, Hoyer LL, Hube B, Klis FM, Kodira C, Lennard N, Logue ME, Martin R, Neiman AM, Nikolaou E, Quail MA, Quinn J, Santos MC, Schmitzberger FF, Sherlock G, Shah P, Silverstein KA, Skrzypek MS, Soll D, Staggs R, Stansfield I, Stumpf MP, Sudbery PE, Srikantha T, Zeng Q, Berman J, Berriman M, Heitman J, Gow NA, Lorenz MC, Birren BW, Kellis M, et al. 2009. Evolution of pathogenicity and sexual reproduction in eight Candida genomes. Nature 459:657-62.
49. Braun BR, van Het Hoog M, d'Enfert C, Martchenko M, Dungan J, Kuo A, Inglis DO, Uhl MA, Hogues H, Berriman M, Lorenz M, Levitin A, Oberholzer U, Bachewich C, Harcus D, Marcil A, Dignard D, Iouk T, Zito R, Frangeul L, Tekaia F, Rutherford K, Wang E, Munro CA, Bates S, Gow NA, Hoyer LL, Kohler G, Morschhauser J, Newport G, Znaidi S, Raymond M, Turcotte B, Sherlock G, Costanzo M, Ihmels J, Berman J, Sanglard D, Agabian N, Mitchell AP, Johnson AD, Whiteway M, Nantel A. 2005. A human-curated annotation of the Candida albicans genome. PLoS Genet 1:36-57.
50. Xiong K, Su C, Sun Q, Lu Y. 2021. Efg1 and Cas5 Orchestrate Cell Wall Damage Response to Caspofungin in Candida albicans. Antimicrob Agents Chemother 65.
51. Zavrel M, Majer O, Kuchler K, Rupp S. 2012. Transcription factor Efg1 shows a haploinsufficiency phenotype in modulating the cell wall architecture and immunogenicity of Candida albicans. Eukaryot Cell 11:129-40.
52. Noble SM, French S, Kohn LA, Chen V, Johnson AD. 2010. Systematic screens of a Candida albicans homozygous deletion library decouple morphogenetic switching and pathogenicity. Nature genetics 42:590-598.
53. Nobile CJ, Fox EP, Nett JE, Sorrells TR, Mitrovich QM, Hernday AD, Tuch BB, Andes DR, Johnson AD. 2012. A recently evolved transcriptional network controls biofilm development in Candida albicans. Cell 148:126-138.
54. Rossi DCP, Gleason JE, Sanchez H, Schatzman SS, Culbertson EM, Johnson CJ, McNees CA, Coelho C, Nett JE, Andes DR, Cormack BP, Culotta VC. 2017. Candida albicans FRE8 encodes a member of the NADPH oxidase family that produces a burst of ROS during fungal morphogenesis. PLoS Pathog 13:e1006763.
55. Aguirre J, Lambeth JD. 2010. Nox enzymes from fungus to fly to fish and what they tell us about Nox function in mammals. Free Radic Biol Med 49:1342-53.
56. Vyas VK, Barrasa MI, Fink GR. 2015. A Candida albicans CRISPR system permits genetic engineering of essential genes and gene families. Sci Adv 1:e1500248.
57. Nguyen N, Quail MMF, Hernday AD. 2017. An Efficient, Rapid, and Recyclable System for CRISPR-Mediated Genome Editing in Candida albicans. mSphere 2.
58. Uthayakumar D, Sharma J, Wensing L, Shapiro RS. 2021. CRISPR-Based Genetic Manipulation of Candida Species: Historical Perspectives and Current Approaches. Frontiers in Genome Editing 2:31.

59. Chamilos G, Nobile CJ, Bruno VM, Lewis RE, Mitchell AP, Kontoyiannis DP. 2009. Candida albicans Cas5, a regulator of cell wall integrity, is required for virulence in murine and toll mutant fly models. J Infect Dis 200:152-7.
60. Turner SA, Butler G. 2014. The Candida pathogenic species complex. Cold Spring Harbor perspectives in medicine 4:a019778.
61. Polvi EJ, Veri AO, Liu Z, Hossain S, Hyde S, Kim SH, Tebbji F, Sellam A, Todd RT, Xie JL, Lin ZY, Wong CJ, Shapiro RS, Whiteway M, Robbins N, Gingras AC, Selmecki A, Cowen LE. 2019. Functional divergence of a global regulatory complex governing fungal filamentation. PLoS Genet 15:e1007901.
62. Xu D, Jiang B, Ketela T, Lemieux S, Veillette K, Martel N, Davison J, Sillaots S, Trosok S, Bachewich C, Bussey H, Youngman P, Roemer T. 2007. Genome-wide fitness test and mechanism-of-action studies of inhibitory compounds in Candida albicans. PLoS Pathog 3:e92.
63. West SA, Griffin AS, Gardner A, Diggle SP. 2006. Social evolution theory for microorganisms. Nat Rev Microbiol 4:597-607.
64. Domingo-Calap P, Segredo-Otero E, Duran-Moreno M, Sanjuan R. 2019. Social evolution of innate immunity evasion in a virus. Nat Microbiol 4:1006-1013.
65. Kreft JU. 2004. Biofilms promote altruism. Microbiology (Reading) 150:2751-2760.
66. Seher TD, Nguyen N, Ramos D, Bapat P, Nobile CJ, Sindi SS, Hernday AD. 2021. AddTag, a two-step approach with supporting software package that facilitates CRISPR/Cas-mediated precision genome editing. G3 Genes|Genomes|Genetics doi:10.1093/g3journal/jkab216.
67. Hall BG, Acar H, Nandipati A, Barlow M. 2014. Growth rates made easy. Molecular biology and evolution 31:232-238.
68. Lohse MB, Gulati M, Valle Arevalo A, Fishburn A, Johnson AD, Nobile CJ. 2017. Assessment and optimizations of Candida albicans in vitro biofilm assays. Antimicrobial agents and chemotherapy 61:e02749-16.
69. Gulati M, Lohse MB, Ennis CL, Gonzalez RE, Perry AM, Bapat P, Arevalo AV, Rodriguez DL, Nobile CJ. 2018. In Vitro Culturing and Screening of Candida albicans Biofilms. Curr Protoc Microbiol 50:e60.
70. Dobin A, Davis CA, Schlesinger F, Drenkow J, Zaleski C, Jha S, Batut P, Chaisson M, Gingeras TR. 2013. STAR: ultrafast universal RNA-seq aligner. Bioinformatics 29:15-21.
71. Ritchie ME, Phipson B, Wu D, Hu Y, Law CW, Shi W, Smyth GK. 2015. limma powers differential expression analyses for RNA-sequencing and microarray studies. Nucleic Acids Res 43:e47.
72. Robinson MD, McCarthy DJ, Smyth GK. 2010. edgeR: a Bioconductor package for differential expression analysis of digital gene expression data. Bioinformatics 26:139-40.
73. Team RC. 2020. R: A Language and Environment for Statistical Computing, https://www.R-project.org.
74. Arnaud MB, Costanzo MC, Skrzypek MS, Binkley G, Lane C, Miyasato SR, Sherlock G. 2005. The Candida Genome Database (CGD), a community resource

for Candida albicans gene and protein information. Nucleic Acids Research 33:D358-D363.

75. Ashburner M, Ball CA, Blake JA, Botstein D, Butler H, Cherry JM, Davis AP, Dolinski K, Dwight SS, Eppig JT, Harris MA, Hill DP, Issel-Tarver L, Kasarskis A, Lewis S, Matese JC, Richardson JE, Ringwald M, Rubin GM, Sherlock G. 2000. Gene ontology: tool for the unification of biology. The Gene Ontology Consortium. Nat Genet 25:25-9.

Chapter 2

A markerless CRISPR-mediated system for genome editing in *Candida auris* reveals a conserved role for Cas5 in the caspofungin response

Craig L. Ennis, Aaron D. Hernday, Clarissa J. Nobile

Microbiology Spectrum 2021

2.1 Abstract

Candida auris is a multidrug resistant human fungal pathogen that has recently emerged worldwide. It can cause life-threatening disseminated infections in humans, with mortality rates upwards of 50%. The molecular mechanisms underlying its multidrug resistance and pathogenic properties are largely unknown. Few methods exist for genome editing in *C. auris*, all of which rely on selectable markers that limit the number of modifications that can be made. Here we present a markerless CRISPR/Cas9-mediated genome editing system in *C. auris*. Using this system, we successfully deleted genes of interest and subsequently reconstituted them at their native loci in isolates across all five *C. auris* clades. This system also enabled us to introduce precision genome edits to create translational fusions and single point mutations. Using Cas5 as a test case for this system, we discovered a conserved role for Cas5 in the caspofungin response between *Candida albicans* and *C. auris*. Overall, development of a system for precise and facile genome editing in *C. auris* that can allow for edits to be made in a high-throughput manner is a major step forward in improving our understanding of this important human fungal pathogen.

2.2 Introduction

Candida auris is a human fungal pathogen that can cause both superficial skin and mucosal infections as well as disseminated bloodstream infections (1, 2). *C. auris* was first identified in Japan in 2009 from a patient with an external ear canal infection (3). Since then, *C. auris* has emerged worldwide, nearly simultaneously, across five different continents (4). Isolates of *C. auris* currently belong to five distinct geographic clades according to where they were first isolated: South Asia (clade I), East Asia (clade II), South Africa (clade III), South America (clade IV), and Iran (clade V) (4, 5). Based on current *C. auris* genome annotations, thousands of unique single nucleotide polymorphisms (SNPs) exist between the different clades (4-6). The majority of *C. auris* clinical isolates are resistant to one or more of the three major antifungal drug classes used to treat invasive infections (the azoles, echinocandins, and polyenes), nearly a third of isolates are resistant to two drug classes, and a handful of isolates are pan-resistant to all three of the major drug classes (4, 7). Within hospital settings, *C. auris* has been the cause of several outbreaks to date (7-10), and in the current coronavirus disease 2019 (COVID-19) pandemic, coinfections of *C. auris* with severe acute respiratory syndrome coronavirus 2 (SARS-CoV-2) have been increasingly reported (10-13). Mortality rates associated with *C. auris* infections are high (upwards of 50%) and are frequently attributed to treatment failures (14, 15). With its recent emergence and multidrug resistant properties, *C. auris* is often referred to as a "superbug" that is a serious public health threat.

The ability to manipulate a microbial genome and identify genes and pathways of interest is a valuable tool in microbial genetics. In the *Candida* species, genome editing has historically been time and resource intensive, relying heavily on the incorporation of auxotrophic and/or resistance markers (16). Since its first application in *Candida albicans* in 2015 (17), CRISPR/Cas9-mediated genome editing has greatly increased the speed and efficiency of creating mutations in several *Candida* species (reviewed in (18)). These systems rely on a unique RNA guided DNA nuclease that directs a double-strand break (DSB) at a locus of interest. The DSB can be repaired by error prone non-homologous end joining (NHEJ) or homology directed repair (HDR), the latter relying on user supplied repair templates to make mutations as small as a single base pair in size or to incorporate large heterologous sequences.

A handful of recent studies have created genome modifications in *C. auris*. Grahl et al. (2017) used a Cas9/RNA complex to create a DSB in the *C. auris* ortholog of *CAT1* in *C. albicans*, replacing the gene with the nourseothricin resistance marker gene (*NAT1*) (19). Similar methods have been utilized by two other groups to construct deletion mutant strains and to replace native promoters with inducible promoters (20, 21). Two studies utilized different selectable markers, such as nourseothricin and hygromycin B, to create gene deletion mutant strains in *C. auris* (21, 22). Collectively, these studies have developed and validated tools that have undoubtedly increased the pace of research on this important human fungal pathogen. However, all prior systems for genome editing in *C. auris* have relied on the incorporation of permanent selectable markers, ultimately reducing the numbers and types of genome modifications that are possible in a given strain.

Additionally, the integration of markers and gene deletion cassettes has been demonstrated to be highly variable across *C. auris* clades (23), and all prior studies have genetically manipulated *C. auris* using clade I isolates only. Together, these issues highlight the need for the development of a facile and efficient genome editing system in *C. auris* that does not rely on the integration of permanent selectable markers and that is compatible with isolates across all known *C. auris* clades.

Here we report a markerless CRISPR/Cas9 mediated genome editing system for *C. auris*, adapted from the *C. albicans* LEUpOUT system (24). This system relies on the temporary integration of Cas9 and target-specific guide RNA (gRNA) expression constructs by HDR at the *C. auris LEU2* locus and integration of a DNA repair template ("donor DNA", or dDNA) at the target site of Cas9 cutting during transformations. After verification of the intended genome edits at the Cas9/gRNA target site, the gRNA, Cas9, and selectable marker expression cassettes are "recycled" and removed from the genome, resulting in a modified strain without the introduction of permanent markers. With this *C. auris* system, we successfully deleted and reconstituted the putative ortholog of *C. albicans CAS5* in a representative isolate from each of the five *C. auris* clades. *CAS5* encodes an important cell wall regulator in *C. albicans* that controls sensitivity to the echinocandin drug caspofungin, and we discovered that this function is conserved in *C. auris*. We further tested the versatility of our system by engineering a single point mutation at a conserved phosphorylation site in Cas5 and confirmed that this mutation prevents nuclear localization upon caspofungin treatment. Overall, this new *C. auris* CRISPR system enables rapid genome editing in *C. auris* to easily create deletion mutant strains and reconstituted (complementation/addback) strains, as well as small-scale precision genome edits, which should significantly advance the field in understanding this important and recently emerged human fungal pathogen.

2.3 Results

Construction of a markerless Candida auris CRISPR system

The *C. auris* CRISPR system presented here is based on the widely used LEUpOUT system previously developed for *C. albicans* (24). Briefly, this system utilizes Cas9 and gRNA expression cassettes that are either amplified or digested from plasmids and

integrated within the *LEU2* locus to create a *LEU2* disruption strain that is resistant to nourseothricin or hygromycin B and auxotrophic for leucine (Figure 2.1A).

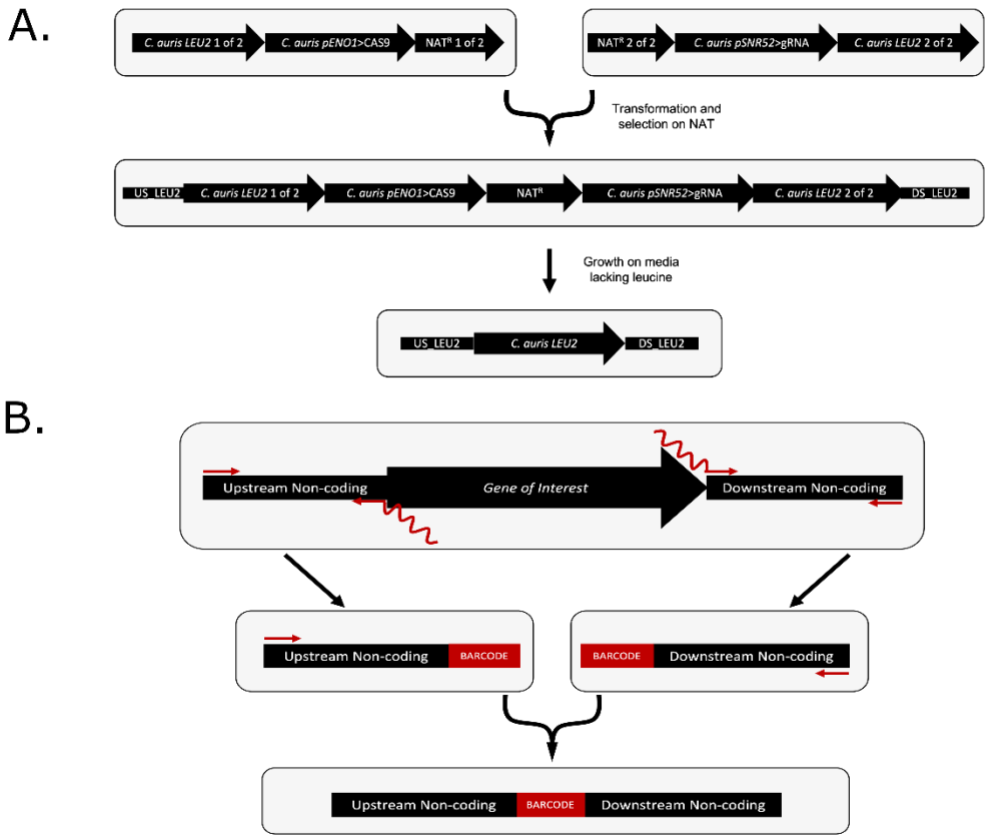

Figure 2.3.1 Schematic of the *C. auris* CRISPR system design. (A) Diagram of the individual and combined gRNA and Cas9 fragments and the transient *C. auris* genotypes at each stage of the transformation and LEUpOUT process. (B) Illustration of the repair template design used for constructing gene deletion strains. Two (100-200 bp) fragments are amplified, and PCR stitched together, to create a larger (200-400 bp) fragment with homology to the genome lacking the gene of interest.

In contrast to the predominantly diploid strains of *C. albicans*, the majority of *C. auris* strains are haploid, and thus creation of a *LEU2/leu2Δ* hemizygous base strain is not typically required for genome edits in *C. auris*. Following confirmation of the intended edits at the target locus, which is determined by the unique gRNA sequence encoded within the gRNA cassette, the CRISPR components are removed along with the resistance marker via selection on media lacking leucine, which creates a selective pressure for cells that have undergone homologous recombination between the flanking direct repeats of the disrupted *LEU2* locus (Fig. 2.1A). This method for transient integration of the CRISPR components and the selectable marker enables efficient precision genome editing at the gRNA target locus and rapid marker recycling to allow for essentially limitless serial genome editing.

The Cas9 plasmid contains homology to the 5' end of the *C. auris LEU2* locus (B9J08_000229) with the *C. auris ENO1* promoter (B9J08_000274) driving expression of

Cas9 (Fig. 2.1A). This fragment contains part "1 of 2" of the nourseothricin gene (*NAT*) or hygromycin B gene (*HYG*) resistance selectable markers, while part "2 of 2" of the selectable markers is included in a separate gRNA plasmid. The "1 of 2" and "2 of 2" segments of each marker overlap by approximately 200 bp of homology, and the intact marker is reconstituted via homologous recombination following transformation into *C. auris*. In addition to the *NAT* or *HYG* "2 of 2" selectable markers, the gRNA construct carries the *C. auris SNR52* promoter driving expression of an *ADE2* (B9J08_003951) spacer sequence, which directs Cas9 to introduce DSBs at the target locus, fused to the conserved trans-activating CRISPR RNA (tracrRNA) sequence that associates with Cas9 to direct cutting to the *ADE2* locus. This construct also contains homology to the 3' end of *LEU2*, allowing these fragments to integrate at this locus.

High throughput gRNA design and amplification

Our *C. auris* system enables simple, versatile, and high throughput generation of unique gRNA expression cassettes via either of two simple PCR-mediated methods (24). The first method, the cloning-free method, involves PCR-based stitching of "universal A" and "unique B" fragments into a custom gRNA expression cassette that can be transformed directly into *C. auris* along with the accompanying Cas9 expression cassette. Using this method, a PCR plate full of unique gRNAs can be amplified in two reactions followed by a PCR stitching step, enabling the quick creation of transformant libraries. Our gRNA design is described in detail in File S1 ("*Candida auris* Markerless CRISPR/Cas9 Genome Editing Protocol"), where Data Set S1 ("Oligo Calculator") was used to create a 60 bp oligonucleotide with standardized 20 bp sequences flanking the ends of the user defined target sequence. The standardized flanking sequences facilitate amplification of unique gRNAs using a standard PCR protocol. The second method, the cloning method, uses a single oligonucleotide-based PCR strategy to generate unique gRNA expression cassettes via circularization of a linearized plasmid, followed by transformation into *E. coli*. The custom gRNA expression cassette can subsequently be excised from the cloned plasmid via restriction digestion and transformed directly into *C. auris* along with the accompanying Cas9 expression cassette. In either approach, only a single custom oligonucleotide is required to introduce a unique target sequence into the gRNA expression cassette and can be designed using the "Oligo Calculator" in Data Set S1. Our base gRNA expression cassette, which is contained in plasmids pCE27 (containing the *NAT* resistance marker) and pCE41 (containing the *HYG* resistance marker), includes a spacer sequence that targets the *C. auris ADE2* locus, allowing users to easily perform *ADE2* editing as a control for CRISPR-mediated editing efficiency in *C. auris*. We note that the editing efficiency of our system at the *C. auris ADE2* locus is ~20%. pCE27 and pCE41 also serve as templates for the incorporation of custom gRNA target sequences by either of the two methods mentioned above.

Rapid generation of gene deletion strains across all C. auris clades

A prior study has indicated that strains within *C. auris* clades III and IV have highly variable efficiencies for integration of selectable markers via homologous recombination (23), thus we sought to determine whether our system could be effective for use in all *C. auris* clades. Using a representative isolate from each *C. auris* clade (AR0387 (clade I),

AR0381 (clade II), AR0383 (clade III), AR0385 (clade IV), and AR1097 (clade V)), we measured editing efficiency by deleting the *C. auris* gene (B9J08_000765) that is a putative ortholog of the *C. albicans CAS5* gene. These *C. auris* base strains were selected because they have been previously used in virulence studies and have predetermined minimum inhibitory concentrations (MICs) for the three major antifungal drug classes used in the clinic. In *C. albicans*, *CAS5* encodes for the extensively studied transcription factor Cas5 that controls cell wall integrity, and *C. albicans cas5*Δ/Δ mutants exhibit hypersensitivity to the echinocandin drug caspofungin (25-27). *C. auris* transformations were performed on three separate occasions using the *NAT* selectable marker version of the LEUpOUT system (Fig. 2.1A) along with amplified dDNA with a 20 bp barcode sequence (Fig. 2.1B; described below), and nourseothricin resistant colonies were screened for deletion of *CAS5* by PCR genotyping. Transformations into the representative strain from clade I (AR0387) revealed *CAS5* deletion efficiencies similar to the across-clade average of 40% (Fig. 2.2A). We observed the highest efficiency (62%) of *CAS5* deletion in the representative clade III isolate (AR0383) while the Clade V isolate (AR1097) exhibited the lowest efficiency (18%). Nonetheless, we were successful in obtaining *cas5*Δ strains from each of our representative clinical isolates with good efficiency. Overall, these results demonstrate our abilities to construct markerless deletion mutant strains in *C. auris*.

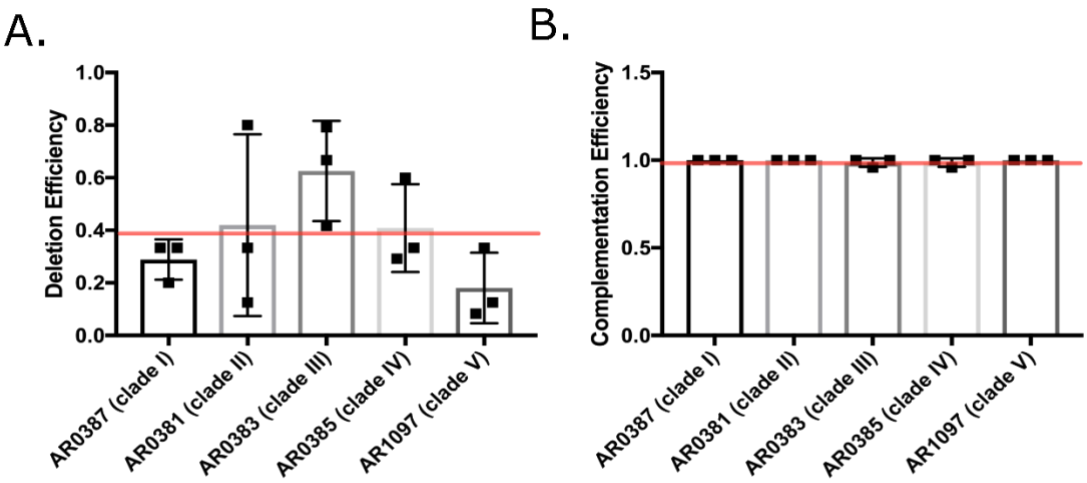

Figure 2.3.2 Editing efficiency of *CAS5* deletion and complementation across *C. auris* clades. (A) *CAS5* was deleted in a representative isolate from each of the five *C. auris* genetic clades (AR0387 (clade I), AR0381 (clade 2), AR0383 (clade III), AR0385 (clade IV), and AR1097 (clade V)). All colonies obtained from each transformation were assessed. Three independent transformations were performed for each isolate. Average deletion efficiencies and standard deviations for each isolate were calculated and is represented by the red line. (B) *CAS5* was complemented to the native locus in a *cas5*Δ mutant from each genetic clade. All colonies obtained from each experiment were assessed. Three independent transformations were performed for each mutant strain. The average efficiency of *CAS5* integration and standard deviation for each strain constructed is shown.

We note that while developing this method, we tested various approaches for generating the necessary dDNA fragments that result in deletion of a target gene upon integration via homologous recombination at the site of Cas9 cutting. We first attempted to create gene deletion mutants using relatively short dDNA fragments with 50-70 bp of homology to sequences on either side of the Cas9/gRNA target locus, which is typically sufficient for comparable *C. albicans* transformations; however, we observed extremely low editing efficiencies using these shorter fragments. To overcome this issue, we utilized a PCR stitching approach to generate dDNA fragments with 100-200 bp of upstream and downstream flanking homology to the *C. auris CAS5* (B9J08_000765) ORF, using primers that bridge the upstream and downstream fragments together via a 22 bp barcode (Fig. 2.1B). Since the barcode sequence is not found within the *C. auris* genome and contains an additional GG sequence, it also serves as a unique gRNA target sequence for subsequent Cas9-mediated editing of the deleted locus.

We also note that during PCR-based screening for *CAS5* deletion transformants, we identified a low frequency (2-6%) of colonies across isolates that had duplicated the *CAS5* locus (duplication of *CAS5* was most frequent in the clade V isolate at a frequency of ~6%). These duplication events were observed while using either the *NAT* or *HYG* selectable markers and were evident based on the presence of distinct PCR bands signifying one intact copy and one deleted copy of *CAS5*. Both PCR bands were observed after obtaining single-colony isolates, confirming that these distinct bands were not the result of background growth of wildtype cells on the transformation plate.

Facile complementation of deleted genes at their native loci

Since the dDNA used to delete *CAS5* (Fig. 2.1B) created a unique "landing pad" site for subsequent genome editing, we tested the ability of this system to complement (i.e., addback) the deleted *CAS5* gene at its native locus. Similar landing pads, also called "AddTags", have been previously utilized in *C. albicans* to reintegrate deleted genes at their native loci (24, 28). Briefly, we generated a new gRNA cassette to target our landing pad using the *HYG* selectable marker version of the *C. auris* LEUpOUT system. We then amplified our *CAS5* addback dDNA via PCR amplification of *C. auris* genomic DNA from a wildtype *C. auris* strain using primers that flank the *CAS5* gene to generate 80 bp of upstream and downstream flanking homology to the *cas5*Δ landing pad. Using this method, we were successful in complementing the five clades with the *HYG* selectable marker, noting exceptionally high overall efficiency (99%) (Fig. 2.2B). Together, these results indicate that our *HYG* and/or *NAT* selectable marker constructs support facile deletion and complementation of genes in representative isolates from each of the five *C. auris* clades.

Cas5 is a conserved regulator of the caspofungin response in C. auris

Nearly half of the predicted proteins encoded within the *C. auris* genome have putative orthologs in *C. albicans* (6). One of many putative orthologs that remains uncharacterized is the transcriptional regulator Cas5. In *C. albicans*, *CAS5* encodes a well characterized transcriptional regulator of cell wall integrity, and deletion of *CAS5* results in hypersensitivity to the frequently used antifungal drug caspofungin (25-27). Global alignment using BLASTP between *C. albicans* Cas5 and its putative ortholog in *C. auris* (B9J08_000765) revealed 88% conservation of the DNA-binding domain (*C. albicans*

743-801; *C. auris* 617-675) (Fig. 2.3A) and 33% conservation across the entire protein, thus we asked whether this putative Cas5 ortholog retains the same function in *C. auris*. Caspofungin sensitivity analyses of the *C. auris* clade I wildtype and its corresponding *cas5*Δ mutant and complementation strains by plate spot assays and growth rate

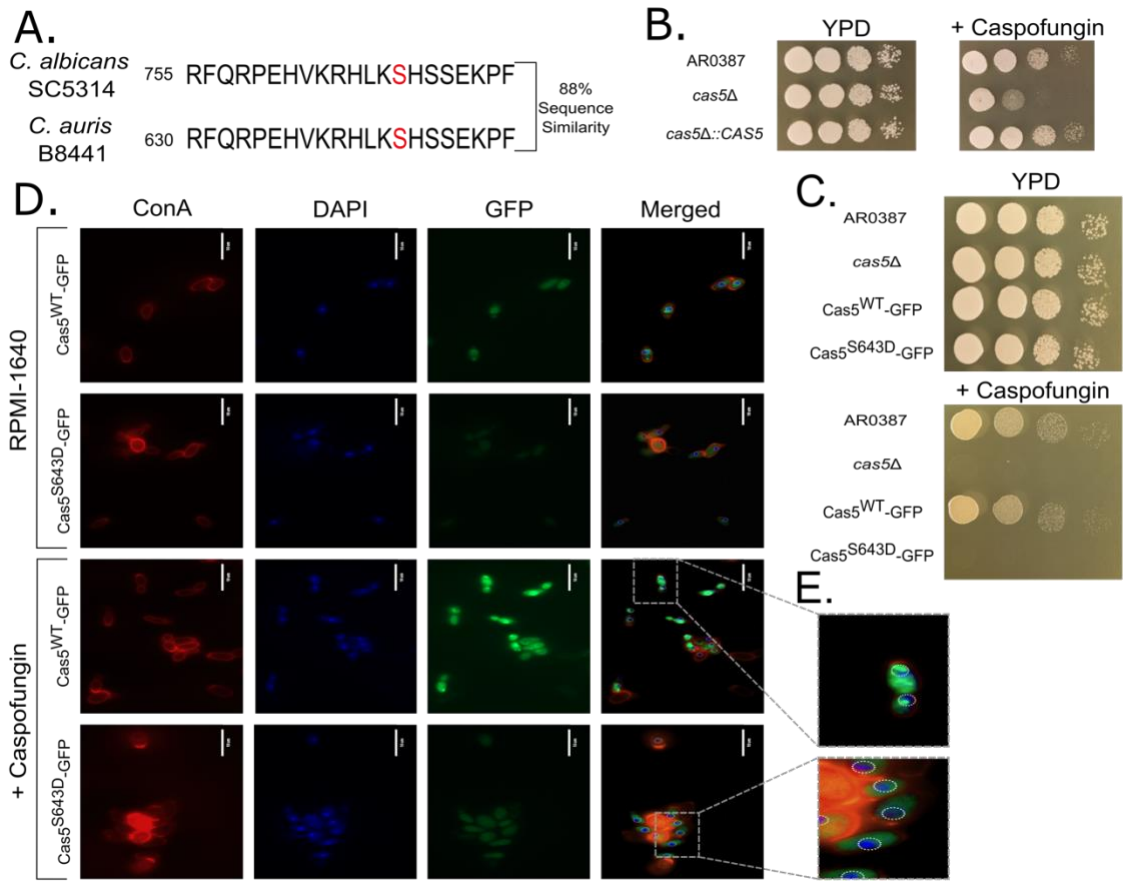

Figure 2.3.3 Cas5 is a conserved regulator of the caspofungin response. (A) Alignment using BLASTP of the *C. albicans* and *C. auris* Cas5 amino acid sequences focusing on a portion of the conserved DNA-binding domain and phosphorylation site (red). (B) Serial spot dilution plate assays performed on YPD medium and YPD medium supplemented with 62.5 ng/mL caspofungin with the AR0387 (clade I) wildtype, *cas5*Δ, and *cas5*Δ::*CAS5* strains. Plates were grown at 30°C and images were acquired after 24 h of growth. (C) Serial spot dilution plate assays performed on YPD medium and YPD medium supplemented with 62.5 ng/mL caspofungin with the AR0387 (clade I) wildtype, *cas5*Δ, Cas5^{WT}-GFP, and Cas5^{S643D}-GFP strains. Plates were grown at 30°C and images were acquired after 24 h of growth. (D) Fluorescence microscopy images of the Cas5^{WT}-GFP and Cas5^{S643D}-GFP strains incubated in the presence and absence of 125 ng/mL caspofungin. Fungal cell walls were stained with ConA and nuclei were stained with DAPI. Cells were imaged with a 100X oil immersion objective. Scale bars represent 10 μm. (E) Representative zoomed-in inset images from a subset of representative cells in Fig. 2.3D of the Cas5^{WT}-GFP and Cas5^{S643D}-GFP strains depicting GFP localization after incubation with 125 ng/mL caspofungin.

experiments confirmed that Cas5 is indeed a conserved regulator of the caspofungin response in *C. auris* (Fig. 2.3B and Fig. S2.1).

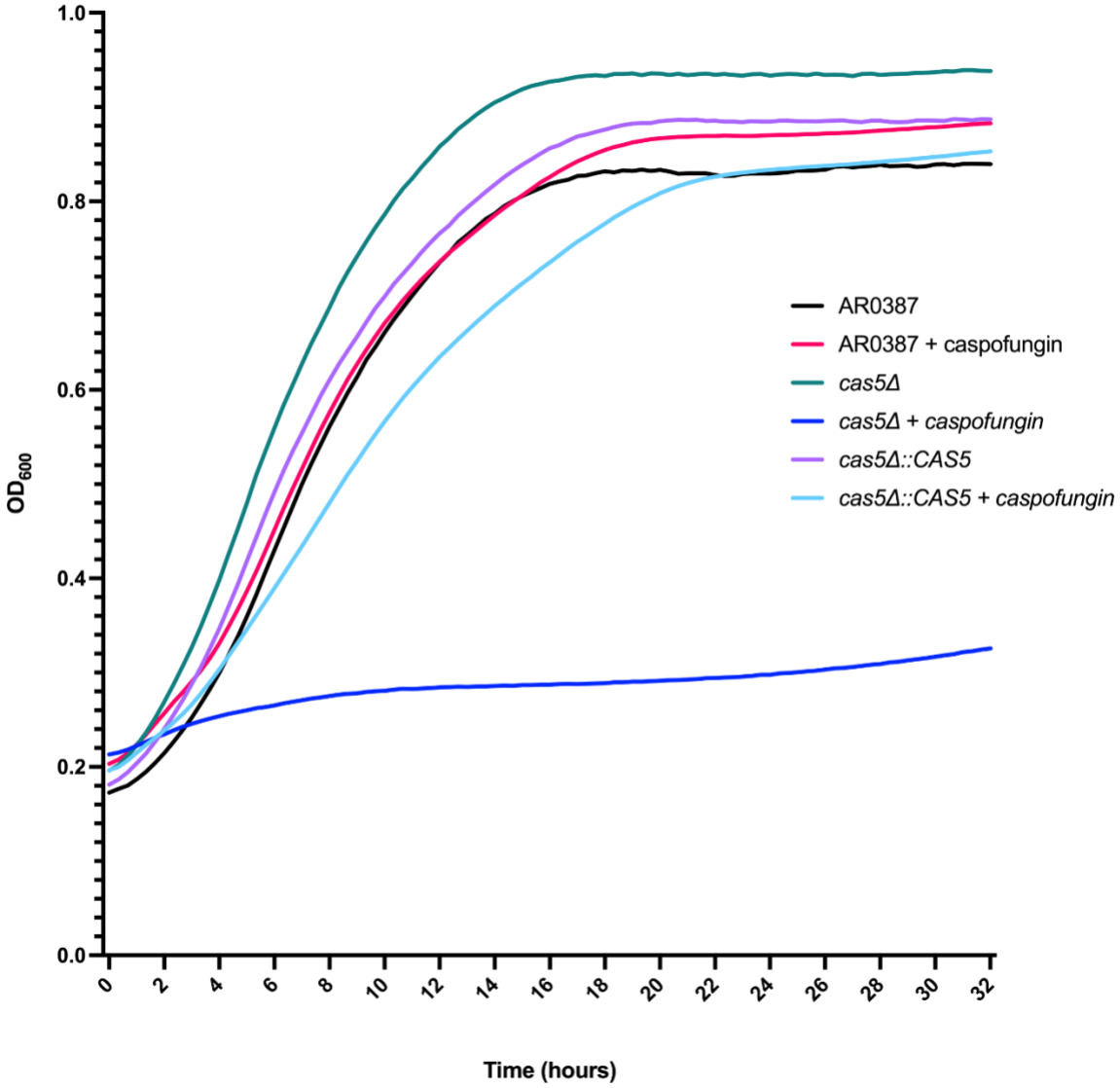

S Figure 2.1 Growth rate measurements confirm a conserved role for Cas5 in the caspofungin response. Growth rate experiment of AR0387 (clade I) wildtype, *cas5*Δ, and *cas5*Δ::*CAS5* strains in RPMI-1640 with and without 62.5 ng/mL caspofungin. Cells were diluted 10^5 in their respective media and grown over 32 h with OD_{600} measurements occurring every 20 mins.

Efficient GFP tagging and codon editing in C. auris

In general, the *C. auris* genome is largely unexplored and many of its genes remain uncharacterized. Using Cas5 as our test case, we also asked whether our *C. auris* genome editing system could support the integration of heterologous sequences, such as fluorescent protein coding sequences, and the introduction of small-scale edits, such as codon

substitutions. *C. albicans* Cas5 is localized to the cytoplasm under basal conditions and is nuclear localized during caspofungin treatment (26), and this translocation is controlled by the dephosphorylation of a serine residue at amino acid position 769. The C-terminal DNA-binding domain as well as this putative phosphorylation site (S643) is highly conserved between the two species (Fig. 2.3A). We first created a Cas5-GFP C-terminal translational fusion (100% editing efficiency) using a CTG optimized eGFP coding sequence that also encodes a seven amino acid linker sequence (RIPLING). Cas9 was directed to induce DSBs at a site 10 bp upstream of the *CAS5* stop codon, and the dDNA used to introduce GFP was designed to ablate this Cas9 target site upon successful integration at the *CAS5* locus to create a $Cas5^{WT}$-GFP *C. auris* strain. We note that the dDNA for this purpose utilized 52 bp of homology, which is substantially less homology than was required for making gene deletion strains. Plate spot assays and fluorescence microscopy confirmed the functionality of our $Cas5^{WT}$-GFP fusion *C. auris* strain and that *C. auris* Cas5 also translocates from the cytoplasm to the nucleus upon exposure to caspofungin (Fig. 2.3C-E).

We next asked whether we could use our genome editing system to mutate the conserved serine residue in our GFP-tagged *C. auris* strains to create an amino acid substitution (S643D) that should mimic a constitutively phosphorylated Cas5. We directed Cas9 to cut at a target sequence that overlaps the S643 codon (AGC) and used the same dDNA stitching approach outlined in Fig. 1B to introduce an S643D substitution (GAT) into a *C. auris* strain that already harbored our Cas5-GFP translational fusion. Since this codon partially overlaps the reverse complement of the TGG PAM site used to target Cas9 cutting at this location, incorporation of our modified dDNA ablated this PAM site and replaced it with the sequence TGA. To further ensure that the dDNA or modified target site would not be cut by Cas9, eight synonymous substitutions were also incorporated within the region of the dDNA representing the original 20 bp gRNA target site (40% of the sequence altered), while retaining the wildtype amino acid coding sequence (10% editing efficiency). This newly constructed $Cas5^{S643D}$-GFP *C. auris* strain was then assessed for GFP localization and caspofungin sensitivity. As expected, the S643D substitution caused *C. auris* Cas5 to largely remain in the cytoplasm, even in the presence of caspofungin (Fig. 2.3D-E). Quantitation of the Cas5 cellular localization results from the microscopy images for each of the strains tested are as follows: $Cas5^{WT}$-GFP (untreated) = 80% ± 10% cytoplasmic and 20% ± 10% nuclear; $Cas5^{WT}$-GFP (caspofungin treated) = 31% ± 10% cytoplasmic and 69% ± 10% nuclear; $Cas5^{S643D}$-GFP (untreated) = 100% ± 0% cytoplasmic and 0% ± 1% nuclear; $Cas5^{S643D}$-GFP (caspofungin treated) = 76% ± 6% cytoplasmic and 24% ± 6% nuclear. Furthermore, caspofungin sensitivity analysis confirmed that the $Cas5^{S643D}$-GFP *C. auris* strain is hypersensitive to caspofungin (Fig. 2.3C-E), which is consistent with previously published results for *C. albicans* (26). Taken together, these results not only highlight the conserved function and regulation of Cas5 between *C. auris* and *C. albicans*, but also the utility of our *C. auris* genome editing system to incorporate heterologous sequences and explore the consequences of small-scale precision genome edits on gene function.

2.4 Discussion

The recent emergence of *C. auris* coupled with its high virulence and inherent antifungal drug resistant properties make it a pressing microorganism for study. Here, we developed a genome editing system that enables efficient, facile, and inexpensive precision genome editing in *C. auris*. An additional advantage of this system is that it does not rely on the incorporation of permanent selectable markers, and the Cas9 and gRNA expression cassettes are removed along with the selectable marker following successful verification of the intended genome edits at the Cas9 target site. In this way, the system enables essentially limitless serial genome edits in the same genetic background. We display the versatility of our system to make sequential edits in clinical isolates in two different ways. First, gene deletion strains of our gene of interest in all five *C. auris* clades were made that were subsequently complemented at their native loci. Second, we created a translational fusion with GFP followed by an additional edit to introduce a non-synonymous substitution within the coding sequence of the GFP tagged gene of interest.

Since most *C. auris* clinical isolates are haploid, and thus directly compatible with our LEUpOUT system, most *C. auris* isolates should be amenable to our genome editing system without requiring any prior strain engineering. One group has recently identified highly virulent diploid isolates of *C. auris* (29), which would require prior strain modification to be compatible with our genome editing system; however, we anticipate that the generation of *LEU2* hemizygous strains using traditional gene deletion approaches should enable the use of our genome editing system in *C. auris* diploids, as has been demonstrated with a similar genome editing system in *C. albicans* (24).

Two sets of plasmids are available for use in our genome editing system, each relying on a different selectable marker, allowing for transformation in strains previously constructed with a selectable marker. For example, if one were to attempt genome editing in a diploid *C. auris* isolate, it should be possible to use the *NAT* marker system to delete a single copy of the *LEU2* gene via integrative transformation, and then subsequently to use the *HYG* selectable marker system for precision genome editing. Beyond the versatility of having two selectable markers, the *HYG* selectable marker system reduces the cost of transforming strains since hygromycin B is a more affordable alternative to nourseothricin. In our experience, the *HYG* selectable marker system is superior to the *NAT* selectable marker system at reducing background growth of *C. auris* on selective media. This variable background growth can make isolating single colonies more difficult if performing a subsequent transformation with the *NAT* marker system. While both systems work well for markerless genome editing in *C. auris*, we find that using hygromycin B provides a more robust selection with consistently lower background colony growth than using nourseothricin, making subsequent complementation and downstream edits easier.

While the genome editing system presented here is based on the widely used *C. albicans* LEUpOUT system published by Nguyen et al. (24), the plasmids and repair template designed here were modified and optimized to increase the editing efficiency in *C. auris*. When developing this system, we initially replaced the *C. albicans LEU2* with the *C. auris LEU2* sequences, while retaining the native *C. albicans* promoters to test if these heterologous promoters were sufficient for gene editing. With this plasmid design, *C. auris* readily incorporated the CRISPR components, yet *cas5*Δ mutants were

exceptionally rare in all isolates tested. With the additional incorporation of *C. auris*-specific promoters (*SNR52* and *ENO1*), we were able to successfully perform genome editing at the *CAS5* locus across all clades and isolates tested.

We tested several different repair template designs to further improve efficiency. Previous studies have used repair templates with as little as 50 bp homology upstream and downstream of the target locus (22, 23). Using annealed oligonucleotides with 40-50 bp homology, as is common with the *C. albicans* system, gene deletion mutants with the new plasmids were infrequent in clades I and IV and were exceptionally rare in clades II, III, and IV, whereas increasing the homology length to 100-200 bp substantially increased our gene deletion efficiencies (across-clade average of 40% for deleting *CAS5*). Interestingly, the repair template used for creating the Cas5-GFP translational fusion strain contained 52 bp homology upstream and downstream to the target locus and was more than sufficient for GFP tagging (100% efficiency), indicating that *C. auris* can integrate sequences that contain shorter regions of homology with high efficiency. Furthermore, we observed extremely high (99%) complementation efficiency for adding back *CAS5* to its native locus. The *C. albicans* LEUpOUT system boasts editing efficiencies for complementation ranging from 60-80% (24), requiring integration of two copies of the gene of interest in a diploid organism. We believe that the higher complementation efficiency observed here is due to the haploid genome architecture of *C. auris*, requiring integration of only a single copy of the gene of interest. In addition to deleting and complementing entire protein coding genes, we also demonstrate the ability to modify single codons as a proof of concept that this system can also be used to study the functional consequences of small-scale genome edits.

Genomic rearrangements and aneuploidy are common stress response mechanisms in the *Candida* species (30, 31), and *C. auris* is no exception. Genomic rearrangements are frequent across *C. auris* isolates and clades, with the highest degree of rearrangements and gene losses occurring in clade II isolates (32, 33). While the mechanism of the *CAS5* duplication events observed in our deletion transformations is unknown, we note that the standard lithium acetate fungal transformation process is known to induce genomic rearrangements and aneuploidy in *C. albicans* (34). A common concern regarding Cas9-mediated genome editing is the potential for off-target cutting, which could result in unwanted genetic modifications; however, we do not believe this is the primary mechanism responsible for the *CAS5* duplication events that we observed. Two independent studies have concluded that off-target effects of Cas9 genome editing in *C. albicans* are likely to be rare (34, 35); however, Marton et al. found that lithium acetate-based transformations frequently induce genomic rearrangements, regardless of whether or not Cas9 is used in the method (34). Furthermore, off-target cutting is believed to be more of a concern in larger eukaryotic genomes (36), such as mammals, which have ~500-fold larger genomes than *Candida* species, and thus contain fewer unique 20 bp sequences from which to select gRNA targets. Even so, off-target cutting in mammalian genomes has been shown to be relatively rare, even at sites that differ from the intended target by as few as three nucleotides (37, 38). Considering the relatively small genome size of *C. auris*, and assuming the selection of highly specific 20 bp gRNA target sites, we believe that off-target cutting is unlikely to be a significant problem when using our genome editing system. However, the observation of *CAS5* duplication events highlights the importance of careful

evaluation of engineered strains (through, for example, genetic complementation experiments), regardless of the transformation methodology being used. In addition, our facile gene complementation approach is another advantage of our system that enable researchers to easily control and monitor for unintended modifications in gene deletion strains.

While assessing the functionality of our genome editing system, we chose to focus on *CAS5* in *C. auris* because its ortholog in *C. albicans* is well characterized and its deletion in *C. albicans* results in a clearly discernable hypersensitivity to caspofungin. Alignment of *C. albicans* and *C. auris* Cas5 indicates that the C-terminal domain containing the DNA-binding domain and phosphorylation site is highly conserved (88% identity), while the remaining amino acid sequences have greatly diverged (33% identity). Based on this striking sequence identity within the DNA-binding domain, we hypothesized that the function of Cas5 is likely to be conserved between the two species, despite the fact that the two species are evolutionarily quite distant. Using this system, we constructed a GFP-tagged Cas5 *C. auris* strain containing codon substitutions that mimic a constitutively phosphorylated form of Cas5 (a Cas5^{S643D}-GFP strain), and observed that this strain was hypersensitive to caspofungin, matching the phenotype of the *cas5*Δ strain. We observed decreased GFP fluorescence by microscopy in the Cas5^{S643D}-GFP *C. auris* strain relative to the Cas5^{WT}-GFP *C. auris* strain. This finding could be the result of Cas5 regulating its own expression and would be consistent with previous work in *C. albicans* observing decreased Pol II occupancy at the *CAS5* locus in the *cas5*Δ/Δ *C. albicans* strain compared to the wildtype *C. albicans* strain in both the presence and absence of caspofungin (26). Interestingly we observed an increase in GFP fluorescence under caspofungin treatment in the Cas5^{S643D}-GFP *C. auris* strain. We suspect that either the Cas5^{S643D}-GFP *C. auris* strain is still capable of inducing its own expression (26) or there are unidentified transcriptional regulators contributing to caspofungin-induced *CAS5* expression in *C. auris*. Additionally, our findings suggest that the caspofungin hypersensitivity of this Cas5^{S643D}-GFP *C. auris* strain is due to the inability of this modified form of Cas5 to effectively translocate into the nucleus in response to caspofungin treatment. Overall, consistent with its role in *C. albicans*, we discovered that Cas5 in *C. auris* is also a key regulator of the caspofungin response.

Broadly, this study contributes to our understanding of the cell wall stress response in *Candida* species. The CTG clade, which is named for species that translate CTG as serine rather than leucine (39), comprises many *Candida* species (e.g., *C. albicans*, *Candida dubliniensis*, *Candida parapsilosis*, and *C. auris*) and excludes certain *Candida* species (e.g., *Candida glabrata* and *Candida krusei*). The most recent common ancestor of *C. albicans* and *S. cerevisiae* diverged approximately 235 million years ago, with *S. cerevisiae* lacking a Cas5 ortholog (26, 40). Prior to this study, Cas5 was identified as a critical caspofungin response regulator in only *C. albicans* and *C. parapsilosis* (25, 41). The evolutionary distance between *C. albicans* and *C. auris* is large, much larger than the evolutionary distance between *C. albicans* and *C. parapsilosis* (6), and thus the conserved role of Cas5 in the caspofungin response in *C. auris* that we observe here is not necessarily expected. In the non-CTG clade species, *C. glabrata*, *MOT3* encodes a transcriptional regulator with synteny to both *CAS5* in *C. albicans* and *MOT3* in *S. cerevisiae;* however, Mot3 in *C. glabrata* is dispensable for the caspofungin response (42, 43). *C. krusei* has a

"Cas5-like" regulator with greater conservation at the DNA-binding domain to Cas5 in *C. albicans* (66% identity) than to Mot3 in *S. cerevisiae* (48% identity) or Mot3 in *C. glabrata* (37% identity, (26)), yet a role for this Cas5-like regulator in *C. krusei* has yet to be established. Future work characterizing putative Cas5 orthologs across the *Candida* species would greatly improve our understanding of how these important human fungal pathogens respond to cell wall stress.

Essential genes are promising drug targets in fungal pathogens as interference with their protein products leads to fungal cell death (17, 18, 44). As such, essential genes are not amenable to deletion, yet their expression can be controlled using CRISPR/Cas9 technologies (18). A CRISPR interference (CRISPRi) system utilizing a catalytically inactive Cas9 (dCas9) for stable gene repression is available in *C. albicans* and has been demonstrated to be a useful tool for studying essential genes (45). A similar system using dCas9-tethered transcriptional activation domains has been shown to be an effective means of targeted transcriptional activation in *C. albicans* (46). Adaptation of our genome editing system to incorporate similar tools to allow for facile repression or activation of genes of interest in *C. auris* should facilitate the future identification of fungal-specific drug targets in *C. auris*.

In summary, we present a versatile CRISPR/Cas9-mediated genome editing system for use in *C. auris* that is the first system that does not create a terminal strain retaining a selectable marker in the genome. We believe this system is a major genetic advance in the field that should facilitate future discoveries into the biology of this important and recently emerged human fungal pathogen.

2.5 Materials and Methods

Strains and culturing conditions

Wildtype *C. auris* clinical isolate strains AR0387 (clade I), AR0381 (clade II), AR0383 (clade III), AR0385 (clade IV), and AR1097 (clade V) used in this study were obtained from the Centers for Disease Control and Prevention (CDC) and U.S. Food and Drug Administration (FDA) Antimicrobial Resistance (AR) Isolate Bank, Drug Resistance *Candida* species panel; https://wwwn.cdc.gov/ARIsolateBank/; accessed on 05/24/2021. Transformed strains constructed in this study are listed in Data Set S2 and oligonucleotides used in this study are listed in Data Set S3. A detailed protocol describing necessary regents, dDNA and gRNA amplification procedures, and the *C. auris* transformation process is available in File S1 ("*Candida auris* Markerless CRISPR/Cas9 Genome Editing Protocol").

Genotypes of the edited strains were verified by colony PCR. The *cas5*Δ mutant strains (CEC97 (AR0383), CEC98 (AR0385), CEC99 (AR0387), CEC100 (AR1097), CEC140 (AR0381)) were made with stitched PCR products from pCE27 and *Mss*I digested pCE35 in their respective isogenic wildtype strains. The complemented strains (CEC141 (AR0383), CEC142 (AR0385), CEC183 (AR0387), CEC144 (AR1097), CEC165 (AR0381)) were made in their respective *cas5*Δ deletion mutant strains with stitched PCR products from pCE41 and *Mss*I digested pCE38. Wildtype *CAS5* for complemented strains was amplified from genomic DNA from each isolate with flanking homology to the *CAS5*

upstream and downstream noncoding regions. The Cas5^{WT}-GFP strain (CEC68) was made by amplifying *Candida* optimized monomeric GFP (pCE1) with a short linker (RIPLING) with flanking homology to 3' end of *CAS5* and the downstream non-coding region of the gene. This GFP-tagged strain was edited an additional time with dDNA amplified from the Cas5^{WT}-GFP strain (CEC68) genomic DNA using primers CJNO4368, CJNO4369, CJNO4372, and CJNO4373 to introduce a mutation creating a Cas5^{S643D}-GFP strain (CEC146), which was verified by PCR and sanger sequencing. The oligonucleotides used to amplify the Cas5^{S643D} dDNA contained synonymous point mutations to ablate future Cas9 cutting and a nonsynonymous substitution to introduce the S643D mutation. Changes to the DNA sequence in the Cas5^{S643D}-GFP strain are denoted with bold lowercase font in Data Set S3.

C. auris cells were stored at -80°C and were streaked on YPD plates (2% peptone, 2% dextrose, and 1% yeast extract) and grown for two days at 30°C. Single colonies were inoculated into liquid YPD medium and grown overnight with shaking at 30°C for use in all downstream experiments.

Plasmid construction

Plasmids pADH118 and pADH137 (24) were used as base plasmids to construct the gRNA and Cas9 plasmids, respectively. All primers were designed based on the B8441 (AR0387) genome and B8441 genomic DNA was used for amplification of all promoters. The gRNA plasmid was constructed by PCR amplification of pADH118 to integrate the 3' end of the B8441 B9J08_000229 (*LEU2*) ORF, which was amplified using genomic DNA and gap repaired using chemically competent DH5α *E. coli* (Lucigen, Catalog # 60107-1) creating pCE8. pCE8 was further linearized by PCR amplification to remove the *C. albicans SNR52* promoter, which was replaced with the *C. auris SNR52* promoter amplified using genomic DNA. This again was gap repaired with chemically competent DH5α *E. coli* to create pCE27. The Cas9 plasmid was constructed by linearizing pADH137 and the 5' end of the of the B8441 B9J08_000229 (*LEU2*) ORF, which was amplified using genomic DNA, and integrated using gap repair to create pCE4. This plasmid was linearized an additional time to replace the *ENO1* promoter driving expression of Cas9 with gap repair to create pCE35.

The plasmid containing monomeric GFP was constructed by gap-repair cloning into a linearized pADH98 entry vector created by PCR amplification followed by *Dpn*I digestion and gel extraction. GFP was codon optimized for CUG clade species and purchased from ThermoFisher Scientific with homology to the pADH98 entry vector added to each end. This synthetic fragment and entry vector were gap repaired as described above using chemically competent DH5α *E. coli* to create pCE1. All plasmids constructed in this study were verified by sequencing and are available on AddGene with the following accession numbers (pCE1 (174434), pCE27 (174405), pCE35 (174409), pCE38 (174432), pCE41 (174433)).

Transformation of C. auris cells by heat shock

C. auris cells were transformed as previously described for *C. albicans* cells (24). Briefly, *C. auris* overnight cultures were diluted to an optical density (OD_{600}) of 0.1 in YPD medium and grown at 30°C shaking until they reached an OD_{600} between 0.4–0.7.

Cells were pelleted and washed twice in sterile water before being transferred to a DNA mixture of the unique gRNA fragment, Cas9 fragment, dDNA repair template, and single-stranded salmon sperm DNA (pre-boiled). Fresh PLATE mix (50% PEG-3350, 25 mM lithium acetate, 1X TE) was added to each transformation and incubated overnight. Incubated cells were heat shocked at 44°C for 15 min, washed, and recovered in YPD medium at 30°C shaking for 4 h before plating on YPD medium supplemented with 200 μg/mL nourseothricin or 500 μg/mL hygromycin B. Individual colonies were checked after two days of growth at 30°C and patched onto YPD plates supplemented with 200 μg/mL nourseothricin or 500 μg/mL hygromycin B and verified by colony PCR for the genome edit of interest. Colonies that had the correct genome edit were restreaked on Synthetic Complete (SC) medium lacking leucine and isoleucine (6.7% yeast nitrogen base without ammonium sulfate, 2% glucose, and auxotrophic supplements) to remove the CRISPR components. Individual colonies were patched onto YPD plates with and without 200 μg/mL nourseothricin or 500 μg/mL hygromycin B to confirm loss of the *NAT* or *HYG* resistance markers and CRISPR components.

Plate spot dilution assays

Overnight cell cultures were diluted to an OD_{600} of 0.2 in YPD medium and grown to mid log phase with shaking at 30°C. OD_{600} of the back-diluted culture was measured and diluted to an OD_{600} of 0.2. This was serial diluted 1:10 four times for each strain and plated onto YPD plates supplemented with and without 62.5 ng/mL caspofungin. Plates were incubated at 30°C for 24 h and imaged.

Fluorescent microscopy

C. auris $Cas5^{WT}$-GFP and $Cas5^{S643D}$-GFP strains (CEC68 and CEC146) were grown overnight, and diluted to an OD_{600} of 0.5 in RPMI-1640 medium buffered with MOPS and incubated at 30°C in the presence and absence of 125 ng/mL caspofungin for 60 min. Cells were fixed with 2% formaldehyde, stained with 4′,6-diamidino-2-phenylindole (DAPI) and concanavalin A (ConA), and washed prior to being imaged on an EVOS FL microscope with a 100X oil immersion objective using the DAPI, GFP, and Texas Red filters. Quantification of nuclear and cytoplasmic Cas5-GFP localization was determined by counting at least 100 cells from representative images of each strain using the Fiji software package (47) in ImageJ (48). The proportion of cells with nuclear or cytoplasmic Cas5 localization was averaged across all images.

Growth curves

Growth curves were performed by diluting overnight *C. auris* cultures to 10^5 CFU/mL in RPMI-1640 medium buffered with MOPS. Cells were further diluted (3:4) in a 384 well plate with RPMI-1640 medium buffered with MOPS with or without caspofungin at a concentration of 62.5 ng/mL and grown for 32 h with linear shaking at 30°C in a Biotek Cytation5 plate reader. The OD_{600} of each well was measured in 20 min intervals. The averages of twelve replicates per strain and treatment condition were calculated.

2.6 References

1. Horton MV, Johnson CJ, Kernien JF, Patel TD, Lam BC, Cheong JZA, Meudt JJ, Shanmuganayagam D, Kalan LR, Nett JE. 2020. *Candida auris* Forms High-Burden Biofilms in Skin Niche Conditions and on Porcine Skin. *mSphere* 5:e00910-19.
2. Du H, Bing J, Hu T, Ennis CL, Nobile CJ, Huang G. 2020. *Candida auris*: Epidemiology, biology, antifungal resistance, and virulence. *PLoS Pathog* 16:e1008921.
3. Satoh K, Makimura K, Hasumi Y, Nishiyama Y, Uchida K, Yamaguchi H. 2009. *Candida auris* sp. nov., a novel ascomycetous yeast isolated from the external ear canal of an inpatient in a Japanese hospital. *Microbiol Immunol* 53:41-4.
4. Lockhart SR, Etienne KA, Vallabhaneni S, Farooqi J, Chowdhary A, Govender NP, Colombo AL, Calvo B, Cuomo CA, Desjardins CA, Berkow EL, Castanheira M, Magobo RE, Jabeen K, Asghar RJ, Meis JF, Jackson B, Chiller T, Litvintseva AP. 2017. Simultaneous Emergence of Multidrug-Resistant *Candida auris* on 3 Continents Confirmed by Whole-Genome Sequencing and Epidemiological Analyses. *Clin Infect Dis* 64:134-140.
5. Chow NA, de Groot T, Badali H, Abastabar M, Chiller TM, Meis JF. 2019. Potential Fifth Clade of *Candida auris*, Iran, 2018. *Emerg Infect Dis* 25:1780-1781.
6. Munoz JF, Gade L, Chow NA, Loparev VN, Juieng P, Berkow EL, Farrer RA, Litvintseva AP, Cuomo CA. 2018. Genomic insights into multidrug-resistance, mating and virulence in *Candida auris* and related emerging species. *Nat Commun* 9:5346.
7. Zhu Y, O'Brien B, Leach L, Clarke A, Bates M, Adams E, Ostrowsky B, Quinn M, Dufort E, Southwick K, Erazo R, Haley VB, Bucher C, Chaturvedi V, Limberger RJ, Blog D, Lutterloh E, Chaturvedi S. 2020. Laboratory Analysis of an Outbreak of *Candida auris* in New York from 2016 to 2018: Impact and Lessons Learned. *J Clin Microbiol* 58: e01503-19.
8. Rhodes J, Abdolrasouli A, Farrer RA, Cuomo CA, Aanensen DM, Armstrong-James D, Fisher MC, Schelenz S. 2018. Genomic epidemiology of the UK outbreak of the emerging human fungal pathogen *Candida auris*. *Emerg Microbes Infect* 7:43.
9. Schelenz S, Hagen F, Rhodes JL, Abdolrasouli A, Chowdhary A, Hall A, Ryan L, Shackleton J, Trimlett R, Meis JF, Armstrong-James D, Fisher MC. 2016. First hospital outbreak of the globally emerging *Candida auris* in a European hospital. *Antimicrob Resist Infect Control* 5:35.
10. Villanueva-Lozano H, Trevino-Rangel RJ, Gonzalez GM, Ramirez-Elizondo MT, Lara-Medrano R, Aleman-Bocanegra MC, Guajardo-Lara CE, Gaona-Chavez N, Castilleja-Leal F, Torre-Amione G, Martinez-Resendez MF. 2021. Outbreak of *Candida auris* infection in a COVID-19 hospital in Mexico. *Clin Microbiol Infect* 8:813-816.
11. Chowdhary A, Sharma A. 2020. The lurking scourge of multidrug resistant *Candida auris* in times of COVID-19 pandemic. *J Glob Antimicrob Resist* 22:175-176.
12. Allaw F, Kara Zahreddine N, Ibrahim A, Tannous J, Taleb H, Bizri AR, Dbaibo G, Kanj SS. 2021. First *Candida auris* Outbreak during a COVID-19 Pandemic in a Tertiary-Care Center in Lebanon. *Pathogens* 10:157.

13. de Almeida JN, Jr., Francisco EC, Hagen F, Brandao IB, Pereira FM, Presta Dias PH, de Miranda Costa MM, de Souza Jordao RT, de Groot T, Colombo AL. 2021. Emergence of *Candida auris* in Brazil in a COVID-19 Intensive Care Unit. *J Fungi* (Basel) 7:220.
14. Lee WG, Shin JH, Uh Y, Kang MG, Kim SH, Park KH, Jang HC. 2011. First three reported cases of nosocomial fungemia caused by *Candida auris*. *J Clin Microbiol* 49:3139-42.
15. Chowdhary A, Sharma C, Duggal S, Agarwal K, Prakash A, Singh PK, Jain S, Kathuria S, Randhawa HS, Hagen F, Meis JF. 2013. New clonal strain of *Candida auris*, Delhi, India. *Emerg Infect Dis* 19:1670-3.
16. Noble SM, Johnson AD. 2005. Strains and strategies for large-scale gene deletion studies of the diploid human fungal pathogen *Candida albicans*. *Eukaryot Cell* 4:298-309.
17. Vyas VK, Barrasa MI, Fink GR. 2015. A *Candida albicans* CRISPR system permits genetic engineering of essential genes and gene families. *Sci Adv* 1:e1500248.
18. Uthayakumar D, Sharma J, Wensing L, Shapiro RS. 2021. CRISPR-Based Genetic Manipulation of *Candida* Species: Historical Perspectives and Current Approaches. *Frontiers in Genome Editing* 2:606281.
19. Grahl N, Demers EG, Crocker AW, Hogan DA. 2017. Use of RNA-Protein Complexes for Genome Editing in Non-*albicans Candida* Species. *mSphere* 2:e00218-17.
20. Day AM, McNiff MM, da Silva Dantas A, Gow NAR, Quinn J. 2018. Hog1 Regulates Stress Tolerance and Virulence in the Emerging Fungal Pathogen *Candida auris*. *mSphere* 3:e00506-18.
21. Kim SH, Iyer KR, Pardeshi L, Munoz JF, Robbins N, Cuomo CA, Wong KH, Cowen LE. 2019. Genetic Analysis of *Candida auris* Implicates Hsp90 in Morphogenesis and Azole Tolerance and Cdr1 in Azole Resistance. *mBio* 10:e02529-18.
22. Rybak JM, Doorley LA, Nishimoto AT, Barker KS, Palmer GE, Rogers PD. 2019. Abrogation of Triazole Resistance upon Deletion of *CDR1* in a Clinical Isolate of *Candida auris*. *Antimicrob Agents Chemother* 63:e00057-19.
23. Mayr EM, Ramirez-Zavala B, Kruger I, Morschhauser J. 2020. A Zinc Cluster Transcription Factor Contributes to the Intrinsic Fluconazole Resistance of *Candida auris*. *mSphere* 5:e00279-20.
24. Nguyen N, Quail MMF, Hernday AD. 2017. An Efficient, Rapid, and Recyclable System for CRISPR-Mediated Genome Editing in *Candida albicans*. *mSphere* 2:e00149-17.
25. Bruno VM, Kalachikov S, Subaran R, Nobile CJ, Kyratsous C, Mitchell AP. 2006. Control of the *C. albicans* cell wall damage response by transcriptional regulator Cas5. *PLoS Pathogens* 2:e21.
26. Xie JL, Qin L, Miao Z, Grys BT, Diaz JC, Ting K, Krieger JR, Tong J, Tan K, Leach MD, Ketela T, Moran MF, Krysan DJ, Boone C, Andrews BJ, Selmecki A, Ho Wong K, Robbins N, Cowen LE. 2017. The *Candida albicans* transcription factor Cas5 couples stress responses, drug resistance and cell cycle regulation. *Nat Commun* 8:499.
27. Chamilos G, Nobile CJ, Bruno VM, Lewis RE, Mitchell AP, Kontoyiannis DP. 2009. *Candida albicans* Cas5, a regulator of cell wall integrity, is required for virulence in murine and toll mutant fly models. *J Infect Dis* 200:152-7.

28. Seher TD, Nguyen N, Ramos D, Bapat P, Nobile CJ, Sindi SS, Hernday AD. 2021. AddTag, a two-step approach with supporting software package that facilitates CRISPR/Cas-mediated precision genome editing. *G3 Genes|Genomes|Genetics* 11:jkab216.
29. Fan S, Li C, Bing J, Huang G, Du H. 2020. Discovery of the Diploid Form of the Emerging Fungal Pathogen *Candida auris*. *ACS Infect Dis* 6:2641-2646.
30. Bhattacharya S, Holowka T, Orner EP, Fries BC. 2019. Gene Duplication Associated with Increased Fluconazole Tolerance in *Candida auris* cells of Advanced Generational Age. *Sci Rep* 9:5052.
31. Selmecki A, Forche A, Berman J. 2006. Aneuploidy and isochromosome formation in drug-resistant *Candida albicans*. *Science* 313:367-70.
32. Munoz JF, Welsh RM, Shea T, Batra D, Gade L, Howard D, Rowe LA, Meis JF, Litvintseva AP, Cuomo CA. 2021. Clade-specific chromosomal rearrangements and loss of subtelomeric adhesins in *Candida auris*. *Genetics* 218:iyab029.
33. Sekizuka T, Iguchi S, Umeyama T, Inamine Y, Makimura K, Kuroda M, Miyazaki Y, Kikuchi K. 2019. Clade II *Candida auris* possess genomic structural variations related to an ancestral strain. *PLoS One* 14:e0223433.
34. Marton T, Maufrais C, d'Enfert C, Legrand M. 2020. Use of CRISPR-Cas9 To Target Homologous Recombination Limits Transformation-Induced Genomic Changes in *Candida albicans*. *mSphere* 5:e00620-20.
35. Shapiro RS, Chavez A, Porter CB, Hamblin M, Kaas CS, DiCarlo JE, Zeng G, Xu X, Revtovich AV, Kirienko NV. 2018. A CRISPR–Cas9-based gene drive platform for genetic interaction analysis in *Candida albicans*. *Nature Microbiology* 3:73-82.
36. Naeem M, Majeed S, Hoque MZ, Ahmad I. 2020. Latest Developed Strategies to Minimize the Off-Target Effects in CRISPR-Cas-Mediated Genome Editing. *Cells* 9:1608.
37. Garrood WT, Kranjc N, Petri K, Kim DY, Guo JA, Hammond AM, Morianou I, Pattanayak V, Joung JK, Crisanti A, Simoni A. 2021. Analysis of off-target effects in CRISPR-based gene drives in the human malaria mosquito. *Proceedings of the National Academy of Sciences* 118:e2004838117.
38. Kim D, Bae S, Park J, Kim E, Kim S, Yu HR, Hwang J, Kim J-I, Kim J-S. 2015. Digenome-seq: genome-wide profiling of CRISPR-Cas9 off-target effects in human cells. *Nature Methods* 12:237-243.
39. Turner SA, Butler G. 2014. The *Candida* pathogenic species complex. *Cold Spring Harbor perspectives in medicine* 4:a019778.
40. Taylor JW, Berbee ML. 2006. Dating divergences in the Fungal Tree of Life: review and new analyses. *Mycologia* 98:838-49.
41. Holland LM, Schröder MS, Turner SA, Taff H, Andes D, Grózer Z, Gácser A, Ames L, Haynes K, Higgins DG. 2014. Comparative phenotypic analysis of the major fungal pathogens *Candida parapsilosis* and *Candida albicans*. *PLoS Pathogens* 10:e1004365.
42. Schwarzmüller T, Ma B, Hiller E, Istel F, Tscherner M, Brunke S, Ames L, Firon A, Green B, Cabral V. 2014. Systematic phenotyping of a large-scale *Candida glabrata* deletion collection reveals novel antifungal tolerance genes. *PLoS Pathogens* 10:e1004211.

43. Byrne KP, Wolfe KH. 2005. The Yeast Gene Order Browser: combining curated homology and syntenic context reveals gene fate in polyploid species. *Genome Research* 15:1456-1461.
44. Segal ES, Gritsenko V, Levitan A, Yadav B, Dror N, Steenwyk JL, Silberberg Y, Mielich K, Rokas A, Gow NAR, Kunze R, Sharan R, Berman J, Pietro AD, Springer N, Hube B. 2018. Gene Essentiality Analyzed by *In Vivo* Transposon Mutagenesis and Machine Learning in a Stable Haploid Isolate of *Candida albicans*. *mBio* 9:e02048-18.
45. Wensing L, Sharma J, Uthayakumar D, Proteau Y, Chavez A, Shapiro RS. 2019. A CRISPR Interference Platform for Efficient Genetic Repression in *Candida albicans*. *mSphere* 4:e00002-19.
46. Román E, Coman I, Prieto D, Alonso-Monge R, Pla J, Mitchell AP. 2019. Implementation of a CRISPR-Based System for Gene Regulation in *Candida albicans*. *mSphere* 4:e00001-19.
47. Schindelin J, Arganda-Carreras I, Frise E, Kaynig V, Longair M, Pietzsch T, Preibisch S, Rueden C, Saalfeld S, Schmid B. 2012. Fiji: an open-source platform for biological-image analysis. *Nature Methods* 9:676-682.
48. Schindelin J, Rueden CT, Hiner MC, Eliceiri KW. 2015. The ImageJ ecosystem: An open platform for biomedical image analysis. *Molecular reproduction and development* 82:518-529.

Chapter 3

Combination of Clearitas® with common oxidizing disinfectants is effective at disrupting mature bacterial and fungal biofilms

In preparation for submission; Authors: Craig L. Ennis & Clarissa J. Nobile

3.1 Abstract

Biofilms are surface-attached microbial communities that are the predominant mode of growth of microorganisms in nature. Biofilms are of critical consequence in medical, ecological, and industrial settings. In terms of the drinking water industry, biofilms can cause water systems to clog and drinking water to become contaminated. Oxidizing disinfectants, such as chloramine and chlorine dioxide, are frequently used by municipalities to reduce microbial growth in water systems. Here we report on Clearitas®, an NSF60 listed product that is a safe and non-toxic product used to treat drinking water for human consumption. We found that Clearitas® on its own is effective at disrupting mature biofilms formed by pathogenic bacterial and fungal species, and that this efficacy is increased when Clearitas® is combined with other commonly used oxidizing agents. The improvement observed when Clearitas® is combined with other oxidizing disinfectants is not seen when these oxidizing disinfectants are combined with each other (e.g., a mixture of Clearitas® and bleach is more effective than a mixture of bleach and chloramine). We also found that Clearitas® on its own is effective at inhibiting biofilm development under controlled flow conditions, similar to conditions of a municipal water system. Overall, Clearitas® is an effective product at inhibiting and disrupting bacterial and fungal biofilms that should be useful alone and in combination with oxidizing disinfectants at reducing microbial growth in water systems.

3.2 Introduction

Biofilms are communities of microbial cells adhered to a surface and surrounded by a protective extracellular matrix and are the predominant microbial growth form found in nature (1-2). Biofilms can form on both biotic (e.g. epithelial linings) and abiotic surfaces (e.g. rocks in streams, water distribution systems, and implanted medical devices) in natural and artificial settings (3). Compared to planktonic (free-floating) cells, biofilms are highly resistant to chemical and mechanical disruption, and provide a recalcitrant reservoir of cells that can colonize new sites and proliferate within the biofilm structure (4). Due to the protective nature of the biofilm structure, biofilms are extremely difficult to remove and are significantly challenging to deal with in medical and industrial settings (4-7).

Water distribution systems are a common industrial setting for biofilm formation, providing a complex and diversely rich ecological niche for microorganisms to interact with one another in the context of biofilms (8-10). When biofilms form in these industrial settings (termed biofouling), this can have profound impacts on water quality and the utility of the system, and can be extremely costly and challenging to address (10, 11). Over time, biofilms within water distribution systems can accumulate biomass to such a degree that the flow rates within the pipes in the system are significantly decreased, eventually leading to complete clogging of the system (12).

There are few, if any, cost-effective methods for clearing this type of biofouling that are also safe to use in potable water systems (13). Ultraviolet (UV) light, for example, is commonly utilized in the water industry to inhibit microbial growth and sterilize drinking water (14). Although UV treatment of biofilms does reduce overall cell numbers, it is often ineffective at biofilm removal, and cannot be used to reach inaccessible pipes and pumps within the water distribution system (14, 15). The other common option to reduce microbial growth in water systems is to chemically treat the system with oxidant disinfectants (14). The most frequently used chemical oxidants for water systems include chlorine, chlorine dioxide, and chloramine, which are inexpensive and highly effective against planktonic microorganisms; they are also effective at preventing biofilm growth (14, 16-18). These oxidants, however, are largely ineffective at breaking up mature biofilms once they have already been established (17, 19-21). The development of effective biofilm disinfectants that can be used to disrupt mature biofilms and that are safe for use in potable water systems presents a significant challenge for the water distribution industry.

Here we compare the efficacies of several standard oxidant disinfectants, including a new oxidant disinfectant (Clearitas®), for their abilities to both inhibit and disrupt common pathogenic biofilms. Our findings indicate that Clearitas®, which is a NSF 60 listed product that is safe for use in drinking water (22), has similar broad-spectrum inhibitory and disruptive activities against both bacterial and fungal biofilms when compared to similar oxidant-based disinfectants. Furthermore, we found that when combined with standard chlorine oxidants, we observed a significant increase in biofilm disruption above that of any of the chlorine disinfectants alone. This additive effect, however, was not seen with the non-chlorine disinfectants tested, such as hydrogen peroxide. Overall, these results can be used to inform best practices for mitigating

biofouling in industrial drinking water facilities as well as in other industrial settings facing similar biofouling issues.

3.3 Results

Chlorine-based oxidants are effective at disrupting bacterial and fungal biofilms

To assess the effects of commonly used disinfectants on disrupting biofilms, we tested three standard chlorine-based oxidants (bleach/sodium hypochlorite, chlorine dioxide, and chloramine), a new chlorine-based oxidant (Clearitas®), and a frequently used non-chlorine-based oxidant (hydrogen peroxide) on biofilms formed by the pathogenic species *Candida albicans* and *Staphylococcus aureus*. *C. albicans* is among the most common fungal pathogens of humans (23) and *S. aureus* is a predominant bacterial pathogen of humans (24). These species were selected because of their pathogenic potential and because both form robust biofilms.

Throughout the course of the study, clinical isolate strain SC5314 was used for the *C. albicans* biofilm experiments, and the methicillin-resistant *S. aureus* (MRSA) strain JE2/USA300 JE2 was used for the *S. aureus* biofilm experiments. We tested the chlorine-based and non-chlorine-based oxidants alone and in combination with Clearitas® at 50, 25, 12.5 mg/L in species-specific biofilm-inducing medium using standard biofilm protocols to determine the levels of biofilm disruption on mature biofilms (25, 26). Treatment of mature *C. albicans* and *S. aureus* biofilms with the chlorine-based oxidizing disinfectants alone resulted in decreased biofilm thickness at all chlorine concentrations tested with little to no change in overall biofilm disruption at all concentrations tested (S Fig 3.1A and B).

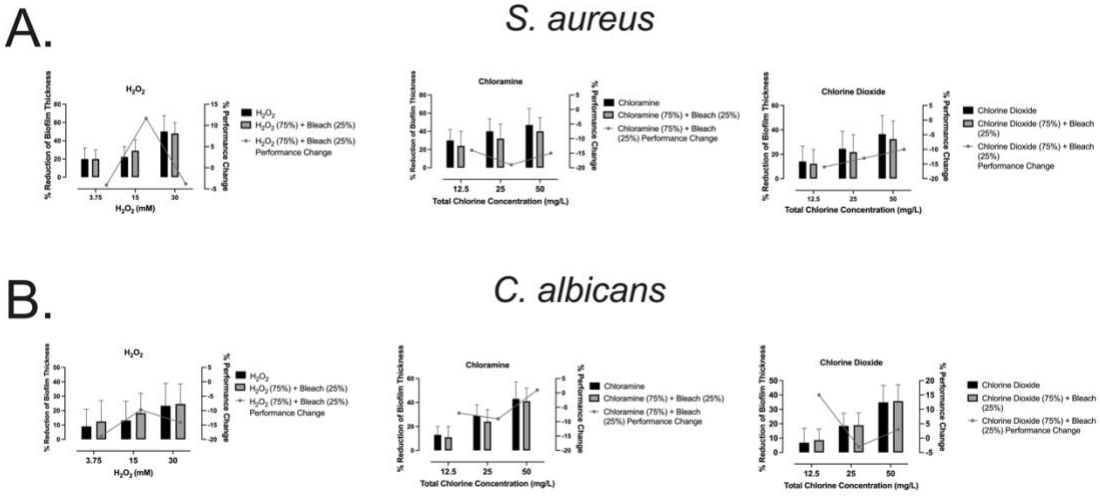

S Figure 3.1 Treatment of bleach in combination with chloramine, chlorine dioxide, or hydrogen peroxide does not improve biofilm disruption over bleach alone. A) *S. aureus* and B) *C. albicans* biofilms were treated with hydrogen peroxide, chloramine, and chlorine dioxide alone or in combination with bleach (25 oxidizing agent:75 bleach). Biofilm disruption was measured with 5 x 5 scanning optical density (OD_{600}) readings. Four replicates were included per experiment and three biological replicates were performed; the average of the experiments is presented.

Combining these chlorine-based oxidizers with Clearitas® in a 75:25 ratio resulted in greater overall reduction of biofilms for both species (Fig 3.1A and B). This 75:25 chlorine-

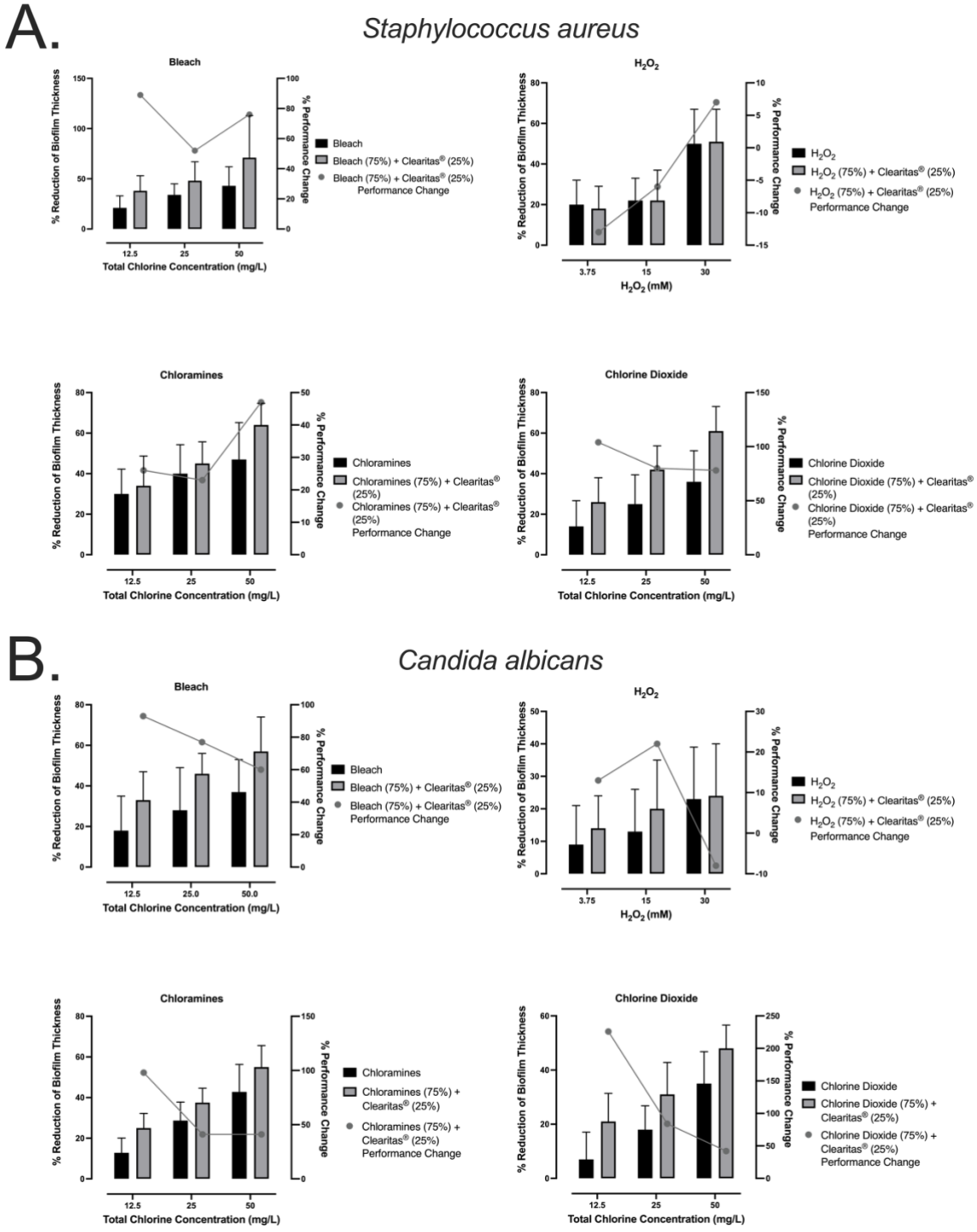

Figure 3.1 Combination of Clearitas and oxidizing disinfectants improves biofilm disruption over bleach alone. Biofilms of A) *Staphylococcus aureus* and B) *Candida albicans* were treated with 12.5, 25, and 50 mg/L Clearitas®, an oxidizing agent, or a 75:25 combination of the two respectively. Hydrogen peroxide was tested alone and in combination with Clearitas® at 3.75, 15, and 30 mM. Oxidizing agents tested included bleach (top left), chloramine (top right), chlorine dioxide (bottom left), and hydrogen peroxide (bottom right). Overall biofilm eradication was measured by scanning optical density reading, and graphed values represent the average of four technical replicates repeated across three biological replicates. The left-axis represents the overall reduction of biofilm thickness and the right-axis the performance change of mixing Clearitas® with an oxidizing agent. The equation used to calculate performance enhancement can be found in the Materials and Methods.

based oxidizer:Clearitas® ratio was chosen to mimic a realistic scenario in the field where Clearitas® may be added to water systems in combination with chlorine-based oxidizers. We note that increasing the relative levels of Clearitas® provides an effect similar to that observed for the 75:25 chlorine-based oxidizer:Clearitas® ratio (S Fig 3.1), i.e. the effect is not increased upon addition of higher levels of Clearitas®. Interestingly, the disruptive abilities against *C. albicans* biofilms were greatest at lower chlorine concentrations (12.5 mg/L) and decreased as the chlorine concentration increased. In contrast, the effect against *S. aureus* biofilms generally increased with the chlorine concentration of the solution. By comparison, hydrogen peroxide, a non-chlorine based oxidizing disinfectant, had little effect against fungal biofilms, and a small improvement in disruption was observed when hydrogen peroxide was combined with Clearitas® (Fig 3.1A and B, S Fig 3.1B).

To manufacture Clearitas®, a brine solution consisting of NaCl undergoes a proprietary oxidation step, resulting in the chlorinated solution. Since our results indicate that Clearitas® and bleach + Clearitas® are effective at disrupting mature biofilms, we sought to determine whether the antibiofilm properties of Clearitas® can be achieved by using the brine precursor or whether this is a unique property of Clearitas®. The brine

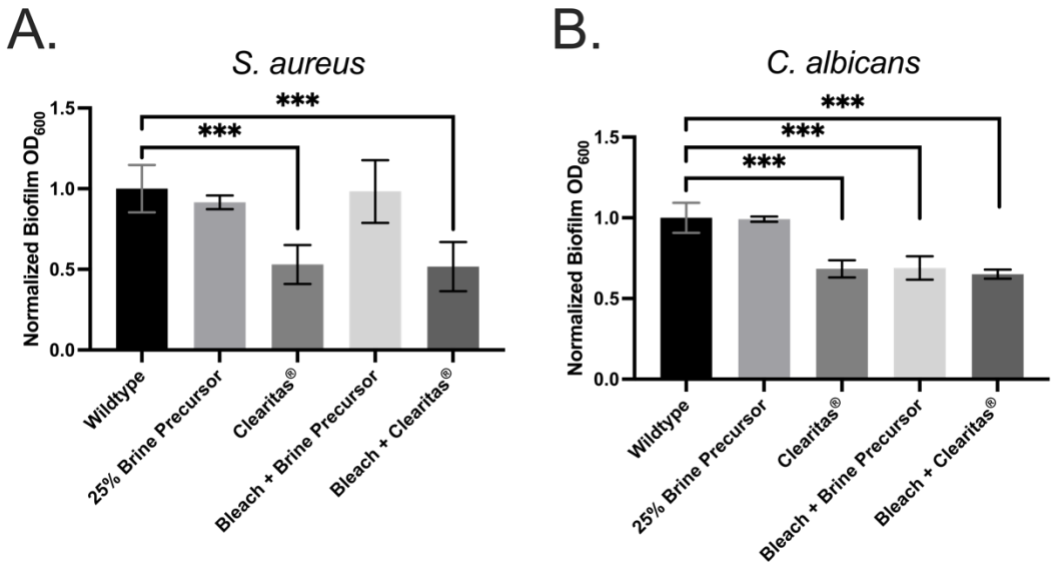

S Figure 3.2 Clearitas® is effective at disrupting biofilms above its brine precursor. Clearitas® is manufactured in part by a proprietary oxidization method of a brine solution. A 25% brine precursor, Clearitas®, 25% brine precursor supplemented with bleach (50 mg/L), and a 75:25 mixture of bleach and Clearitas® (50 mg/L) were used to disrupt A) *S. aureus* and B). *C. albicans* biofilms. The experiment was repeated on two occasions with six technical replicates per experiment, with the average across all experiments displayed. Statistical significance was determined by a student's t-test; p-value < 0.05 (*), < 0.01 (**), < 0.001 (***).

solution alone and the bleach + brine mixture had little disruptive effects on both *C. albicans* and *S. aureus* biofilms (S Fig 3.3A and B), however Clearitas® alone and the bleach + Clearitas® mixture significantly disrupted biofilms of both species. This finding indicates that the proprietary oxidation step occurring during the manufacturing process of Clearitas® is responsible for the antibiofilm properties of Clearitas®.

Clearitas® alone is effective at reducing viable cells within a biofilm

Biofilms are notorious for their high levels of resistance to physical and chemical stresses, where the biofilm structure protects the cells within the biofilm from exposure to the environment (27). Treatment of a biofilm with a disinfectant often leaves behind surviving cells that can then repopulate the biofilm once treatment has ended. Since Clearitas® in combination with bleach is highly effective at biofilm disruption, we sought to determine whether this combination effectively reduces the number of viable cells within a biofilm. To measure viable cells within a biofilm, we repeated assays similar to those used to determine the disruptive properties of these oxidizing agents, but we diluted and plated the remaining biofilm and counted viable cells. Contrary to what was expected, Clearitas® alone at 50 mg/L had the greatest reduction in viable cell counts when tested

against *C. albicans* and *S. aureus* biofilms (Fig 3.2A and 2B).

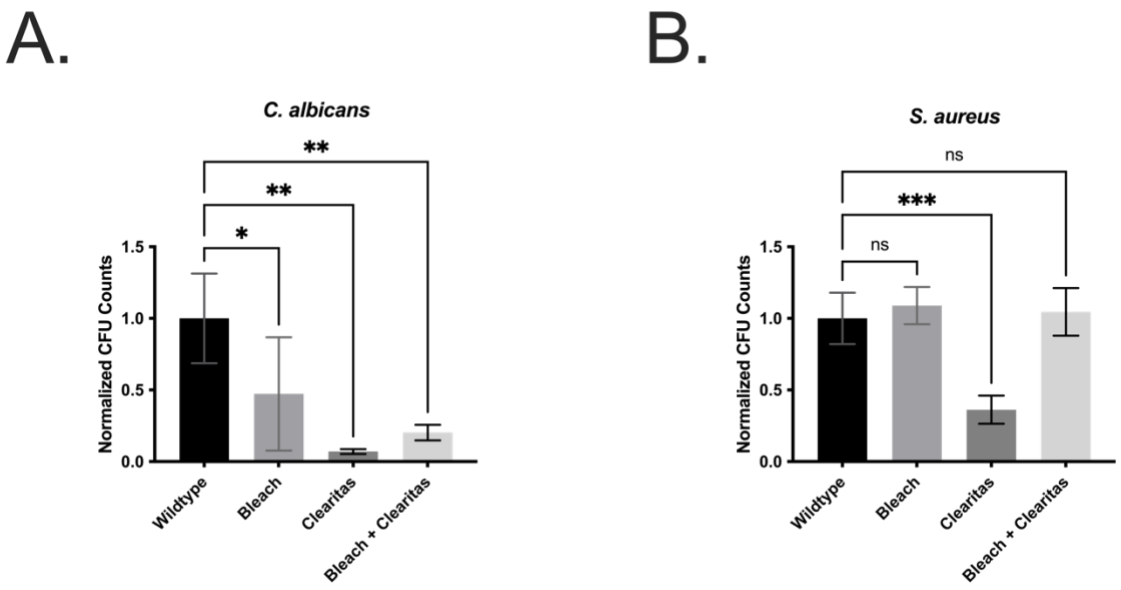

Figure 3.2 Clearitas® is effective at reducing viable cell counts in biofilms. A) *S. aureus* and B) *C. albicans* biofilms were grown to maturation and challenged with 50 mg/L bleach, Clearitas®, or a 75:25 admixture of the two. Biofilms were manually disrupted and diluted in Letheen Broth supplemented with 0.1% sodium thiosulfate neutralizing residual chlorine, and plated. Cell viability experiments were repeated twice with four replicates included per experimental condition; the average of all biological and technical replicates is graphed. CFU counts were normalized to the untreated wildtype control for each species. Significance was determined by a student's t-test; p value < 0.05 (*), < 0.01 (**), < 0.001 (***).

Treatment of *C. albicans* biofilms with bleach alone and a mixture of bleach and Clearitas® resulted in significant reduction of viable cells within the biofilm. A similar trend was observed in *S. aureus* biofilms; bleach alone reduced viability of cells, but not with the same efficacy as Clearitas® alone or the mixture with bleach. It is possible that Clearitas® is better at penetrating the biofilm structure than other frequently used oxidizing agents, however the mechanism of its disruptive properties remains unknown. Taken together, Clearitas® is an effective measure of disrupting biofilms and reducing viable cell counts of bacterial and fungal microorganisms.

Clearitas® has long-acting inhibitory properties against the development of biofilms under controlled flow conditions

Since Clearitas® is able to disrupt mature biofilms, we tested its ability to inhibit biofilm development in a way that closely mimics biofilm growth under controlled flow, similar to that found in pipes supplying drinking water. We utilized a customizable microfluidic device to monitor *C. albicans* and *S. aureus* biofilm growth over the course of 12 hours in the presence and absence of bleach, Clearitas®, and the mixture of bleach and Clearitas®. All solutions tested strongly inhibited *S. aureus* biofilm growth, noting

minimal cell proliferation relative to the biofilm (Fig 3.3A, S Fig 3.4). In contrast, *C. albicans* was still capable of biofilm development in the presence of all disinfectants tested,

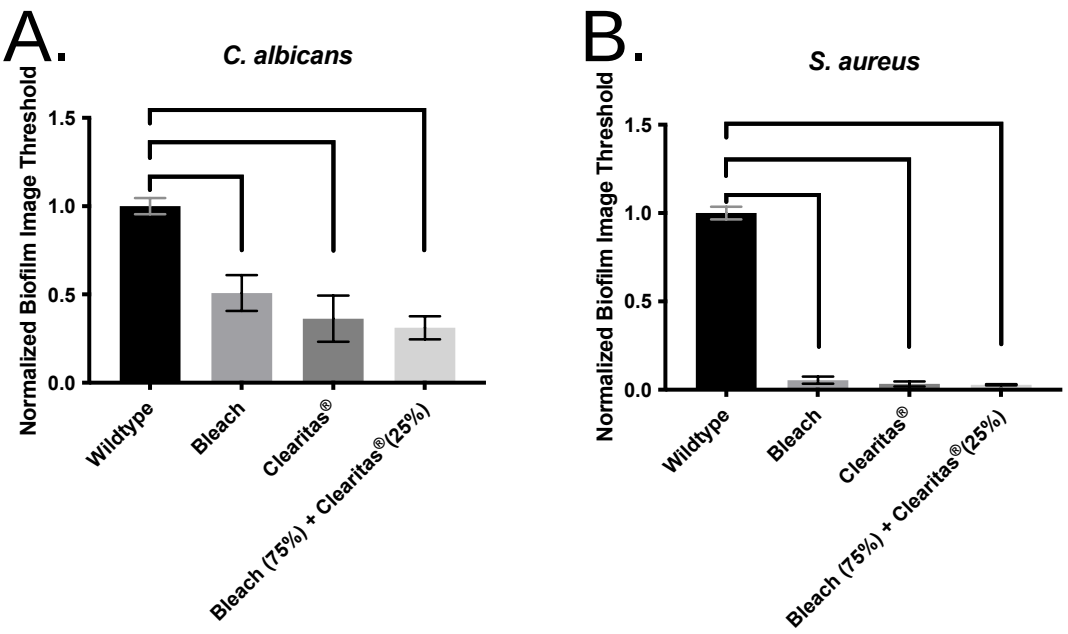

Figure 3.3 Combination of Clearitas® and bleach together significantly inhibit biofilm development under controlled flow conditions. A) *C. albicans* and B) *S. aureus* biofilms were grown under controlled laminar flow conditions in a Bioflux 1000Z microfluidic system and imaged over the course of 12hrs. Both species biofilms were subjected to a flow rate of 0.5 dyn/cm^2 at 37 °C with oxidizing disinfectants at a concentration of 50 mg/L. Images were acquired every five minutes at two different wavelengths. Three replicates were included per experiment and three points of the viewing chamber were imaged per replicate. Overall biofilm development was measured by image thresholding of the final time-point (12 h, frame 145) and was averaged across all replicate and viewpoints per condition. Threshold values were normalized to the untreated control. Statistical significance was determined by a student's t-test; p-value < 0.05 (*), < 0.01 (**), < 0.001 (***).

yet we note significant reduction in overall biofilm growth after 12 hours, and the bleach + Clearitas® mixture had the greatest inhibition (Fig 3.3B, S Fig 3.5). The longevity of *S. aureus* biofilm inhibition compared to *C. albicans* highlights a need for a broadly effective inhibitor of biofilm development in municipal water systems. Altogether, we propose that Clearitas® can be used as an effective measure to ensure inhibit development of bacterial biofilms in piping used for drinking water.

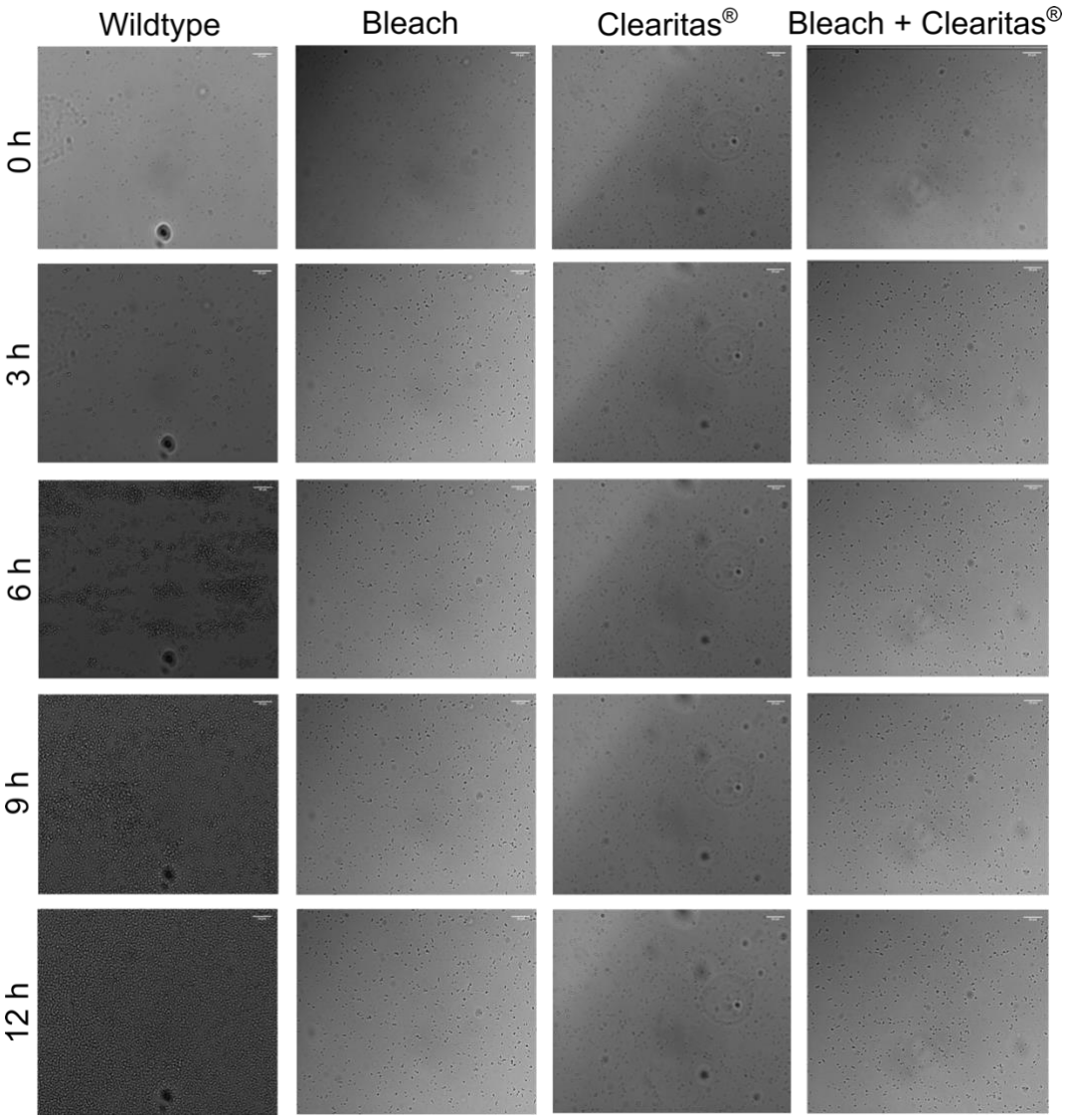

S Figure 3.3 Clearitas® inhibits *S. aureus* biofilm development under controlled flow conditions. Brightfield images from time lapse biofilm inhibition experiment quantified in Fig 3.3B for *S. aureus* at 0, 3, 6, 9, and 12 h time points. *S. aureus* biofilms were grown in TSBG alone or supplemented with 50 mg/L of either bleach, Clearitas®, or a mixture of the two. Images were acquired using a 40X objective, and the scale bar represents 20 μm.

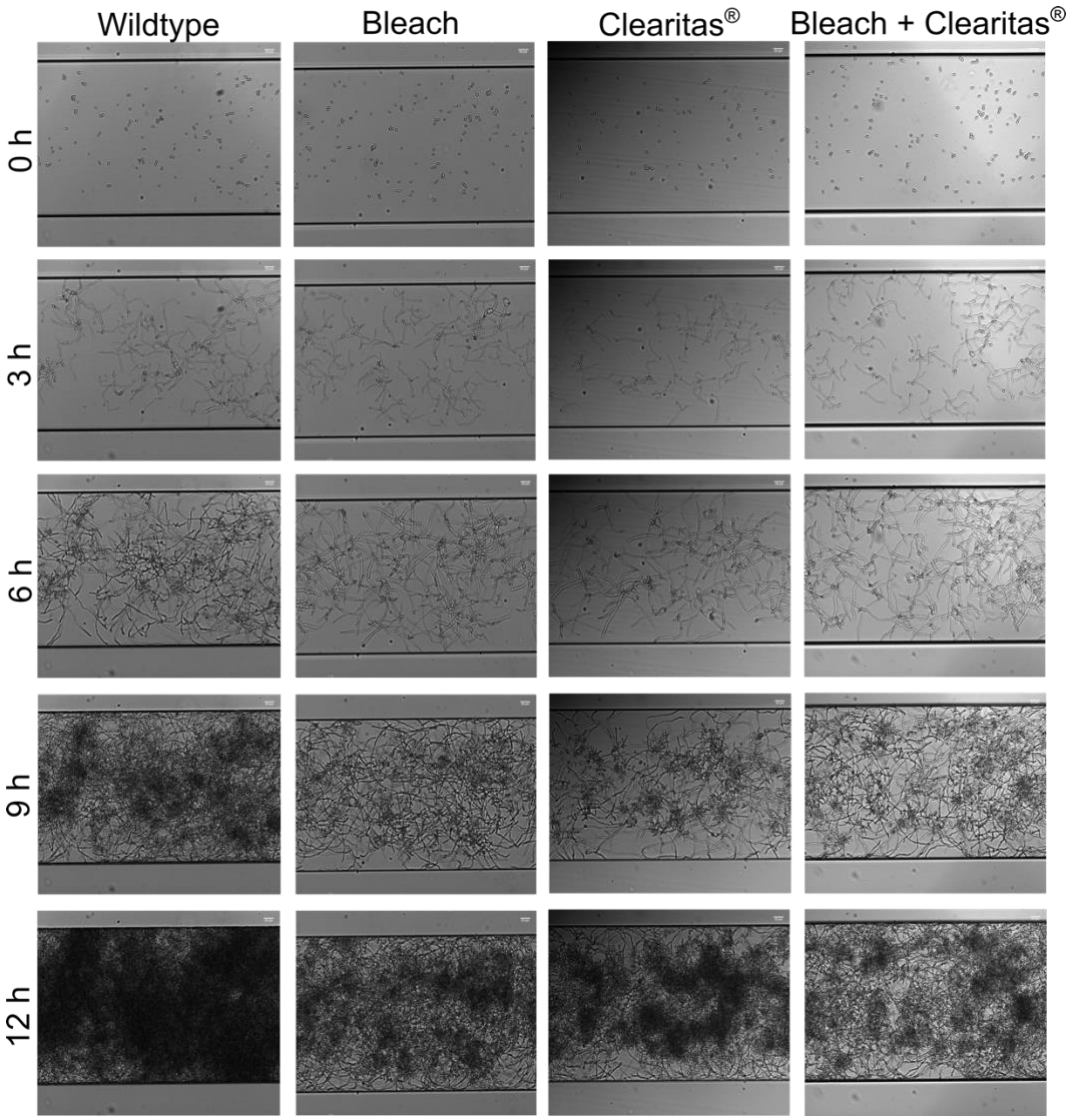

S Figure 3.4 Clearitas® inhibits *C. albicans* biofilm development under controlled flow conditions. Brightfield images from time-lapse biofilm inhibition experiment quantified in Fig 3.3A for *C. albicans* at 0, 3, 6, 9, and 12 h time points. *C. albicans* biofilms were grown in Spider alone or supplemented with 50 mg/L of either bleach, Clearitas®, or a mixture of the two. Images were acquired using a 20X objective, and the scale bar represents 20 μm.

Disruptive capability of Clearitas® against pathogenic biofilm forming bacteria

Microbial communities in drinking water are incredibly diverse, and opportunistic pathogens are frequently isolated from contaminated water systems (2, 5, 10, 11). We sought to test the application of Clearitas® in disrupting biofilms from equally diverse biofilm forming microorganisms that have the potential to cause infection. Biofilms of the gram-negative pathogen *Escherichia coli*, and gram-positive pathogens *Enterococcus faecalis*, and *Staphylococcus epidermidis*, were grown under biofilm inducing conditions,

and challenged with bleach, Clearitas®, and bleach mixed with Clearitas®. Clearitas® alone at all concentrations tested had little effect on biofilms formed by *E. coli*. When mixed with bleach there is a mild additive effect observed for these species, consistent with our findings for *C. albicans and S. aureus* biofilms (Figure 3.4).

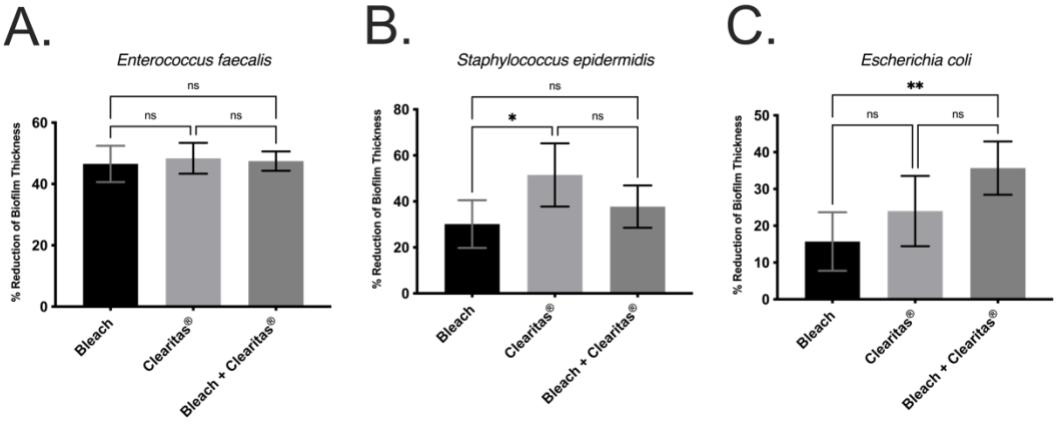

Figure 3.4 Combination of Clearitas® with bleach is effective at disrupting biofilms formed by several bacterial species. Biofilms of A) *Enterococcus faecalis*, B) *Staphylococcus epidermidis*, and C) *Escherichia coli* were grown to maturation and challenged with 50 mg/L bleach, Clearitas®, or a 75:25 combination of the two. Biofilm disruption was measured by scanning optical density (OD_{600}) reading, averaged across four replicates, and normalized to the untreated control. Statistical significance was determined by a student's t-test; p-value < 0.05 (*), < 0.01 (**), < 0.001 (***).

Treatment of *E. faecalis* biofilms with bleach, Clearitas®, and a mixture of the two effectively reduced overall biofilm biomass at 50 mg/L, yet all solutions tested had nearly equal disruptive properties. Similarly, exposure of *S. epidermidis* biofilms with the same concentration of these oxidizing agents resulted in efficient disruption of the biofilm. Contrary to what was seen in disruption assays against *S. aureus* (Fig 3.1A), Clearitas® alone was most effective at disrupting *S. epidermidis* biofilms, and improved biofilm disruption was not evident. This suggests that the disruptive properties of these disinfectants may be species specific, with some microorganisms having more resilient biofilms than others.

Clearitas® is an effective against both gram-positive and negative pathogens that are notorious biofilm forming microorganisms. These pathogens commonly form within municipal water systems and are able to contaminate drinking water systems. Furthermore, some of these pathogens are known to cause nosocomial infections, and thus Clearitas® may be an effective solution for disinfecting surfaces in a hospital setting.

3.4 Discussion

Here we show the utility of, Clearitas®, a novel chlorine-based oxidizing disinfectant with broad-spectrum activity against bacterial and fungal biofilms. Chlorine (bleach, chlorine dioxide, and chloramine) and non-chlorine (hydrogen peroxide) oxidizing

disinfectants are commonly used to reduce biofilm buildup in industrial settings, such as municipal water systems, to reduce biofouling. Consistent with previously published literature, we find that these disinfectants on their own are largely ineffective at greatly reducing microbial biofilms once developed. When combined with Clearitas®, chlorine-based oxidants have a synergistic effect, resulting in greater reduction of mature biofilms. Based on experiments (Fig 3.1 and S Fig 3.3), we believe that the manufacturing process of Clearitas® is what provides its potency against biofilms. A chlorine-based oxidizing agent, in conjunction with Clearitas®, can inhibit the development of a biofilm as well. Furthermore, we note that Clearitas® alone is highly effective at reducing the number of viable cells within a biofilm, and this is consistent in both bacterial and fungal biofilms, suggesting this effect may be seen in other microbial species. This product was originally patented for use in municipal water systems (22); however, its broad-spectrum activity against both gram-negative and positive bacteria suggest that it may prove useful in other settings where biofilms are a problem (e.g., hospitals, agriculture, food processing). Taken together, we believe Clearitas® is an effective measure at both reducing biofilm biomass and killing both fungal and bacterial cells harbored within these structures presenting a useful method for providing safe, clean drinking water.

3.5 Materials and Methods

Strains, Medias, and Equipment

Species used in this study were *Candida albicans* (SC5314; ATCC® MYA-2876™), *Staphylococcus aureus* (USA300; ATCC® BAA-1556™), *Staphylococcus epidermidis, Escherichia coli, Enterococcus faecalis.* The *C. albicans* and *S. aureus* strains are available through atcc.org and the S. epidermidis, E. coli, and E. faecalis strains clinical isolates gifted by the UCSF clinical microbiology lab (28).

Candida albicans was streaked on Yeast Peptone Dextrose (YPD) (2% Peptone, 2% Dextrose, 1% Yeast Extract) and incubated for 48 hours at 30 °C. A single colony was inoculated in 4mL YPD broth, and grown for 12 hours at 30 °C shaking at 225 rpm.

Staphylococcus aureus, *Streptococcus epidermidis*, and *Enterococcus faecalis* were streaked on Tryptic Soy Agar (TSA) plates and incubated for 24 hours at 37 °C. A single colony was inoculated in 4mL Tryptic Soy Broth (TSB), and grown for 12 hours at 37 °C shaking. *Escherichia coli* was streaked on Luria Bertani (LB) plates, and incubated for 24 hours at 37 °C. A single colony was inoculated in 4mL LB broth and grown for 12 hours at 37 °C shaking.

For all *C. albicans* biofilms, all solutions were prepared in Spider (1% nutrient broth, 1% mannitol, and 0.2% K_2HPO_4) as described previously (25, 26, 29). All bacterial biofilms were prepared in TSB supplemented with 1% glucose, henceforth referred to as TSBG. All subsequent steps were completed in a fashion that maintained sterility. Solutions of Clearitas®, bleach, chloramine, and/or chlorine dioxide were created at a concentration of 50 mg/L Cl_2, and homogenized by vortexing. Hydrogen peroxide was diluted in media to 30mM. For solutions containing chlorine (Clearitas®, bleach, chloramine, and chlorine

dioxide), the Cl_2 concentration was measured by the iodometric technique using a Hach Chlorine mid and high range digital titrator (Catalog # 2471100) and H_2O_2 concentration was determined with a Hach H_2O_2 drop count titration test kit (Catalog # 2291700). Solutions were tested against mature biofilms in 96-well polystyrene plates.

Optical density measurements for cuvettes and plates were performed using a Biotek Epoch2.

96-well Biofilm Disruption

The method used to disrupt *Candida albicans* biofilms was performed as previously described using a 96-well polystyrene plate (23, 26). This protocol was further modified to support biofilm growth of bacterial species. Briefly, over-night culture was diluted to 0.5 for *C. albicans* in Spider media and 0.3 for *S. aureus, S. epidermidis, E. coli,* and *E. faecalis* in TSBG. *C. albicans* biofilms were allowed to adhere for ninety minutes shaking at 250 rpm at 37 °C in an ELMI Shaker. Bacterial species were adhered for sixty minutes under static conditions at 37 °C. All plates were sealed with breathable film throughout during biofilm adherence and maturation. After initial adherence, the media is removed, and the wells are washed with 1X PBS removing non-adhered cells and resupplied with fresh media. Biofilms were allowed to develop for 24 hours under their respective conditions. Afterwards media was removed, and media supplemented with disinfectant was added slowly in a drop-wise manner to avoid mechanical disruption. Biofilms were incubated for 24 hours with the conditioned media which was then removed and biofilm disruption was measured by 5 x 5 scanning optical density readings at OD_{600}. Optical density readings were normalized to the wildtype condition and analyzed using a two-tailed students t-test. Percent Performance Change (PC) measures the change in biofilm disruption when mixing two compounds using the equation, $PC = \frac{\%RBT_{Disinfectant+Clearitas®}}{(0.75)\%RBT_{Disinfectant\ Alone}+(0.25)\%RBT_{Clearitas®}} - 1$, where RBT is the percent reduction in biofilm thicknes.

Biofilm Water Disruption

The method used is a modified version of the previously published 384-well biofilm disruption method (25). 384-well polystyrene plates were filled with 80 µl TSBG or Spider for *S. aureus* and *C. albicans* biofilms respectively. 1 µl of overnight cell culture was inoculated into each well. *C. albicans* biofilms were allowed to adhere for 90 minutes at 37 °C shaking at 350 rpm in an ELMI Shaker. *S. aureus* biofilms were allowed to adhere for 60 minutes under static conditions at 37 °C in an ELMI Shaker. After the adherence step, biofilms were washed with 1X PBS and resupplied with fresh media. *C. albicans* and *S. aureus* biofilms were incubated under the aforementioned conditions for 24 hours. Clearitas® and bleach were diluted into autoclaved distilled water, and chlorine concentrations were measured using the colorimetric method using a Palintest compact chlorometer (Catalog # APO31). Media was removed from the wells after 24 hour incubation, and supplied with the disinfectant diluted in water. Biofilms were placed back to their respective conditions for 24 hours. Water was removed from the wells, and biofilm disruption was measured using OD_{600} readings with a Epoch 2 plate reader.

Bioflux Microfluidic Assay

Inhibition assays were performed as published using Bioflux 48-well low-sheer plates (Fluxion Biosciences), the BioFlux 1000Z (Fluxion Biosciences) microfluidic device, and a Zeiss AX10 microscope (30). Briefly the channels of the Bioflux plate were primed using wildtype and conditioned media with bleach, Clearitas®, and bleach + Clearitas® at 50 mg/L Cl_2 prewarmed to 37 °C. Liquid cell culture was diluted to an optical density of 0.5 and 0.3 in unconditioned Spider and TSBG media for *C. albicans* and *S. aureus* respectively. Cells were flushed into the viewing window of a plate at 2 dyn/cm^2 for four seconds, and were allowed to adhere for 10 minutes. Wildtype and conditioned media was flushed through at 2 dyn/cm^2 for five minutes to remove non-adhered cells after the initial image acquisition. The flow rate was then set to 0.5 dyn/cm^2 for the remainder of the assay with image acquisition occurring every five minutes over twelve hours using brightfield microscopy. Temperature was maintained at 37 °C during the course of the experiment. *C. albicans* biofilm development was imaged using the 20X objective and *S. aureus* biofilm development was imaged using the 40X objective. Compiled timelapse images were compressed into .wav files at 10 frames per second (fps) using FIJI (31).

Biofilm inhibition was quantified measuring the percentage of the viewing area covered by the biofilm using the Bioflux Montage software (Fluxion Biosciences) as described (30). Values were normalized to the wildtype condition, and statistical analysis was performed using a two-tailed students t-test.

Cell Viability Testing of Clearitas

Biofilm cell viability tests were carried out as follows. *C. albicans* and *S. aureus* biofilms were grown in 96 well polystyrene plates for 24 hours in Spider media. Media was removed and biofilms were challenged with either bleach, Clearitas®, or bleach + Clearitas® in growth media with 50 mg/L chlorine to measure the impact on cell viability. Once the 24 hour treatment was completed, media was removed, biofilms were washed with 1X PBS to remove non-adhered cells. Biofilms were resuspended in 1X PBS, and mechanically disrupted and scrapped off the bottom of the wells. Resuspended biofilms in PBS were diluted 1:10 in Leftheen Broth (VWR Catalog # DF0681-17-7) + 0.1% Sodium Thiosulfate to neutralize residual chlorine. Samples were serially diluted to 10^6 in 1X PBS and plated on YPD or TSA plates. Colonies were counted and multiplied by the dilution factor, and statistical analysis was done using a two-tailed students t-test.

Acknowledgments

We are thankful for Blue Earth Labs for providing their Clearitas® product to us free of charge. We are also grateful to Jason Peters at Blue Earth Labs for his advice on product usage.

3.6 References

1. Nobile CJ, Mitchell AP. Microbial biofilms: e pluribus unum. Current Biology. 2007;17(10):R349-R53.

2. Watnick P, Kolter R. Biofilm, city of microbes. Journal of bacteriology. 2000;182(10):2675-9.
3. Nobile CJ, Johnson AD. Candida albicans biofilms and human disease. Annual review of microbiology. 2015;69:71-92.
4. Gulati M, Nobile CJ. Candida albicans biofilms: development, regulation, and molecular mechanisms. Microbes and infection. 2016;18(5):310-21.
5. Martiny AC, Jørgensen TM, Albrechtsen H-J, Arvin E, Molin S. Long-term succession of structure and diversity of a biofilm formed in a model drinking water distribution system. Applied and Environmental Microbiology. 2003;69(11):6899-907.
6. Stoodley P, Sauer K, Davies DG, Costerton JW. Biofilms as complex differentiated communities. Annual Reviews in Microbiology. 2002;56(1):187-209.
7. Hall-Stoodley L, Costerton JW, Stoodley P. Bacterial biofilms: from the natural environment to infectious diseases. Nature reviews microbiology. 2004;2(2):95-108.
8. Wang H, Masters S, Edwards MA, Falkinham III JO, Pruden A. Effect of disinfectant, water age, and pipe materials on bacterial and eukaryotic community structure in drinking water biofilm. Environmental science & technology. 2014;48(3):1426-35.
9. Inkinen J, Jayaprakash B, Santo Domingo J, Keinänen-Toivola M, Ryu H, Pitkänen T. Diversity of ribosomal 16S DNA-and RNA-based bacterial community in an office building drinking water system. Journal of applied microbiology. 2016;120(6):1723-38.
10. Abdel-Nour M, Duncan C, Low DE, Guyard C. Biofilms: the stronghold of Legionella pneumophila. International journal of molecular sciences. 2013;14(11):21660-75.
11. El-Chakhtoura J, Prest E, Saikaly P, van Loosdrecht M, Hammes F, Vrouwenvelder H. Dynamics of bacterial communities before and after distribution in a full-scale drinking water network. water research. 2015;74:180-90.
12. Vrouwenvelder H, Van Paassen J, Folmer H, Hofman JA, Nederlof M, Van der Kooij D. Biofouling of membranes for drinking water production. Desalination. 1998;118(1-3):157-66.
13. Chapman JS. Disinfectant resistance mechanisms, cross-resistance, and co-resistance. International biodeterioration & biodegradation. 2003;51(4):271-6.
14. Schwartz T, Hoffmann S, Obst U. Formation of natural biofilms during chlorine dioxide and uv disinfection in a public drinking water distribution system. Journal of applied microbiology. 2003;95(3):591-601.
15. Emtiazi F, Schwartz T, Marten SM, Krolla-Sidenstein P, Obst U. Investigation of natural biofilms formed during the production of drinking water from surface water embankment filtration. Water research. 2004;38(5):1197-206.
16. Vaid R, Linton RH, Morgan MT. Comparison of inactivation of Listeria monocytogenes within a biofilm matrix using chlorine dioxide gas, aqueous chlorine dioxide and sodium hypochlorite treatments. Food Microbiology. 2010;27(8):979-84.
17. Richardson S, Thruston A, Caughran T, Chen P, Collette T, Schenck K, et al. Identification of new drinking water disinfection by-products from ozone, chlorine dioxide, chloramine, and chlorine. Water, air, and soil pollution. 2000;123(1):95-102.

18. Mayack LA, Soracco RJ, Wilde EW, Pope DH. Comparative effectiveness of chlorine and chlorine dioxide biocide regimes for biofouling control. Water Research. 1984;18(5):593-9.
19. Simoes LC, Simoes M, Vieira MJ. Influence of the diversity of bacterial isolates from drinking water on resistance of biofilms to disinfection. Applied and Environmental Microbiology. 2010;76(19):6673-9.
20. Shaw JL, Monis P, Fabris R, Ho L, Braun K, Drikas M, et al. Assessing the impact of water treatment on bacterial biofilms in drinking water distribution systems using high-throughput DNA sequencing. Chemosphere. 2014;117:185-92.
21. Behnke S, Camper AK. Chlorine dioxide disinfection of single and dual species biofilms, detached biofilm and planktonic cells. Biofouling. 2012;28(6):635-47.
22. Peters JE, O'connor SD, Yu C-j. Methods and stabilized compositions for reducing deposits in water systems. Google Patents; 2013.
23. Lohse MB, Gulati M, Johnson AD, Nobile CJ. Development and regulation of single-and multi-species Candida albicans biofilms. Nature Reviews Microbiology. 2018;16(1):19-31.
24. Archer NK, Mazaitis MJ, Costerton JW, Leid JG, Powers ME, Shirtliff ME. Staphylococcus aureus biofilms: properties, regulation, and roles in human disease. Virulence. 2011;2(5):445-59.
25. Lohse MB, Gulati M, Valle Arevalo A, Fishburn A, Johnson AD, Nobile CJ. Assessment and optimizations of Candida albicans in vitro biofilm assays. Antimicrobial agents and chemotherapy. 2017;61(5):e02749-16.
26. Gulati M, Lohse MB, Ennis CL, Gonzalez RE, Perry AM, Bapat P, et al. In Vitro Culturing and Screening of Candida albicans Biofilms. Curr Protoc Microbiol. 2018;50(1):e60.
27. Stewart PS, Costerton JW. Antibiotic resistance of bacteria in biofilms. The lancet. 2001;358(9276):135-8.
28. Fox E, Cowley E, Nobile C, Hartooni N, Newman D, Johnson A. Anaerobic bacteria grow within Candida albicans biofilms and induce biofilm formation in suspension cultures. Current biology. 2014;24(20):2411-6.
29. Liu H, Kohler J, Fink GR. Suppression of hyphal formation in Candida albicans by mutation of a STE12 homolog. Science. 1994;266(5191):1723-6.
30. Gulati M, Ennis CL, Rodriguez DL, Nobile CJ. Visualization of Biofilm Formation in Candida albicans Using an Automated Microfluidic Device. J Vis Exp. 2017(130).
31. Schindelin J, Arganda-Carreras I, Frise E, Kaynig V, Longair M, Pietzsch T, et al. Fiji: an open-source platform for biological-image analysis. Nature methods. 2012;9(7):676-82.

Chapter 4

Conclusions and Future Directions

4.1 Conclusions

In the United States alone, fungal infections result in approximately nine million hospital visits with nearly half of these visits caused by *Candida* species (1). Of these species, *C. albicans* is the most frequently isolated species and is often referred to as the most common human fungal pathogen (2). Although *C. albicans* is the most common fungal species found in patients, other species, such as *C. auris* are emerging and gaining notoriety (3). Development of tools for the study of these non-*albicans Candida* species is lacking and is a critical step towards the development of new therapeutics to treat these life-threatening infections.

Chapter one of this dissertation describes the identification of three adhesion regulators (Bcr1, Efg1, and Flo8) and a NOX enzyme, Cfl11, and its novel contribution to adhesion during the formation of flocs, which have similar properties to biofilms. Biofilms, and we hypothesize flocs as well, provide protection from antifungal drug treatment (4). Disruption of these microbial communities is important for the penetration of therapeutics and eradication of infections (5). My results suggest that Cfl11 contributes to adhesion by creating H_2O_2 bursts that are critical for Als1 function. Enzyme inhibition is a promising mechanism to target for the development of novel antifungal drugs, and Cfl11's location on the cell periphery and its role in adhesion make it an intriguing biofilm-specific drug target. Although Cfl11 is unique to *C. albicans* and *C. dublinieinsis*, the *Candida* species broadly encode several NOX-like enzymes in their genomes, thus these enzymes are likely generally important for virulence. In addition to the identification of Cfl11, we serendipitously identified Pga23 as a critical mediator of the caspofungin response. In response to antifungal and host induced stress, *C. albicans* remodels its cell wall, altering the composition of mannans, chitins, and β-glucans to withstand stress. It remains unclear how Pga23 specifically protects the fungal cell from caspofungin cell wall stress and the structure and function of this protein is undiscovered; however, we suspect it is critical for cell wall remodeling and/or stability.

Chapter two describes the development and optimization of the first markerless CRISPR/Cas9 genome editing tool for *C. auris*. To show the utility of this tool, we explored the conservation of Cas5 in the caspofungin response. Towards this we deleted and complemented *CAS5* in a representative clinical isolate from each of the five *C. auris* genetic clades. We additionally confirmed that activation of Cas5 is mediated by dephosphorylation of the S643 amino acid and our results suggest this event contributes to Cas5's nuclear translocation during caspofungin exposure. Given the evolutionary distance between *C. albicans* and *C. auris*, our results suggest that Cas5 is likely conserved in the *Candida* clade species as a regulator of the caspofungin response. Work characterizing the

Cas5 targets across *Candida* clade species would greatly improve our understanding of how fungal pathogens respond to this critically important antifungal drug.

Biofilm growth within industrial water supply settings is a significant challenge for providing safe drinking water (6, 7). Presently oxidizing disinfectants, such as chloramine and chlorine dioxide, and UV radiation exposure are used to reduce biofilm growth, yet alone these methods are ineffective at disrupting already formed biofilms (8). Chapter three investigates a new oxidizing disinfectant, Clearitas®, that has increased efficacy at disrupting biofilms when it is combined with other oxidizing disinfectants, such as bleach, chloramine, or chlorine dioxide. This disinfectant combination is highly effective against biofilms formed by many bacterial and fungal species, making it a promising disinfection method for industrial water systems.

4.2 Future Directions

Only three antifungal drug classes currently exist for treating systemic fungal infections in humans, and these drug classes can be toxic to humans and some fungal species are rapidly evolving resistance/tolerance to certain drug classes (9). Further work to develop biofilm-specific therapeutics or those capable of rendering resistant species sensitive are important for treating life-threatening fungal infections. Based on my findings in Chapter one, future work to identify small molecules capable of enzymatically inhibiting Cfl11 could be important in the development of novel therapeutics for the disruption of fungal flocs and biofilms. Furthermore, this chapter led to the identification of Pga23 as an important protein for the caspofungin response. Characterization of cell wall carbohydrates (e.g., mannans, chitins, and β-glucans) in the wildtype and *pga23*Δ/Δ strain coupled with high resolution microscopy (e.g., scanning electron microscopy) could help to piece together a role for Pga23 in the antifungal response. We hypothesize that high resolution microscopy of the wildtype and *pga23*Δ/Δ strain in the presence and absence of caspofungin would reveal differences in the cell wall architecture.

Development of the CRISPR/Cas9 tool in Chapter two provides an exciting advancement in our abilities to genetically manipulate an important human fungal pathogen. Historically, genetic manipulation of fungal pathogens has been cumbersome, as well as time and resource intensive. Collections of deletion mutant libraries, like the one described in Chapter one for *C. albicans* (e.g., a transcription factor mutant library), have been an invaluable resource for the study of antifungal drug resistance, commensalism, and virulence. Development of similar deletion mutant libraries in *C. auris* would greatly improve our understanding of this emerging pathogen, and would also facilitate future evolutionary studies of fungal pathogens. Furthermore, using unbiased genome-wide profiling (RNA-seq and CUT&RUN) of Cas5 and its downstream target genes could identify downstream targets important for cell wall remodeling or the response to caspofungin across *Candida* species.

4.3 References

1. Vallabhaneni S, Mody RK, Walker T, Chiller T. 2016. The Global Burden of Fungal Diseases. Infect Dis Clin North Am 30:1-11.
2. Tsay SV, Mu Y, Williams S, Epson E, Nadle J, Bamberg WM, Barter DM, Johnston HL, Farley MM, Harb S, Thomas S, Bonner LA, Harrison LH, Hollick R, Marceaux K, Mody RK, Pattee B, Shrum Davis S, Phipps EC, Tesini BL, Gellert AB, Zhang AY, Schaffner W, Hillis S, Ndi D, Graber CR, Jackson BR, Chiller T, Magill S, Vallabhaneni S. 2020. Burden of Candidemia in the United States, 2017. Clin Infect Dis 71:e449-e453.
3. Du H, Bing J, Hu T, Ennis CL, Nobile CJ, Huang G. 2020. Candida auris: Epidemiology, biology, antifungal resistance, and virulence. PLoS Pathog 16:e1008921.
4. Nobile CJ, Johnson AD. 2015. Candida albicans biofilms and human disease. Annual review of microbiology 69:71-92.
5. Lohse MB, Gulati M, Johnson AD, Nobile CJ. 2018. Development and regulation of single-and multi-species Candida albicans biofilms. Nature Reviews Microbiology 16:19-31.
6. El-Chakhtoura J, Prest E, Saikaly P, van Loosdrecht M, Hammes F, Vrouwenvelder H. 2015. Dynamics of bacterial communities before and after distribution in a full-scale drinking water network. water research 74:180-190.
7. Wingender J, Flemming H-C. 2011. Biofilms in drinking water and their role as reservoir for pathogens. International journal of hygiene and environmental health 214:417-423.
8. Schwartz T, Hoffmann S, Obst U. 2003. Formation of natural biofilms during chlorine dioxide and uv disinfection in a public drinking water distribution system. Journal of applied microbiology 95:591-601.
9. Cowen LE, Sanglard D, Howard SJ, Rogers PD, Perlin DS. 2014. Mechanisms of Antifungal Drug Resistance. Cold Spring Harb Perspect Med 5:a019752.